

**The Role of the HECT-Type Ubiquitin Ligases WWP1 and  
WWP2 in Nerve Cell Development and Function**

**PhD Thesis**  
**in partial fulfillment of the requirements**  
**for the degree “Doctor of Philosophy (PhD)”**  
**at the Georg August University Göttingen,**  
**Faculty of Biology**

**Submitted by**

**Mika Kishimoto-Suga**

**Born in**

**Kyoto, Japan**

**March 2011**



## **Declaration**

I hereby declare that this thesis ‘The Role of the HECT-Type Ubiquitin Ligases WWP1 and WWP2 in Nerve Cell Development and Function’ has been written independently, with no other aids than those cited.

March 15<sup>th</sup>, 2011

Mika Kishimoto-Suga

## Acknowledgments

At first I would like to thank my PhD supervisor, Dr. Hiroshi Kawabe for giving me the opportunity to do my PhD in his group, for his support, his encouragement, and his training in experimental skills. It was a great pleasure to me to conduct this study under his supervision. I am also very grateful to him for his training in presentation and writing skills, and for proofreading this thesis.

I am also indebted to Prof. Dr. Nils Brose for including me as a member in his department. It has been an enriching experience to be a part of his department and his guidance and input to my PhD project has been precious.

I am also truly grateful to the guidance and effort of my other thesis committee member, Prof. Dr. Ernst A. Wimmer.

The interactive scientific environment in Max Planck Institute for Experimental Medicine enabled several collaborations to learn techniques, which were invaluable tools for the progress of my PhD project. These collaborations also gave me an opportunity to interact with highly experienced scientists like Prof. Dr. Victor Taravykin, who was kind and helpful in allowing his experimental set-up to be used for in utero electroporation. I am also truly grateful to the support and effort of Paraskevi Sgourdou. I would also like to thank Dr. Olaf Jahn and Dr. Kalina Dimova for their support in mass spectrometric analyses.

I would also like to express my gratitude to Dr. Daisaku Yokomaku for precious advice during early stages of the study.

I would also like to thank Prof. Hans-Jürgen Kreirnkamp, Prof. Dr. Josh Sanes and Dr. Brendan Lilley for precious advice and providing the various constructs and antibodies.

I am also deeply grateful to Bernd, Sally, Martin, Anja, Ines, Franziska, Klaus, Ivonne, Dayana and Fritz for excellent technical assistance, and the staff of the animal facility at the Max Planck Institute of Experimental Medicine for maintenance of the mouse colony.

Further, I would like to acknowledge the support of all members of the molecular neurobiology department throughout my PhD life: Specially the support of Michiko, Ramya, Christoph Bredack, Tolga, Ben, Matthieu, Rieke, Mirinalini, Noa, Aleksandra, Sonja, Kerstin, Thea, Christoph Biesemann and Marilyn.

I had the privilege of supervising Nadia Mitova as my Lab rotation student, and I would like to acknowledge her support for the characterization of WWP2 in the cultured neuron.

I am also deeply appreciative of the emotional support of my parents and my sister.

Finally and most importantly, I am grateful to my husband, who has supported me immensely, despite being so far away.



## Abstract

Posttranscriptional modification of proteins through the ubiquitin pathway has recently emerged as an essential regulatory mechanism controlling neuronal development and function. WW domain-containing protein-1 and -2 (WWP1 and WWP2) are evolutionarily conserved HECT type E3 ubiquitin ligases in eukaryotes, and the *C. elegans* ortholog of WWP1/2 plays key roles in neuronal functions such as axon guidance and synaptic transmission. In the mammalian brain, however, the functions of WWP1/2 have never been explored and their substrates are unknown. In this study, I discovered a novel function of mammalian WWP1/2 in the developing brain. In analyses of brain specific conditional WWP1/2 deficient mice *in vivo* and *in vitro*, I found that WWP1/2 are critical for the establishment of neuronal polarity - the specification of a single axon and multiple dendrites, which is an essential step during neuronal development. I also show that SAD-A kinase, which is required for neuronal polarization in the cerebral cortex, is ubiquitinated by WWP1/2. Thus I propose that WWP1/2 contribute to neuronal polarization, probably by regulating the SAD kinase signaling pathway. Furthermore, I screened for binding proteins of WWP1/2 in the brain and identified WWP1/2 as specific E3 ligases for the synaptic scaffold proteins liprin- $\alpha$ 3 and shank1a. These findings are consistent with the synaptic localization of WWP1/2 in mature neurons and indicate that WWP1/2 may be involved in synaptic transmission and synaptogenesis. Together, my findings show that WWP1/2 plays multiple roles in neuronal development and synaptic function in the mammalian brain.

# Table of Contents

<b>1</b>	<b>Introduction.....</b>	<b>12</b>
<b>1.1</b>	<b>Nerve cell development in the mammalian brain .....</b>	<b>12</b>
1.1.1	<i>Neural proliferation, neurogenesis and gliogenesis .....</i>	16
1.1.2	<i>Neuronal migration.....</i>	16
1.1.3	<i>Neuritogenesis.....</i>	17
<b>1.2</b>	<b>Ubiquitination .....</b>	<b>19</b>
<b>1.3</b>	<b>HECT type ubiquitin E3 ligases—WWP1 and WWP2.....</b>	<b>22</b>
1.3.1	<i>WWP1 and WWP2 are members of the Nedd4 family of HECT type ubiquitin E3 ligases.....</i>	22
1.3.2	<i>WWP1 and WWP2 regulate cell signaling in mammals .....</i>	23
1.3.3	<i>Nedd4 family E3 ligases in mammalian neuronal development .....</i>	24
1.3.4	<i>Diverse roles of C. elegans WWP1 .....</i>	25
<b>1.4</b>	<b>Aim and outline of the present study: An analysis of the role of WWP1 and WWP2 in nerve cell development and function.....</b>	<b>30</b>
<b>2</b>	<b>Materials and Methods.....</b>	<b>33</b>
<b>2.1</b>	<b>Animals.....</b>	<b>33</b>
<b>2.2</b>	<b>Reagents and DNAs.....</b>	<b>33</b>
2.2.1	<i>Chemicals and reagents .....</i>	33
2.2.2	<i>Kits .....</i>	35
2.2.3	<i>Bacterial strains and yeast strain .....</i>	36
2.2.4	<i>cDNA libraries .....</i>	36
2.2.5	<i>Vector plasmids .....</i>	36
2.2.6	<i>Oligonucleotides .....</i>	37
2.2.7	<i>Antibodies .....</i>	39
<b>2.3</b>	<b>Molecular biology .....</b>	<b>41</b>
2.3.1	<i>Electroporation of plasmid DNA into competent bacterial cells .....</i>	41
2.3.2	<i>Plasmid DNA preparation (Miniprep, Midiprep, and Maxiprep) .....</i>	42
2.3.3	<i>Determination of DNA concentration .....</i>	42
2.3.4	<i>Sequencing of DNA .....</i>	42
2.3.5	<i>DNA digestion with restriction endonucleases .....</i>	42
2.3.6	<i>Dephosphorylation of 5' DNA-ends.....</i>	43
2.3.7	<i>DNA ligation .....</i>	43
2.3.8	<i>Ethanol precipitation of DNA .....</i>	43
2.3.9	<i>Agarose gel electrophoresis .....</i>	43
2.3.10	<i>Agarose gel extraction of DNA fragments .....</i>	44
2.3.11	<i>Polymerase chain reaction (PCR).....</i>	44
2.3.12	<i>Subcloning in TOPO pCR vectors.....</i>	44



2.3.13	<i>Cloning strategies for constructs generated and used in this study</i>	45
<b>2.4</b>	<b>Yeast two-hybrid (YTH) screening</b>	<b>47</b>
2.4.1	<i>Media, buffers, and stock Solutions used in YTH screening</i>	47
2.4.2	<i>Generation of bait constructs for YTH screening</i>	49
2.4.3	<i>Transformation of DNA into yeast</i>	50
2.4.4	<i>Selection of bait constructs for screening</i>	50
2.4.5	<i>Screening</i>	51
2.4.6	<i>Extraction of plasmid DNA from yeast</i>	51
2.4.7	<i>Identification of the intracting cDNA clones</i>	51
<b>2.5</b>	<b>In situ hybridization (ISH)</b>	<b>52</b>
2.5.1	<i>Molecular cloning for ISH probes</i>	52
2.5.2	<i>PCR reaction to generate template DNAs for ISH probe synthesis</i>	52
2.5.3	<i>Transcriptional labeling of RNA probes</i>	52
2.5.4	<i>Tissue preparation</i>	52
2.5.5	<i>Hybridization and Detection</i>	53
<b>2.6</b>	<b>Biochemical experiments</b>	<b>53</b>
2.6.1	<i>Protein assay</i>	53
2.6.2	<i>Sodium dodecyl sulfate polyacrylamide gel electrophoresis (SDS-PAGE)</i>	54
2.6.3	<i>Western blotting</i>	54
2.6.4	<i>Purification of recombinant GST-fusion proteins</i>	55
2.6.5	<i>Antibodies against WWP1 and WWP2 generated in this study</i>	56
2.6.6	<i>Subcellular fractionation of rat brains</i>	57
2.6.7	<i>Affinity purification of GST-WWP1/2 binding proteins</i>	58
2.6.8	<i>Protein identification by mass spectrometry</i>	58
2.6.9	<i>In Vitro ubiquitination assays</i>	59
<b>2.7</b>	<b>Cell cultures</b>	<b>60</b>
2.7.1	<i>Media and solutions</i>	60
2.7.2	<i>Treatment of coverslips for culturing primary neurons</i>	60
2.7.3	<i>Mouse neuronal cultures</i>	60
2.7.4	<i>Rat neuronal cultures</i>	61
2.7.5	<i>HEK 293FT cell line</i>	62
2.7.6	<i>Transfection</i>	62
2.7.7	<i>Lenti-virus production and infection</i>	62
<b>2.8</b>	<b>In utero electroporation</b>	<b>63</b>
<b>2.9</b>	<b>Immunocytochemistry (ICC)</b>	<b>64</b>
<b>2.10</b>	<b>Immunohistochemistry (IHC)</b>	<b>64</b>
<b>2.11</b>	<b>Nissl staining</b>	<b>65</b>
<b>2.12</b>	<b>Image analysis and statistics</b>	<b>65</b>

<b>3</b>	<b>Results</b> .....	<b>68</b>
3.1	Largely overlapping distribution of WWP1 and WWP2 in the brain.....	68
3.2	Subcellular localization of WWP1 and WWP2 in neurons.....	71
3.2.1	Axonal localization of WWP1 and WWP2 in developing neurons.....	71
3.2.2	Synaptic localization of WWP1 and WWP2 in neurons.....	73
3.3	Generation of neuron specific WWP1 and WWP2 conditional KO mouse lines.....	76
3.4	The effect of WWP1 and WWP2 deficiency on axon specification.....	80
3.5	WWP1 and WWP2 are required for polarity formation in developing cortical neurons <i>in vivo</i> .....	87
3.6	Identification of WWP1 and WWP2 interacting proteins in the mammalian brain.....	94
3.6.1	Affinity purification of WWP1- and WWP2-binding proteins from synaptosomes.....	94
3.6.2	Liprin- $\alpha$ 3 is a specific ubiquitination substrate of WWP1 and WWP2.....	95
3.6.3	Ubiquitination of SAD kinase by WWP1 and WWP2.....	95
3.6.4	Yeast two-hybrid screening for proteins interacting with WWP1 and WWP2.....	100
3.6.5	Shank1a is identified as a WWP1 binding protein.....	102
3.6.6	Shank1a is a ubiquitination substrate of WWP1 and WWP2.....	103
<b>4</b>	<b>Discussion</b> .....	<b>108</b>
4.1	WWP1 and WWP2 regulate axon specification and neuronal polarity formation.....	108
4.1.1	Molecular pathways involved in neuronal polarization <i>in vivo</i> .....	109
4.1.2	LKB1-SAD pathway and WWP1/2.....	110
4.1.3	TGF $\beta$ signaling and WWP1/2.....	112
4.2	Role of WWP1 and WWP2 in synaptic function.....	115
4.2.1	Liprin- $\alpha$ 3 and WWP1/2.....	115
4.2.2	SAD-A and WWP1/2.....	116
4.2.3	Shank1a and WWP1/2.....	117
<b>5</b>	<b>References</b> .....	<b>121</b>
	Curriculum vitae.....	133

## Abbreviations

aa	Amino acid
AMP	Adenosine monophosphate
ATP	Adenosine triphosphate
AZ	Presynaptic active zone
bp	Base pairs
<i>C. elegans</i>	Caenorhabditis elegans
CNS	Central nervous system
Cre	Cre recombinase
CSV	Clude synaptic vesicle
DKO	Double knockout
DNA	Deoxyribonucleic acid
dNTPs	Deoxynucleosides triphosphate
<i>E. coli</i>	Escherichia coli
E1	Ubiquitin activating emzyme
E2	Ubiquitin conjugating emzyme
E3	Ubiquitin ligase
EGFP	Enhanced green fluorescent protein
GABA	$\gamma$ -aminobutirric acid
GDP	Guanosine diphosphate
GFP	Green fluorescent protein
GTP	Guanosine triphosphate
HECT	Homologous-to- E6-AP-C-terminus
kDa	Kilo Dalton
KO	Knockout
mRNA	Messenger RNA
NMDA	N-methyl-D-aspartate
RING	Really-Interesting-New-Gene
SEM	Standard error of the mean
SS	Synaptic soluble cytoplasm
SV	Synaptic vesicle
TGF	Transforming growth factor
WT	Wildtype

# **1 Introduction**

## **1.1 Nerve cell development in the mammalian brain**

The brain is a complex organ, which controls vision, hearing, somatic sensation, olfaction, taste, memory, learning and other activities based on the function of the neuron. Neurons are highly specialized for processing and transmitting intracellular and intercellular signals. With their long extended axons and elaborate dendritic arbor, neurons establish a directional flow of information transfer. Synaptic inputs are received at dendrites, integrated toward the cell body, conducted along the axon and converted to synaptic outputs at the axon terminals (Fig. 1-1). The brain contains billions of neurons (the adult human brain contains approximately 100 billion neurons [Shariff, 1953; Lange, 1975]), of which every neuron forms on average 1,000–10,000 synaptic contacts. This allows communication between each neuron by transmitting information through the synapse. Despite this vast complexity, the resulting neuronal networks that control information processing in the brain are highly ordered. The controlled development of individual neurons is of crucial importance for proper network formation in the brain.

Sequentially, the five key steps of nerve cell development are as follows: first, proliferation of neuronal progenitors (neural proliferation); second, the generation of neurons from progenitor cells (neurogenesis); third, their migration to the appropriate target sites (neuronal migration); fourth, their differentiation into extensively arborized cells (neuritogenesis); and fifth, their integration into functional networks through synapse formation and refinement (synaptogenesis and synapse elimination) [Barnes and Polleux, 2009] (Fig. 1-2 and 1-3). Numerous external cues and intracellular signaling processes are tightly regulated in all five key steps.

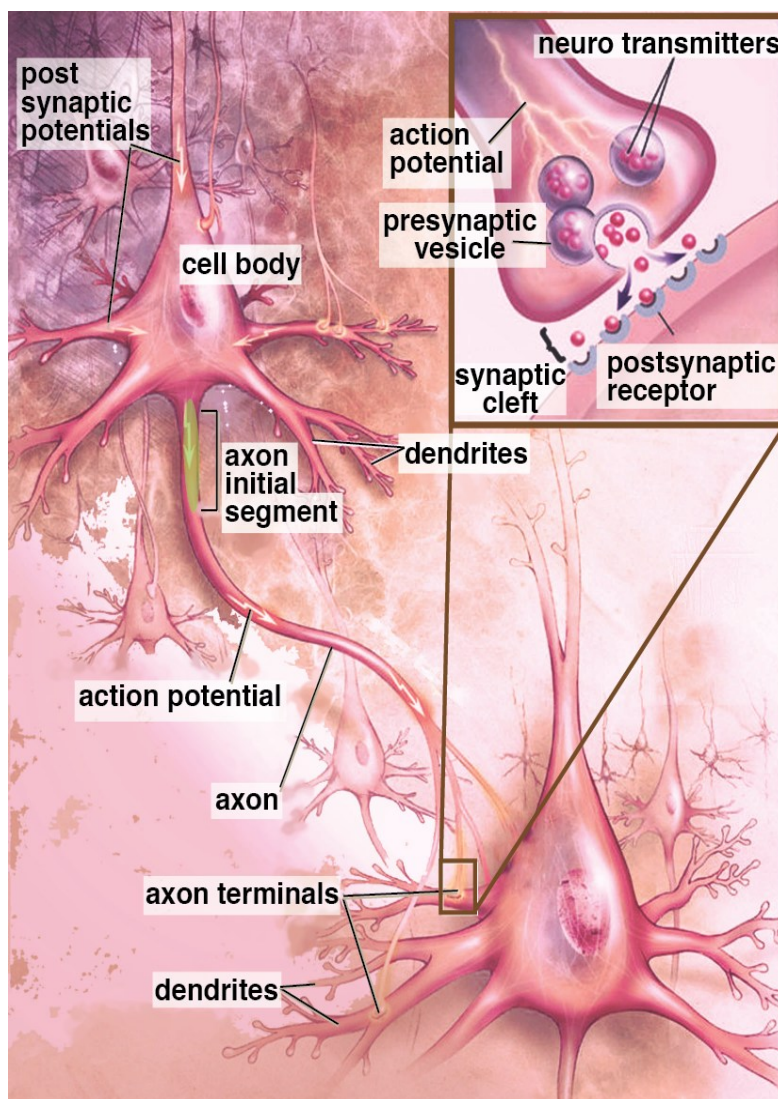


**Figure 1-1 Neuronal polarity and function**

Neurons consist of a cell body, a single axon and multiple dendrites. The dendrites show highly branched structures covering the large field in the brain while the axon shows a less branched and prolonged structure. The neurotransmitter receptors at the dendrite mediate the influx of extracellular ions toward the cytoplasm, which triggers the postsynaptic potential. Once the postsynaptic potentials reach to the threshold, the axon initial segment generates the action potential. The axon transduces this potential like an electrical cable, which can be even thousands times longer than the cell body size. The axonal terminal contains a specialized architecture where the neurotransmitter is released to the synaptic cleft in response to the action potential. Such uni-directed information transfer from the dendrite to the axonal terminal is achieved by the highly polarized structure of individual neurons. Original illustration was quoted from [www.alz.org](http://www.alz.org). (Alzheimer's Association).

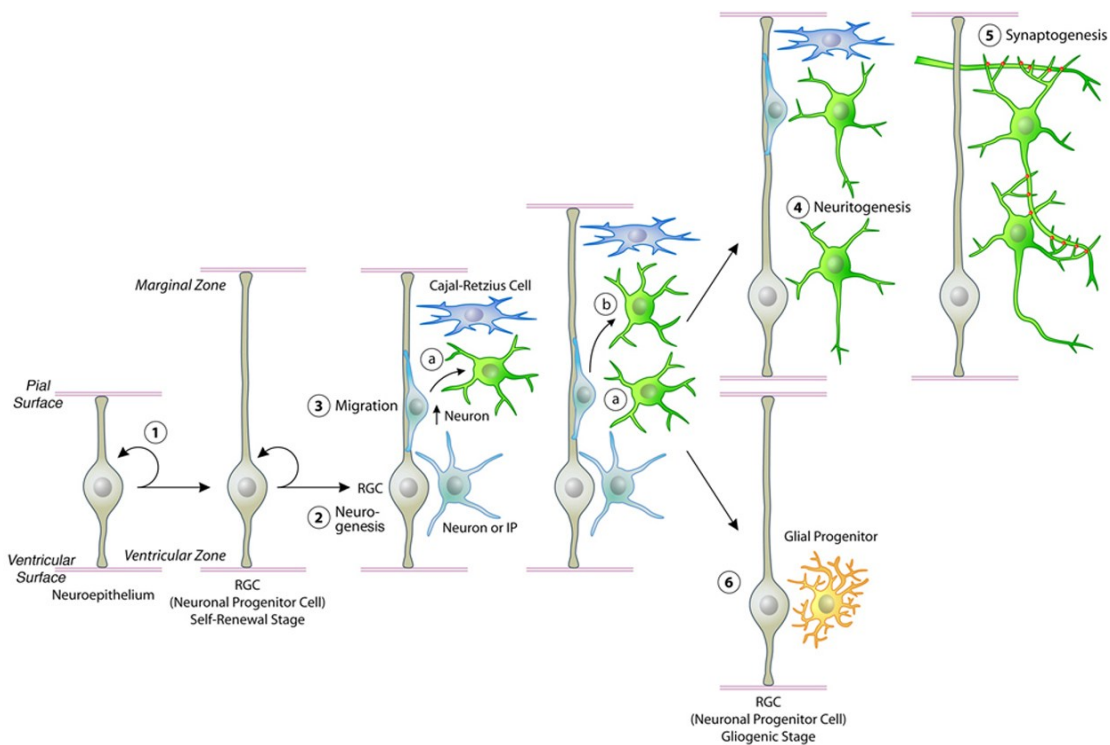


**Figure 1-2 Key steps of neuronal differentiation in the mammalian brain**

Neuroepithelial cells and radial glia cells (RGCs) expand themselves by symmetric cell division (1). Premature neurons or intermediate progenitors (IPs) are generated upon asymmetric division of Neuroepithelial cells and RGCs(2). Cajal-Retzius cells are generated ectopically at the lateral in the very early stage of neurogenesis and migrate tangentially towards the marginal zone. Radial glia cells sustain the potential to differentiate to premature neurons, IPs, and glial progenitors (oligodendrocytes and astrocytes). New neurons migrate along radial glia cell processes (3) until they receive a signal from Cajal-Retzius cells, after which they distribute horizontally in the cortical plate (a). Later migrating neurons go further towards the marginal zone (b). During migration, neurons begin to differentiate, generating two major processes, the future axon and the future main dendrite shaft. Subsequently, the neurons further extend their processes (4) and generate ordered networks by regulated synaptogenesis and synapse elimination (5). Soon after the neurogenesis stage, RGCs start to generate glial progenitors (6). The pink lines in the individual panels indicate the pial (top) and ventricular (bottom) surface, respectively. RGC, radial glia cell; IP, intermediate progenitor cell.

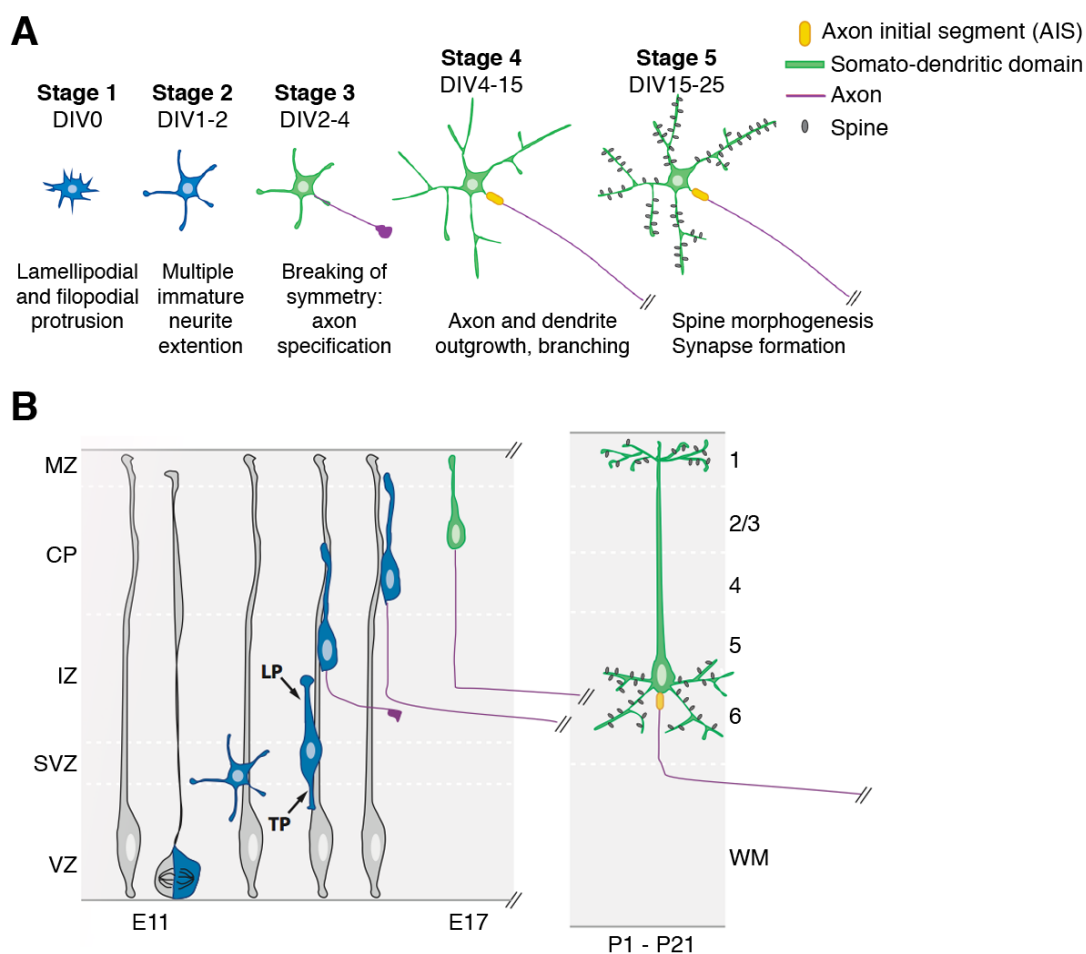


**Figure 1-3 Neuronal polarization during development *in vitro* and *in vivo***

(A) Cultured neurons pass through defined developmental stages. At stage 1, neurons form lamellipodia and filopodia. At stage 2, multiple immature neurites form from filipodia. At stage 3, a single neurite acquires axon identity and grows rapidly. Stage 4 involves rapid axon and dendrite growth, and in stage 5 the neuron is fully differentiated.

(B) Cortical neurons *in vivo* migrate along radial glia cells, forming a leading (LP) and a tailing processes (TP), which form the basis for dendrite-axon polarity. Final differentiation occurs in the first postnatal weeks in rodents.

Original illustration was quoted from *Annu. Rev. Neurosci.* 2009. 32: 347/81 [Barnes and Polleux, 2009].

### **1.1.1 Neural proliferation, neurogenesis and gliogenesis**

Three main types of neuronal progenitors have been identified in the embryonic neocortex: neuroepithelial cells, radial glial cells and intermediate progenitors. At the ventricular zone before neurogenesis (mouse embryonic day 9–11 [E9–E11]), neuroepithelial cells proliferate by symmetric cell division and subsequently generate neurons by asymmetric division. After the onset of neurogenesis (E11–E17), neuroepithelial cells give rise to a distinct yet related cell type, radial glial cells. Radial glial cells normally proliferate by symmetric cell division and undergo asymmetric division to generate one radial glial cell and one neuron [Anthony et al., 2004]. Besides radial glial cells, another type of neuronal progenitor, namely intermediate progenitor cells, appear at the onset of neurogenesis. Intermediate progenitor cells are distinguished from neuroepithelial and radial glial cells. Each intermediate progenitor cell symmetrically divides only once to generate two post-mitotic neurons in the subventricular zone, a more apical part of the developing cortex [Noctor et al., 2004; Hevner et al., 2006; Sessa et al., 2008; Noctor et al., 2008]. Moreover, the gliogenesis of astrocytes and oligodendrocytes occurs mostly in the postnatal stages of the developing cortex [Richardson et al., 2006].

### **1.1.2 Neuronal migration**

In the developing cortex, newly generated neurons migrate along the radial glial cells from their origin in the ventricular or subventricular zones towards the cortical plate. This migration is under the guidance of secreted cues from Cajal-Retzius cells. Upon cell cycle exit through asymmetric cell division in the ventricular or subventricular zones, post-mitotic neurons rapidly form multiple processes. One major process is formed in the radial direction and becomes a leading process before the neuron initiates radial migration along the radial glial process. The migrating neuron leaves a trailing process behind the cell body. Once



neurons receive the Reelin signal from the Cajal-Retzius cells at the top of the cortical plate, they translocate their cell body ventrally as neurons born at later stages bypass their predecessors (the inside-out accumulation pattern) [Noctor et al., 2004].

### **1.1.3 Neuritogenesis**

During migration, neurons develop protrusions or neurites that will ultimately become axons and dendrites. Cortical pyramidal neurons acquire their axon-dendrite polarity from the polarized emergence of the trailing and leading processes during migration. The cell body continues to translocate toward the final destination in the cortical plate, while the axon rapidly elongates toward the intermediate zone. The leading process gives rise to the apical dendrite, which initiates local branching in the marginal zone. Axons begin to invade the target area close to birth and elaborate their arbors so they innervate specific target cells over the subsequent 2–3 weeks. Concurrently, dendrites form complex arbors that connect with axons of other neurons [Barnes and Polleux, 2009]. This neuritogenesis is critical for the formation of functional neuronal networks in the brain.

### **1.1.4 Synaptogenesis and synapse elimination**

Following neuritogenesis, brain development culminates in synaptogenesis, by which functional neuronal networks are generated. Following the establishment of nascent synaptic contacts between axons and their target dendrites, they mature into fully functional synapses. This highly coordinated maturation process, during which hundreds of specific proteins are sorted to the pre- and postsynaptic compartments, is controlled by synapse organizing signals such as cell adhesion proteins or trans-synaptic signaling processes [Margeta and Shen, 2010]. In the mature synapse, a presynaptic transmitter release site or active zone (AZ) is exactly apposed to a postsynaptic signal-receiving compartment, the postsynaptic density (PSD). AZs

and PSDs contain distinct sets of adhesion and scaffolding proteins that are required for the proper equipment of the synapse with presynaptic components of the transmitter release machinery and postsynaptic transmitter receptors and signaling proteins. Given that most synapses in the mammalian forebrain are generated after birth, the activity in the developing neuronal network also has a strong influence on synaptogenesis. In many organisms, particularly in vertebrates, synaptogenesis is paralleled and followed by a process of synapse elimination, which is of crucial importance for the refinement and specification of synaptic connectivity. For example, in the mammalian brain, up to 50% of all initially generated synapses are eliminated in later brain development [Huttenlocher et al., 1982; Zecevic et al., 1991]. Like synaptogenesis, synapse elimination is critically dependent upon synaptic activity.

Although these processes mostly occur in a temporally coordinated and successive manner, the various stages of nerve cell development are partially interdependent. For example, dendrite development is directly influenced by synaptic inputs, and dendrite complexity affects the total number of synapses made by a given neuron [Parrish et al., 2007; Spruston et al., 2008]. Likewise, the guiding cues and signaling processes that control neuronal development are characterized by substantial crosstalk at multiple levels [O'Donnell et al., 2009; Sanes and Yamagata, 2009; Marin et al., 2010]. Subsequently, these guidance and signaling processes are controlled by various intracellular regulatory mechanisms. Among these, ubiquitin-dependent functional modification and/or degradation of signaling proteins has recently emerged as an important process and a thus far underestimated regulatory principle in nerve cell development.

## 1.2 Ubiquitination

Ubiquitination is a post-translational modification of proteins, related to phosphorylation, acylation, alkylation and many other related processes that modify proteins after their translation. Ubiquitination is a multistep process requiring the hierarchical activity cascade of three enzyme classes: ubiquitin-activating (E1), ubiquitin-conjugating (E2) and ubiquitin ligase (E3) enzymes. E3 ligases, the final effectors of the cascade, can append a 76-amino-acid-long ubiquitin to substrate proteins either as a single moiety (monoubiquitination), a double moiety (diubiquitination), or chains of ubiquitin (polyubiquitination). Approximately 600 E3 ligase isoforms are encoded in the human genome [Li et al., 2008] and are classified as Really-Interesting-New-Gene type ligases (RING Finger E3 ligases) or Homologous-to-E6-AP-C-Terminus type ligases (HECT type E3 ligases). The genomes of higher vertebrates encode only one or two E1, and ~30 E2 enzymes, and given that E3 ligases recognize substrates via specific protein-protein interactions, E3 ligases are the main determinants of the substrate specificity of ubiquitination processes.

While all seven ubiquitin lysine residues can be used for ubiquitin chain formation, K48-linked chains have long been thought to represent the major polyubiquitin variant in eukaryotic cells. However, recent studies showed that K11-linked and K63-linked polyubiquitin chains, with poorly understood functions, are similarly abundant [Xu et al., 2009]. The chain type specificity solely depends on the E2 enzyme for RING Finger ligases, whereas protein domains C-terminal to the HECT domains are critical determinants of the ubiquitin chain types generated by HECT type ligases [Kim et al., 2009]. Initially, the focus of research on protein ubiquitination had been on proteasome-dependent degradation of polyubiquitinated cytosolic proteins (the ubiquitin proteasome system). Since the 1990s, a flurry of studies has shown that protein ubiquitination (e.g. mono- and diubiquitination) does not necessarily control proteasomal protein degradation, but also influences many other

cellular processes including cell surface expression of membrane proteins, endocytosis, protein interactions and protein function (Fig. 1-4) [Hicke et al., 2001].

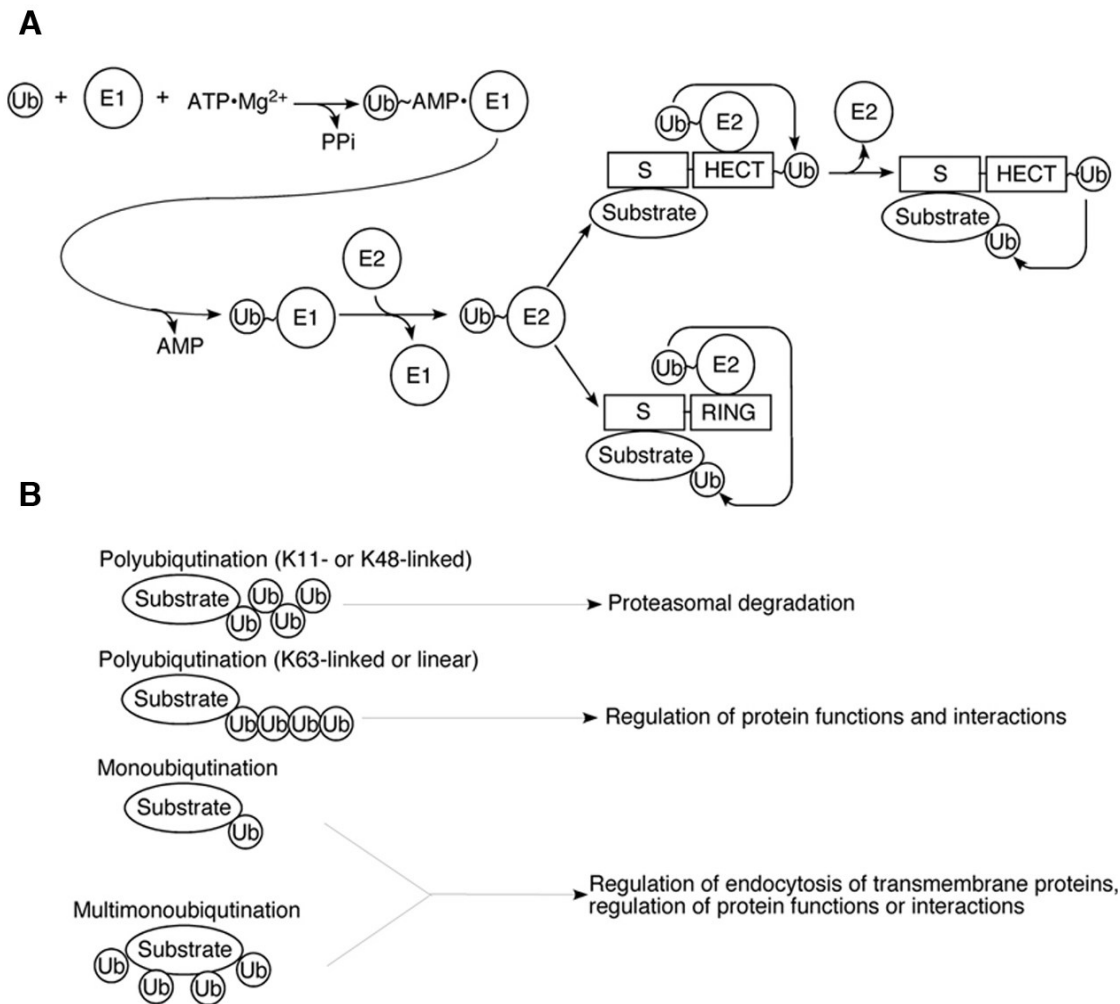


**Figure 1-4 The protein ubiquitination pathway.**

(A) Ubiquitination is a sequential reaction mediated by three classes of enzymes (E1, E2, and E3). A ubiquitin activating enzyme (E1) is conjugated with a free ubiquitin moiety through a thioester bond. This reaction uses ATP·Mg<sup>2+</sup> to form a ubiquitin adenylate intermediate, which is a conjugate of ubiquitin and AMP via a high-energy covalent bond (~). This intermediate is first coupled to the E1 through a non-covalent bond (•). Ubiquitin activated in this manner is then transferred to a cysteine residue of the E1 enzyme. Active ubiquitin conjugated to the E1 enzyme through a high-energy thioester bond (~) is subsequently transferred to a ubiquitin conjugating enzyme (E2), which, in turn, is recognized by a ubiquitin ligase (E3), of which there are two major types, HECT type and RING

finger type ligases. HECT type ligases receive the active ubiquitin from the E2 enzyme, bind it covalently via a cysteine residue in the HECT domain, and subsequently transfer it to a lysine residue in the ultimate ubiquitination substrate protein, which is recognized by the substrate recognition domain of the E3 ligase (S). By contrast, the RING finger type ligases transfer the active ubiquitin directly from the E2 enzyme to the ultimate ubiquitination substrate protein without forming a covalent bond. The human genome encodes two E1, approximately 30 E2, and about 600 E3 enzymes. HECT, Homologous-to-E6-AP-C-Terminus; RING, Really-Interesting-New-Gene. (B) Functional consequences of protein ubiquitination. K48-linked polyubiquitin (polyUb) chains and likely also K11-linked polyUb chains are directly recognized by the proteasome. K63-linked polyUb chains and also head-to-tail-linked linear polyUb chains regulate protein function. Monoubiquitination or multi-monoubiquitination regulate the function or endocytosis of many proteins.

---

That the process of ubiquitination and the ubiquitin proteasome system play a key role in brain development was first indicated by the discovery of the ubiquitin carboxy-terminal hydrolase PGP 9.5 in the somata and dendrites of differentiating neurons in rat embryos [Wilkinson et al., 1989; Kent and Clarke, 1991]. Since then, the analysis of ubiquitination in the developing and mature brain has become a major new focus in neuroscience, not least because ubiquitination seems to play a key role in neurodegenerative disorders [Lowe et al., 1988; Lennox et al., 1988; Tai et al., 2008]. Thus, understanding the molecular mechanisms of the various phases of nerve cell development and differentiation, which are coordinated by ubiquitination, is of substantial importance for our understanding of normal brain development and function as well as the corresponding pathological disorders.

### 1.3 HECT type ubiquitin E3 ligases—WWP1 and WWP2

#### 1.3.1 WWP1 and WWP2 are members of the Nedd4 family of HECT type ubiquitin E3 ligases

WW domain-containing protein-1 and -2 (WWP1 and WWP2) are evolutionarily conserved E3 ligases in eukaryotes and play important roles in the regulation of diverse cellular functions (i.e. protein degradation, endocytosis, vesicular transport and transcription) [Molbert-Colas et al., 2003; Ingham et al., 2004; Zhang et al., 2004; Li et al., 2008]. WWP1 and WWP2 were originally identified as novel human proteins based on their WW domains, 35–40 amino acid regions with two highly conserved tryptophans. This domain exhibits a high affinity towards proline rich motifs such as PPxY, LPxY, PPLP, or PxxP motifs (where x indicates any amino acid, and P, Y and L indicate proline, tyrosine and leucine, respectively) [Pirozzi et al., 1997]. WWP1 and WWP2 share a characteristic domain organization with Nedd4 family HECT type E3 ligases, which consists of an N-terminal C2, two to four WW domains, and a C-terminal catalytic HECT domain [Ingham, 2004](Fig. 1-5). The C2 domain of Nedd4 family E3 ligases binds to phospholipids in a calcium-dependent manner and mediates intracellular targeting to the cell membrane [Dunn, et. al., 2004, Plant, et. al., 2000]. This domain also mediates protein-protein interactions, including the intramolecular interaction with the HECT domain that directs inhibition of the catalytic activity [Morrione, et. al., 1999, Wiesner, et. al., 2007]. WW domains recognize phosphoserine- and phosphothreonine-containing proteins as well as proline-rich motifs [Chen and Sudol, 1995, Gallagher, et. al., 2006]. The HECT domain forms a thioester intermediate with a ubiquitin at a conserved cysteine residue in the C-terminal region and then transfers the ubiquitin to its substrates [Huibregtse, et. al., 1995]. The rodent Nedd4 family is composed of eight members: Nedd4-1 (Neuronal precursor cell expressed and developmentally downregulated protein 4-1), Nedd4-2, WWP1, WWP2, Itch, Smurf1 (Smad ubiquitination regulatory factor

1), Smurf2, and NEDL1 (Nedd4-like ubiquitin-protein ligase-1) [Ingham, 2004]. Among these, WWP1, WWP2, and ITCH contain four highly homologous tandem WW domains and compose the WWP1 sub-family.

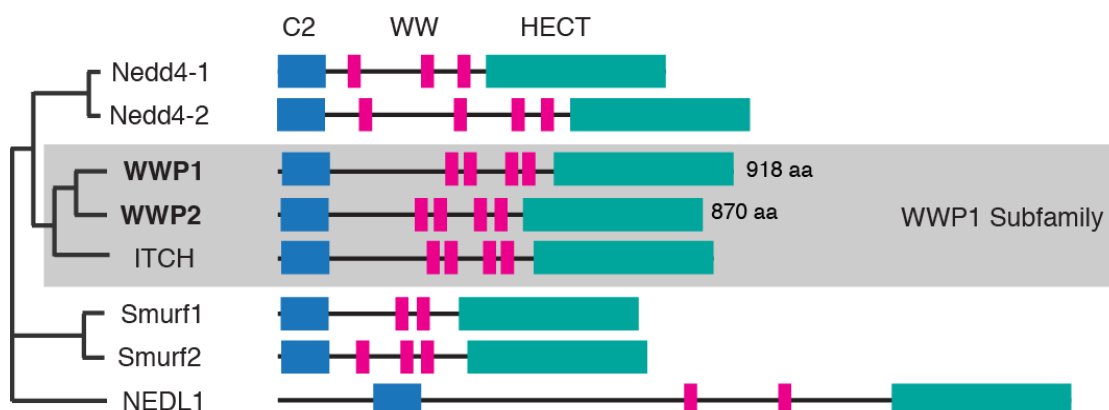


**Figure 1-5 The phylogenetic tree of Nedd4 family HECT type E3 ligases**

All enzymes share similar domain structures with an N-terminal C2 domain (blue boxes), multiple WW domains (magenta boxes), and a C-terminal HECT (homologous to E6-APcarboxyl terminus) domain (green boxes). C2 and WW domains recognize the substrates, while the HECT domain is essential for conjugation of the ubiquitin moiety to the substrates. WWP1 subfamily proteins, WWP1, WWP2, and ITCH are closely related with 80% identity at the amino acid level.

### 1.3.2 WWP1 and WWP2 regulate cell signaling in mammals

WWP1 and WWP2 are ubiquitously expressed in mammalian tissues and regulate diverse biological processes by targeting ubiquitination substrates [Ingham, et. al., 2004, Rotin and Kumar, 2009]. It has also been reported that WWP1 is involved in carcinogenesis in humans. The WWP1 gene is frequently amplified in human cancers including breast and prostate cancer, and RNA interference (RNAi) mediated down-regulation of WWP1 induces tumor cell growth arrest [Chen et al, 2007; Chen et al., 2009]. WWP1 over-expression negatively regulates two distinct tumor suppressor pathways, p53 and transforming growth factor-beta (TGF $\beta$ ) signaling [Chen et al, 2007; Laine et al., 2006; Peschiaroli al., 2010].

WWP2-mediated ubiquitination is involved in the transcriptional regulation of

embryonic stem (ES) cells. This is achieved by maintaining expression levels of two key players in the pluripotent and self-renewing state of ES cells; a large subunit of RNA polymerase II, Rbp1, and the transcription factor Oct-4 [Li et al., 2007; Xu et al., 2009; Liao et al., 2010]. Although recent studies indicate the involvement of WWP1 and WWP2 in general cellular processes, the functions of these HECT type ligases in mammalian nerve cells have never been explored.

### **1.3.3 Nedd4 family E3 ligases in mammalian neuronal development**

All Nedd4 family members, including WWP1 and WWP2, are expressed in neurons or neuronal progenitor cells. Recent studies implicated the important roles of Nedd4 family E3 ligases in developing neurons. It was demonstrated that Nedd4-1, one of the most abundant HECT type E3 ligases in neurons, promotes the growth of developing dendrites by ubiquitinating the small GTPase, Rap2 [Kawabe et al., 2010]. In a complementary study, it was shown that Nedd4-1 promotes the branching of developing axons by ubiquitinating another target, the phosphatase PTEN [Drinjakovic et al., 2010]. Apart from Nedd4-1, additional work has shown that Smurf1 regulates axon specification by switching the substrate preference from the axon determinant protein PAR6 to an axonal growth inhibiting protein, the small GTPase RhoA [Cheng et al., 2011]. These studies demonstrate the central roles of Nedd4 family E3 ligases in promoting neuritogenesis. While there are distinct molecular pathways in the axon and dendrites, these E3 ligases could activate/inactivate specific proteins within each subcellular compartment by switching their substrate preferences. Although the functions of WWP1 and WWP2 in neurons have not been studied, it is likely that substrate-specific protein ubiquitination by WWP1 and WWP2 is also associated with neuronal development and function.



### 1.3.4 Diverse roles of *C. elegans* WWP1

The role of the *C. elegans* ortholog of WWP1 and WWP2 (CeWWP-1) has been studied extensively with RNA interference (RNAi) and genetic approaches. Down-regulation of CeWWP1 by RNAi causes defects in morphogenesis of the developing embryo [Huang et al., 2000], indicating that CeWWP-1 is essential for the later stages of embryogenesis. Independent of the early developmental function of CeWWP-1, the loss of *wwp-1* gene expression decreased stress resistance during adulthood. Loss of *wwp-1* function by RNAi or gene mutation reduces lifespan under high temperature or oxidative stress while *wwp-1* over-expression extends lifespan. It was shown that CeWWP-1 functions in the same pathway as the E2 ubiquitin-conjugating enzyme, UBC-18, to regulate diet-restriction-induced longevity [Carrano et al., 2009]. This may be explained by regulation of body fat storage by CeWWP-1 [ven Haaften et al., 2006; Ashrafi et al., 2003]. Apart from these CeWWP-1 functional studies in non-neuronal tissues, it has been reported that CeWWP-1 is expressed in cholinergic and GABAergic motor neurons and the central nervous system (nerve ring) where it plays several key roles in neuronal functions (i.e. normal acetylcholine neurotransmission, axonal guidance and fasciculation, and patterning of the ventral nerve cord) [McKay et al., 2003; Sieburth et al., 2005; Schmits et al., 2007; Hunt-Newbury et al., 2007; Ch'ng et al., 2008].

Among these reports, Josh Kaplan's group performed a large-scale RNAi screening of genes involved in synaptogenesis using green fluorescent protein-tagged SNB (GFP::SNB; synaptobrevin) as a marker for presynaptic nerve terminals. They detected significant GFP::SNB distribution changes in 11 mutant strains carrying loss-of-function mutations in genes including *wwp-1*, *arr-1* ( $\beta$ -Arrestin) and *osm-9* (transient receptor potential vanilloid channel). These genes had previously not been implicated in synaptic transmission in *C. elegans* or other organisms [Sieburth et al., 2005] (Fig. 1-6C). In a subsequent study, the same group systematically studied morphological changes of the presynaptic terminal in loss-of-function mutants of 24 genes related to synaptic transmission [Ch'ng et al., 2008]. They

quantified several parameters including the intensity and distance between the GFP::SNB punctate pattern and correlated this to loss-of-function mutants based on phenotypic changes (Fig. 1-6B). Expected correlations were shown between some mutants, for example, between *unc-13* and *unc-18*, and between *egl-8* and *pkc-1*. Both *unc-13* and *unc-18* have been identified as “uncoordinated” movement phenotypes. Unc-13 and Unc-18 proteins and their mammalian orthologs, Munc13 and Munc18, are presynaptic proteins and are all essential proteins for neurotransmitter release. *egl-8* (phospholipase C  $\beta$ ) and *pkc-1* (protein kinase C (PKC)  $\eta/\epsilon$ ) show striking defects in signal transduction through trimeric GTPases [Sieburth et al., 2007]. Unexpectedly, the authors found that CeWWP-1 has a functional correlation with two presynaptic AZ proteins: SAD-1, an ortholog of mammalian SAD-A and SAD-B protein kinases, and SYD-2, an ortholog of mammalian liprin- $\alpha$  (Fig. 1-6D). Apart from the presynaptic function of SAD kinase [Inoue et al., 2006], *C. elegans* SAD-1 kinase and mouse SAD-A/SAD-B kinases have been implicated in regulating the axo-dendritic polarity of neurons in worms and mice [Crump et al., 2001; Kishi et al., 2005; Bernes et al., 2007].

These genetic analyses of CeWWP-1 in *C. elegans* indicate that mammalian WWP1 and WWP2 may be involved in regulation of axon formation, synaptogenesis, or neurotransmission in the CNS.



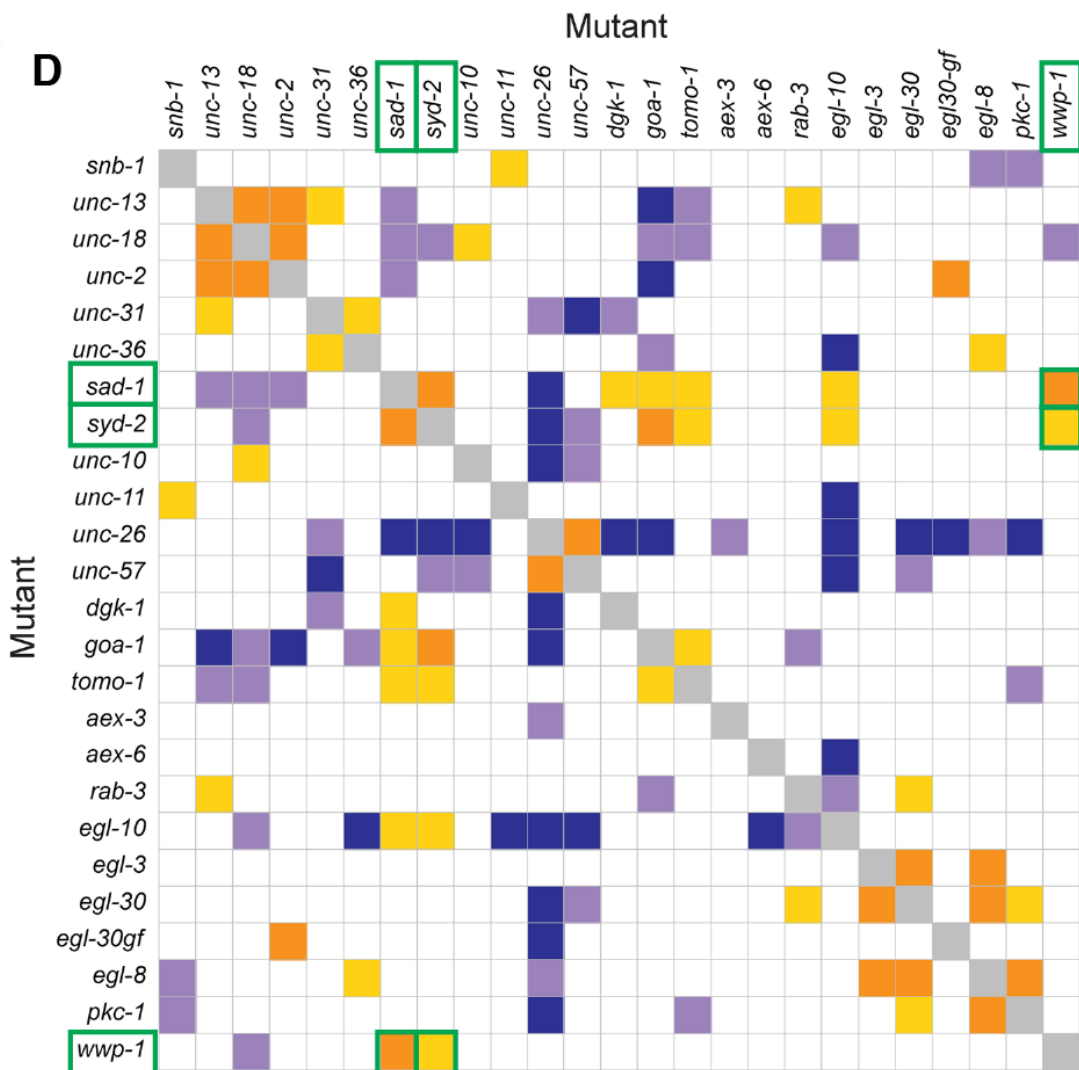
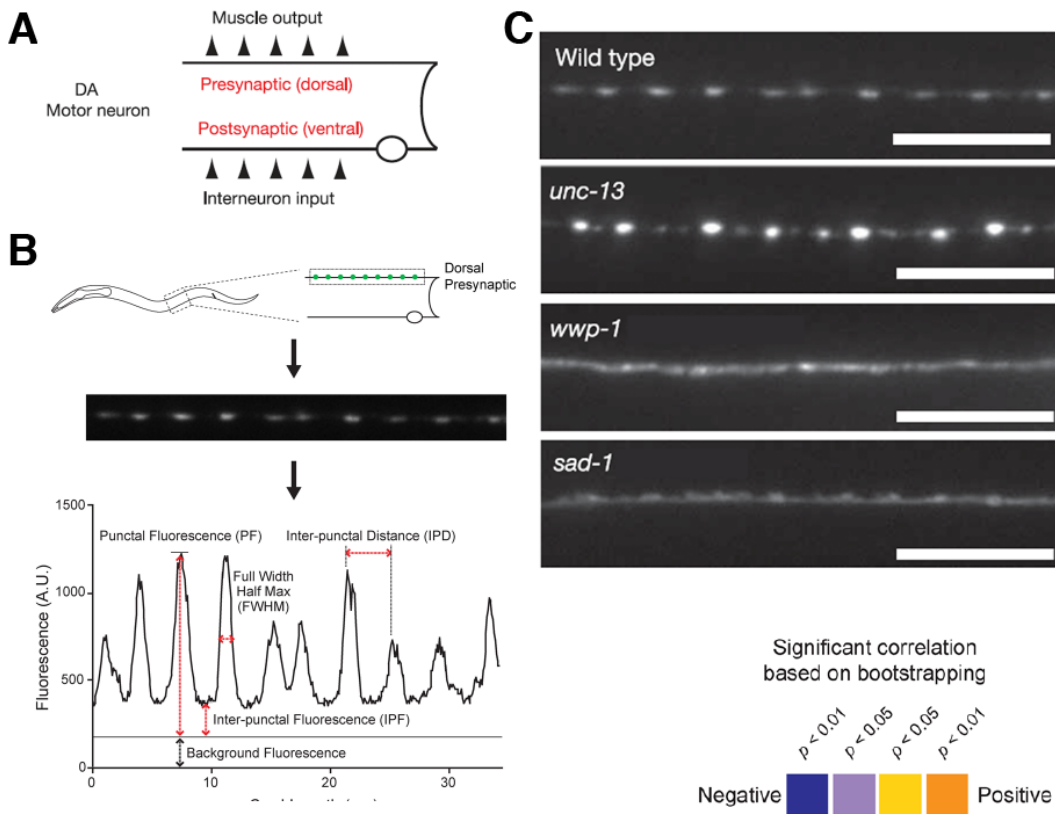


**Figure 1-6 Functional correlation of *sad-1*, *syd-2* and *wwp-1* genes in presynaptic synaptogenesis in *C. elegans*.**

(A) A DA motor neuron has the cell body in the ventral cord, where it receives synaptic inputs. This neuron projects the axon toward the dorsal side of the body wall, where it forms the neuromuscular junction (NMJ).

(B) Top: the scheme of imaging of the presynaptic terminal of the DA neuron expressing SNB-1 synaptobrevin (GFP::SNB-1). Middle: an example of the fluorescence image of GFP::SNB-1 in wild type animals. Each punctum represents the presynaptic terminal at the NMJ. Bottom: a trace representing pixel fluorescence values along the axon. Parameters analyzed in this study are indicated.

(C) Example fluorescence images of GFP::SNB-1 in wild type, *unc-13*, *wwp1*, and *sad-1* loss-of-function mutant animals. Note that *wwp-1* and *sad-1* mutants showed similarly diffused signals along the dorsal axon while *unc-13* mutant show stronger punctate signals than wild type [Sieburth et al., 2005].

(D) Correlations between the phenotypic profiles of mutants analyzed as in (B) [Ch'ng et al., 2008]. Pairwise Pearson's Correlation Coefficients were calculated between all mutations tested, with significant positive or negative correlations indicated by shaded boxes according to the legend.

Images taken from Sieburth et al. (2005) and Ch'ng et al. (2008).

## **1.4 Aim and outline of the present study: An analysis of the role of WWP1 and WWP2 in nerve cell development and function**

The present study was designed and performed with the aim of unveiling the roles of WWP1 and WWP2 E3 ligases in nerve cell development and function. More specifically, my first aim was to characterize the function of WWP1 and WWP2 in developing neurons *in vitro* and *in vivo* using knockout (KO) mice lacking WWP1 and WWP2 in neurons. The second aim was to identify their ubiquitination substrates that link to their characterized function.

### ***Outline of the study***

#### **1. Analysis of the expression profiles of WWP1 and WWP2 in the rodent brain and dissociated primary cultured neurons.**

I found that WWP1 and WWP2 are localized to the axons of developing neurons and to pre- and postsynapses in mature neurons.

#### **2. Establishment of a brain-specific conditional knockout mouse strain for WWP1 and WWP2 genes.**

Functional analysis of a gene-targeted mutant mouse is one of the most straightforward approaches to study gene functions *in vivo*. However, among the reported conventional KO mice lacking ubiquitously expressed E3 ligases, there are many cases of difficulty in analyzing gene functions in neurons *in vivo*. For example, mice homozygous for a loss-of-function mutation of the *Itch* gene develop a variety of inflammatory disorders, indicating that *Itch* has non-redundant functions in the immune response [Hustad et al., 1995; Perry et al., 1998]. My host lab generated *Nedd4-1* KO mice in which *Nedd4-1* gene expression is abolished. Homozygous KO embryos showed retarded development starting at E11.5 and died during late gestation around E16.5, indicating that *Nedd4-1* is an essential E3 ligase in

cellular functions [Kawabe et al., 2010; Cao et al., 2008; Fouladkou et al., 2008]. Mice with either Smurf1 or Smurf2 gene deletion did not show any overt embryonic phenotypic changes. However, those with a deletion of both genes display a failure of neuronal tube closure and only survive up to E10.5 [Narimatsu et al., 2009; Yamashita et al., 2005]. This indicates a functional redundancy between Smurf1 and Smurf2. Given the plastic nature of neurons in the brain, these severe non-neuronal defects could influence normal neuronal/brain functions. In order to study the function of WWP1 and WWP2 *in vivo*, specifically focusing on neuronal function, my supervisors Dr. Kawabe and Prof. Dr. Brose and I generated and established a conditional knockout mouse strain to inactivate WWP1 and WWP2 genes only in the brain.

### **3. Analysis of the conditional WWP1/WWP2 double KO neurons in culture**

I analyzed the morphology of developing neurons prepared from conditional double KO (DKO) mice and found that the neuronal polarity was disrupted in DKO neurons. Re-expressing of recombinant WWP2 in DKO neurons rescued the phenotype while the catalytically inactive mutant of WWP2 failed to rescue.

### **4. *In vivo* analysis of the brain-specific conditional WWP1/WWP2 DKO mice**

I determined the morphology and polarity of DKO neurons *in vivo* by an *in utero* electroporation technique. A severe polarity defect was observed in DKO neurons in the telencephalon.

### **5. Identification of brain-specific ubiquitination substrates of WWP1 and WWP2**

The pre- and postsynaptic scaffold protein liprin- $\alpha$ 3 (*C. elegans* SYD-2 homolog) was identified as a binding partner of WWP1 and WWP2 by affinity chromatography. I showed that liprin- $\alpha$ 3 and SAD-A kinase (*C. elegans* SAD-1 homolog) are ubiquitinated by WWP1 and WWP2 in an *in vitro* ubiquitination assay. I also identified the postsynaptic scaffold

protein shank1 as a binding partner of WWP1 via yeast two-hybrid screening. The shank1 protein was found to be ubiquitinated by WWP1 *in vitro*.



## 2 Materials and Methods

### 2.1 Animals

WWP1<sup>flx/flx</sup> mouse line and WWP2<sup>flx/flx</sup> mouse line were generated by Dr. Hiroshi Kawabe and Prof. Dr. Nils Brose according to the targeting strategy in Figure 14. The Nex-Cre mouse line originally generated by Dr. Goebbles and Prof. Dr. Klaus A. Nave [Goebbles et al., 2006] and the Emx1-Cre mouse line was originally generated by Gorski [Gorski et al., 2002]. All animals were used in compliance with guidelines for the welfare of experimental animals issued by the State Government of Lower Saxony (comparable to NIH guidelines).

### 2.2 Reagents and DNAs

#### 2.2.1 Chemicals and reagents

Acrylamide/ <i>N,N'</i> -Methylene-bis-Acrylamide (29:1)	BioRad
Agarose (UltraPure agarose)	Invitrogen
Alkaline phosphatase	Roche
Amid acids: adenine, uracil, L-tryptophan, L-histidine HCl, L-arginine, L-methionine, L-tyrosine, L-isoleucine, L-lysine HCl, L-phenylalanine, and L-leucine	Sigma-Ardrich
Ammonium persulfate (APS)	Sigma-Ardrich
Ampicillin	Invitrogen
Anti-DIG antibody conjugated with alkali phosphate	Roche
Aprotinin	Roche
Bacto-agar	DIFCO, BD
Bacto-casamino acids	DIFCO, BD
Bacto-peptone	DIFCO, BD
Bacto-yeast extract	DIFCO, BD
BM Purple	Roche
Boric acid (H <sub>3</sub> BO <sub>3</sub> )	Sigma-Ardrich
Bovine serum albumin (BSA), Fraction V	Pierce, Thermo
Comassie brilliant blue R250	BioMol Feinchemikalien

Darbecco modified eagle's medium (D'MEM)	Gibco, Invitrogen
Denhardt's solution (100x)	Sigma-Aldrich
Dextran sulfate	Sigma-Aldrich
DIG RNA labeling mix	Roche
Dimethyl sulfoxide (DMSO)	Sigma-Aldrich
Dionized formamide	Sigma-Aldrich
Dithiothreitol (DTT)	Sigma-Aldrich
DNA ladder mix sample, GeneRuler	Fermentas
DNaseI (RNase free)	Roche
dNTPs	GE Healthcare
Dry milk (skim milk)	Nestle
ECL reagent	Amersham, GE Healthcare
Ethanol	Sigma-Aldrich
Ethidium bromide (1% solution)	Carl Roth
Ethylene glycol tetraacetic acid (EGTA)	Sigma-Aldrich
Ethylenediaminetetraacetic acid (EDTA)	Sigma-Aldrich
FastGreen	Sigma-Aldrich
Glucose	Sigma-Aldrich
Glycerol	Sigma-Aldrich
Glycine	Sigma-Aldrich
Goat serum	Gibco, Invitrogen
HEPES	Sigma-Aldrich
Hydrochloric acid (HCl)	Sigma-Aldrich
IPTG	BioMol Feinchemikalien
Kanamycin	Invitrogen
Leupeptin	Roche
Luria Broth (LB)	Sigma-Aldrich
Methanol	Sigma-Aldrich
<i>N</i> -Ethylmaleimide (C <sub>6</sub> H <sub>7</sub> NO <sub>2</sub> , NEM)	Sigma-Aldrich
<i>N</i> ' <i>N</i> ' <i>N</i> '-tetramethylethyl enediamine (TEMED)	BioRad
Nonidet P40 (NP40)	Fluka
Opti-MEM I	Invitrogen
Phosphate buffered saline (PBS)	PAA Laboratories
PEG (3350)	Sigma-Aldrich
Pfu polymerase	Stratagene

Phenol	Carl Roth
Phenylmethylsulfonyl fluoride (PMSF)	Roche
Potassium acetate (CH <sub>3</sub> CO <sub>2</sub> K)	Sigma-Aldrich
Protein molecular weight standards	Invitrogen
Restriction endonucleases	New England Biolabs (NEB)
Salmon sperm DNA	Sigma-Aldrich
Sodium butyrate	Merck
Sodium chloride	Sigma-Aldrich
Sodium deoxycholate	Sigma-Aldrich
Sodium dodecyl sulfate (SDS)	Roche
Sucrose	Sigma-Aldrich
T4 DNA Ligase	Invitrogen
Taq-Polymerase (REDTaq)	Sigma-Aldrich, D4309
Tri-sodium citrate dihydrate	Sigma-Aldrich
Trichloromethane (Chloroform)	Sigma-Aldrich
Tris Base	Sigma-Aldrich
Triton X-100	Roche
Tween 20	Sigma-Aldrich
X-Gal	BioMol
Z-Leu-Leu-Leu-CHO (MG-132)	Boston Biochem

### 2.2.2 Kits

PureLink Quick Plasmid Miniprep Kit	Invitrogen
PureLink HiPure Plasmid Midiprep Kit	Invitrogen
PureLink HiPure Plasmid Maxiprep Kit	Invitrogen
EndoFree Plasmid Maxi Kit	QIAGEN
PureLink Gel Extraction Kit	Invitrogen
QuickChange II Site-Directed Mutagenesis Kit	Stratagene
Invisorb MSB spin PCRapace kit	Invitex
TOPO TA cloning Kit	Invitrogen
MEGAscript (SP6, T7) transcription kit	Ambion
BCA Protein Assay Kit	Thermo, Pierce
HiTrap NHS-activated HP	GE Healthcare

### 2.2.3 Bacterial strains and yeast strain

<i>E. coli</i> XL-1 Blue competent cells	Stratagene
<i>E. coli</i> Electro10-Blue competent cells	Stratagene
<i>E. coli</i> JM109 competent cells	Promega
<i>E. coli</i> TOP10 competent cells	Invitrogen
<i>E. coli</i> BL21DE3 competent cells	Stratagene
<i>E. coli</i> HB101 competent cells	Promega
<i>S. cerevisiae</i> PJ69-4A strain (James et al., 1996)	Invitrogen

### 2.2.4 cDNA libraries

Mouse Brain Quick-clone cDNA	Clontech (Cat. # 637301)
Mouse Liver Quick-clone cDNA	Clontech (Cat. # 637302)
Mouse brain prey library (constructed in pGAD-GL vector)	Provided by Dr. Hiroshi Kawabe
Rat brain prey library (constructed in pVP16-3 vector)	Provided by Prof. Dr. Nils Brose

### 2.2.5 Vector plasmids

pCR2.1 TOPO, pCRII TOPO	Invitrogen
pCR2.1-WWP1	Generated in this study
pCR2.1-WWP2	Generated in this study
pEGFP-C1, pEGFP-C2	Clontech
pEGFP-WWP1wt	Generated in this study
pEGFP-WWP2wt	Generated in this study
pEGFP-WWP1 C886S	Generated in this study
pEGFP-WWP2 C838S	Generated in this study
pCX-myrVenus	Provided by Dr. Anna-Katerina Hadjantonakis
pCl neo-Myc	Provided by Dr. Hiroshi Kawabe
pCl neo-Myc-WWP2 wt	Generated in this study
pCl neo-Myc-WWP2 C838S	Generated in this study
pFLAG-CMV2b	Provided by Dr. Hiroshi Kawabe
pGEX-4T-1	GE Healthcare Life Sciences
pGEX-WWP1 (1-150aa)	Generated in this study

pGEX-WWP1 (140-345aa)	Generated in this study
pGEX-WWP1 (335/582aa)	Generated in this study
pGEX-WWP2 (1-150aa)	Generated in this study
pGEX-WWP2 (140-300aa)	Generated in this study
pGEX-WWP2 (290-533aa)	Generated in this study
pF(syn)W-RBN	Provided by Dr. Hiroshi Kawabe
pF(syn)W-RBN-EGFP-WWP1wt	Generated in this study
pF(syn)W-RBN-EGFP-WWP2wt	Generated in this study
pFUGW	Salk Inst., Dr. Inder M. Verma
pFUGW-iCre	Provided by Dr. Richard L. Haganir
L21	Provided by Prof. Dr. Pavel Osten
PACK	Provided by Prof. Dr. Pavel Osten
ENV	Provided by Prof. Dr. Pavel Osten
pGAD424-HA	Clontech
pGBD-C2	Provided by Dr. Philip James
pVP16-3	Provided by Prof. Dr. Nils Brose
pFLAG-Liprin-a3	Provided by Dr. Hiroshi Kawabe
pFLAG-SAD-A	Provided by Prof. Dr. Joshua R. Sanes
pN1-Shank1a	Provided by Dr. Hans-Jürgen Kreienkamp
pRK5-HA-Ubiquitin	Provided by Dr. Hans-Jürgen Kreienkamp

### 2.2.6 Oligonucleotides

Oligonucleotide primers used in this study are listed below. They were synthesized in the MPI-EM DNA Core Facility on an ABI 5000 DNA/RNA Synthesizer. Restriction sites used for molecular cloning were underlined.

Primer #	Sequence	Rest. site
89	5'-TGTA AACGACGGCCAGT -3'	-
91	5'-AACAGCTATGACCATGATTACG -3'	-
9339	5'-GCGGCCGCGTCGACTCATTCTGCTTAAACTCTCTGGAG TACGGAAC -3'	Sall
9340	5'-GGGCCCCGAATTCGGTACCATGGAGAGACCCTATACATT TAAGGATTTTCTCC -3'	EcoRI

9343	5'-GGGCCC <u>GAATTC</u> GGTACCGTTGGTGTAACATCCCTGCC TGCAGC -3'	EcoRI
9346	5'-GCGGCCGCGT <u>CGACTC</u> AGTGGCAGAGGAAACGGAACT GGTGATAC -3'	SalI
10400	5'-GGCGT <u>CGACTC</u> ATTCTTGTCCAAATCCCTCTGTC -3'	SalI
10401	5'-GGC <u>GAATTC</u> GGTACCATGGCCACTGCTTCACCAAGATC- 3'	EcoRI
12325	5'-GGC <u>GAATTC</u> TCCATGGCATCTGCCAGCTCCAG -3'	EcoRI
12326	5'-GGCCCT <u>CGAGCT</u> AACTTCCCAGATCAACAGTTGGC -3'	XhoI
12327	5'-GGC <u>GAATTC</u> TTCTGGATGGGCCAACTGTTG -3'	EcoRI
12328	5'-GGCCCT <u>CGAGCT</u> AATCAGGGGCCTGGGCGG -3'	XhoI
12333	5'-GGC <u>GAATTC</u> TCCATGGCCACTGCTTCACCAAGATC -3'	EcoRI
12334	5'-GGCCCT <u>CGAGCT</u> ATGTTACAGGCTCTTGCTCAATCAC -3'	XhoI
12335	5'-GGC <u>GAATTC</u> GATGGATTAGTGATTGAGCAAGAGC -3'	EcoRI
12336	5'-GGCCCT <u>CGAGCT</u> ATTCTGTGTTGGTGTTTCCAGACTG -3'	XhoI
12340	5'-GGCCCT <u>CGAGTC</u> ATTCTTGTCCAAATCCCTCTG -3'	XhoI
12546	5'-CCAAGAAGCCATAACAAGTTTTAATCGCTTGGATCTACC - 3'	-
12547	5'-GGTAGATCCAAGCGATTAAACTTGTATGGCTTCTTGG - 3'	-
12548	5'-CAGGAGCCATACGAGCTTCAACCGTCTGG -3'	-
12549	5'-CCAGACGGTTGAAGCTCGTATGGCTCCTG -3'	-
12919	5'-GGCC <u>GAATTC</u> GGTACCATGGCATCTGCCAGCTCCAG -3'	EcoRI
12920	5'GGCC <u>GAATTC</u> GGTACCATGAGCACTCCGGGACACAGCA G-3'	EcoRI
12921	5'-GGCC <u>GAATTC</u> GGTACCATGGACCATGATCCCTTGGGCC-3'	EcoRI
12923	5'-GGCC <u>GAATTC</u> GGTACCATGAAACCTTACGACCTGCG -3'	EcoRI

12924	5'-GGCC <u>CAGATCT</u> CTACTCCTGTCCGAACCCCTC-3'	BglII
12925	5'-GGCC <u>CAGATCT</u> ACAGTTCATAATCTGTTGGAAAGAATCC-3'	BglII
12927	5'-GGCC <u>CAGATCT</u> ACAAGGGATCATGGTCAGTCG -3'	BglII
12928	5'-GGCC <u>CAGATCT</u> AGGAAGTGCTGGCCTCCTCTC -3'	BglII
12929	5'-GGCC <u>GAATTC</u> GGTACCATGGCCACTGCTTCACCAAG -3'	EcoRI
12930	5'-GGCC <u>GAATTC</u> GGTACCATGCGGCCACAGTCTGGAAA CAC- 3'	EcoRI
12931	5'-GGCC <u>GAATTC</u> GGTACCATGGAATCTGTTGAAATTTGA ACAG -3'	EcoRI
12933	5'-GGCC <u>GAATTC</u> GGTACCATGACATTATTTGAAGATTCCTTC CAACAG -3'	EcoRI
12934	5'-GGCC <u>CAGATCT</u> TCATTCTTGTCCAAATCCCTCTG -3'	BglII
12935	5'-GGCC <u>CAGATCT</u> ACATAATCTGTTGGAAGGAATCTTC -3'	BglII
12937	5'-GGCC <u>CAGATCT</u> AATAGGGGTCATTTTCTGCAGC -3'	BglII
12938	5'-GGCC <u>CTCGAGCT</u> ATGTGTTGGTGTTCAGACTGTG -3'	XhoI
14574	5'-CACGACACTGTGCCTTGATC-3'	-
14575	5'-GTTTAGTCAGCCAGCCATTC-3'	-
14587	5'- CCATTCCCTAAGCTCAATTTAC-3'	-
14588	5'-CTGGTCATTCTCAAGCTTA-3'	-

### 2.2.7 Antibodies

#### Primary antibodies used for Western blotting and immunostaining in this study

	Host Species	Origin	Usage and Dilution		
			WB	IHC	ICC
$\alpha$ -Actin, AC40	Mouse	Sigma	1:500	-	-
$\alpha$ -Actin	Rabiit	Sigma	1:2000	-	-
	Host Species	Origin	Usage and Dilution		
			WB	IHC	ICC
$\alpha$ -AIP2 (WWP2)	Goat	Santa Cruz	1:50	-	-

$\alpha$ -AIP4 (ITCH)	Mouse	BD	1:500	-	1:1000
$\alpha$ -AIP5 (WWP1)	Goat	Santa Cruz	1:50	-	-
$\alpha$ -Ankyrin G	Rabbit	Santa Cruz	-	1:400	1:400
$\alpha$ -Bassoon, SAP7F407	Mouse	Stressgene	-	1:1000	1:1000
$\alpha$ -Cre recombinase	Mouse	Sigma	-	1:200	-
$\alpha$ -Cre recombinase	Rabbit	Covance	-	1:3000	-
$\alpha$ -FLAG, M2	Mouse	Sigma	1:1000	-	1:1000
$\alpha$ -GFP	Mouse	Millipore	-	1:1000	1:1000
$\alpha$ -GFP, clone 7.1/13.1	Mouse	Roche	1:1000	-	-
$\alpha$ -GFP	Rabbit	Synaptic Systems	1:500	-	-
$\alpha$ -HA, HA.11	Mouse	Covance	1:1000	-	-
$\alpha$ -Liprin- $\alpha$ 3	Rabbit	Synaptic Systems	1:500	-	-
$\alpha$ -MAP2	Rabbit	Millipore	-	-	1:2000
$\alpha$ -MAP2	Chicken	Novus	-	1:2000	1:2000
$\alpha$ -Myc, 9E10	Mouse	Sigma	1:1000	-	-
$\alpha$ -c-myc	Rabbit	Santa Cruz	1:1000	-	1:1000
$\alpha$ -PSD95	Mouse	BD	1:500	1:1000	1:1000
$\alpha$ -PSD95, K28/43	Mouse	NeuroMAB	-	1:50	1:50
$\alpha$ -RabGDI	Rabbit	Synaptic Systems	1:2000	-	-
$\alpha$ -Shank	Rabbit	Provided by Dr. Kreienkamp	1:1000	-	-
$\alpha$ -Synapsin	Rabbit	Synaptic Systems	-	-	1:1000
$\alpha$ -Synaptophysin	Mouse	Millipore	1:10000	-	-
$\alpha$ -Tau1	Mouse	Millipore	-	-	1:1000
$\alpha$ -beta-Tubulin, TUB2.1	Mouse	Sigma	1:5000	-	-
$\alpha$ -Ubiquitin	Rabbit	Dako	1:500		



**Secondary antibodies used for Western blotting and immunostaining in this study**

	Host Species	Conjugated substrate/Dye	Origin	Usage, Dilution
$\alpha$ -Goat IgG	Mouse	HRP	Millipore	WB, 1:50000
$\alpha$ -Mouse IgG	Goat	HRP	BioRad	WB, 1:20000
$\alpha$ -Rabbit IgG	Goat	HRP	BioRad	WB, 1:20000
$\alpha$ -Mouse IgG	Goat	IL-COR IRDye 800	Rockland	WB, 1:20000
$\alpha$ -Rabbit IgG	Goat	Alexa Fluor 680	Invitrogen	WB, 1:1000
$\alpha$ -Chicken IgG	Donkey	Alexa Fluor 633	Invitrogen	IHC/ICC, 1:2000
$\alpha$ -Goat IgG	Donkey	Alexa Fluor 350/488/555/633	Invitrogen	IHC/ICC, 1:1000
$\alpha$ -Mouse IgG	Goat	Cy5/ Alexa Fluor 350/488/555	Invitrogen	IHC/ICC, 1:1000
$\alpha$ -Mouse IgG	Donkey	Alexa Fluor 546	Invitrogen	IHC/ICC, 1:1000
$\alpha$ -Rabbit IgG	Goat	Alexa Fluor 350/488/555/633	Invitrogen	IHC/ICC, 1:1000
$\alpha$ -Rabbit IgG	Donkey	Alexa Fluor 546	Invitrogen	IHC/ICC, 1:1000

**2.3 Molecular biology****2.3.1 Electroporation of plasmid DNA into competent bacterial cells**

An aliquot (50  $\mu$ l) of electro-competent cells of the appropriate *E.coli* strain was let thaw on ice and 20 ng of plasmid DNA or 1  $\mu$ l of a ligation reaction were added, mixed gently, and incubated for one minute on ice in a pre-cooled electroporation cuvette (0.1 cm, BioRad). The cuvette was administered an electric pulse of 1.80 kV (E.coli pulser, BioRad). Immediately following the electroporation, the bacterial cells were retrieved from the cuvette with 0.5 ml of pre-warmed LB medium and allowed to recover and express their antibiotic resistance genes for 1 hour at 37°C under moderate shaking. The bacterial cells were carefully centrifuged and the entire pellet was resuspended in 50  $\mu$ l of LB Medium and plated on the appropriate selection plates.

LB medium: 25 g Luria Broth (LB; Invitrogen) powder was dissolved in 1 L ddH<sub>2</sub>O;

autoclaved.

LB plates: 15 g Bacto-agar (Invitrogen) per 1 L of LB medium; autoclaved.

Required selection antibiotic; Ampicillin or Kanamycin was added after autoclaving.

### **2.3.2 Plasmid DNA preparation (Miniprep, Midiprep, and Maxiprep)**

The plasmid DNA preparation was carried out using the PureLink Quick Plasmid Miniprep Kit, HiPure Plasmid Midiprep Kit, HiPure Plasmid Maxiprep Kit (Invitrogen), or EndoFree Plasmid Maxi Kit (QIAGEN), following protocols supplied by manufacturers. The prepared plasmid DNA was let to air-dry and resuspended in TE buffer.

TE: 10 mM Tris-HCl pH 7.4, 1 mM EDTA

### **2.3.3 Determination of DNA concentration**

For the determination of the DNA concentration of aqueous solutions, a DU<sup>®</sup>650 Spectrophotometer (Beckman, USA) was used for absorption measurement at 260 nm/280 nm wavelength. The following formula was used to estimate the DNA concentration: dsDNA concentration =  $OD_{260} * 50 \mu\text{g/ml} * \text{dilution factor}$ . The DNA with the  $OD_{260}/OD_{280}$  ratio at 1.8-2.0 was used as a pure sample relatively free from protein contamination.

### **2.3.4 Sequencing of DNA**

All DNA sequence analysis was done in the MPI-EM DNA Core Facility on an Applied Biosystems 373 DNA Sequencer.

### **2.3.5 DNA digestion with restriction endonucleases**

DNA digestions were carried out for the use of the DNA fragments in further subcloning steps. Instructions in the New England BioLabs manual were followed for the appropriate restriction endonuclease/buffer combination and overall reaction conditions. Generally DNA digests were performed for 1-3 hours at the enzyme specific temperature. When a consecutive digest with a second restriction enzyme was required, reactions were

precleaned using the Invisorb MSB spin PCRapace kit (Invitex) following the protocol supplied by the manufacturer.

### **2.3.6 Dephosphorylation of 5' DNA-ends**

Dephosphorylation of the 5'-ends of DNA plasmids cut with a single restriction endonuclease was carried out in order to prevent recircularization of vectors in further DNA ligation reactions. The plasmid DNA was treated with alkaline phosphatase (Roche) in the supplied buffer according to manufacturer's instructions.

### **2.3.7 DNA ligation**

For ligation, the digested plasmid DNA and the digested insert DNA with compatible ends were mixed in a molar ratio of 1:5 and supplemented with T4 DNA ligase (Invitrogen) and the ligase-specific buffer in a total of 20  $\mu$ l reaction volume. The ligation reaction took place for 16-20 hours at 16°C.

### **2.3.8 Ethanol precipitation of DNA**

15  $\mu$ l of DNA solution was supplemented with 1.5  $\mu$ l of 3 M potassium acetate and 45  $\mu$ l of ethanol and placed at -80°C for 2 hours. The DNA aggregate was precipitated at 16,000 x g for 30 min using a pre-cooled bench-top centrifuge, the pellet was washed with 70 % ethanol and resuspended in 5  $\mu$ l of TE.

### **2.3.9 Agarose gel electrophoresis**

For analyses and purification of PCR products and digested DNA with restriction enzymes, the reactions were subjected to agarose-gel electrophoresis on 0.7-2 % agarose gels in TBE buffer including ethidium bromide. Negatively charged DNA fragments were separated at constant voltage (50-150 V) in TBE buffer and visualized by ethidium bromide under UV-light (254 or 314 nm). DNA fragment sizes were estimated by a GeneRuler DNA Ladder Mix sample (Fermentas) run on the gel in parallel.

TBE buffer: 50 mM Tris-Base, 50 mM boric acid, 2 mM EDTA, pH8.0

### **2.3.10 Agarose gel extraction of DNA fragments**

DNA fragments of interest were excised and isolated from agarose gel with the PureLink Gel Extraction Kit (Invitrogen) according to the protocol supplied by the manufacturer.

### **2.3.11 Polymerase chain reaction (PCR)**

Amplification of DNA *in vitro* was carried out by PCR. The reaction included doublestranded DNA template, oligonucleotide primers, dNTPs, high-fidelity *Pfu* DNA polymerase (Stratagene), and the supplied buffer. All PCR reactions were run on a Gene Amp 9700 PCR cycler (Applied Biosystems) with basic cycle parameters as below:

Step 1: 94°C for 2 minutes

Step 2: 94°C for 20 seconds

Step 3: *Annealing temperature* for 20 seconds

Step 4: 72°C for *extension time* (30-40 cycles from step 2 to step 4)

Step 5: 72°C for 10 min

Annealing temperatures were chosen at 5°C lower than mean calculated melting temperatures of primers used in reactions; extension time was adjusted according to length of PCR products. For genotyping PCR, REDTaq DNA polymerase (Sigma-Ardrich) was used instead of *PfU* DNA polymerase.

### **2.3.12 Subcloning in TOPO pCR vectors**

TOPO TA cloning Kits (Invitrogen) were used for rapid subcloning of PCR products. pCR2.1-TOPO or pCRII-TOPO vectors were used. Protocols supplied by the manufacturer were closely followed. LB plate containing kanamycin, IPTG, and X-gal was used for white colony selection.

### **2.3.13 Cloning strategies for constructs generated and used in this study**

#### pCR2.1-WWP1 (WT, full length)

The cDNA (Accession No. NM\_177327, 2757 bp) encoding full length WWP1 (918 aa) was cloned from the mouse brain cDNA library by PCR amplification using primers 10401/10400. The corresponding fragment was directly subcloned in pCR2.1-TOPO vector.

#### pCR2.1-WWP2 (WT, full length)

The cDNA (Accession No. NM\_025830, 2613 bp) encoding full length WWP2 (870 aa) was cloned from the mouse brain cDNA library by PCR amplification using primers 12325/12340. The corresponding fragment was directly subcloned in pCR2.1-TOPO vector.

#### pEGFP-WWP1 WT

The full length WWP1 cDNA was excised from pCR2.1-WWP1 with EcoRI/SalI and ligated in the same restriction sites on pEGFP-C2 vector.

#### pEGFP-WWP2 WT

The full length WWP2 cDNA was excised from pCR2.1-WWP2 with EcoRI/XhoI and ligated in the EcoRI/SalI restriction sites on pEGFP-C2 vector.

#### pEGFP-WWP1 C886S

Primers 12546/12547 were used for site-directed mutagenesis to generate pEGFP-WWP1 C886S point mutant from pEGFP-WWP1wt.

#### pEGFP-WWP2 C838S

Primers 12548/12549 were used for site-directed mutagenesis to generate pEGFP-WWP2 C838S point mutant from pEGFP-WWP2wt.

#### pCl neo-Myc-WWP2 WT

The full length WWP2 cDNA was excised from pCR2.1-WWP2 with EcoRI and ligated in the same restriction site on pCl neo-Myc vector.

#### pCl neo-Myc-WWP2 C838S

The 2.6 kbp long fragment encoding WWP2 C838S was excised from pEGFP-WWP2 C838S

with EcoRI/XbaI and ligated in the same restriction sites on pCl neo-Myc vector.

pGEX-WWP1 (1-150 aa)

Primers 12333/12334 were used on a pCR2.1-WWP1 template for PCR amplification of a 475 bp long nucleotide fragment corresponding to amino acids 1-150 in mouse WWP1. The fragment was directly subcloned in pCRII-TOPO, further excised with EcoRI/XhoI (restriction sites introduced via the primers) and ligated into the corresponding sites of pGEX-4T-1.

pGEX-WWP1 (140-345 aa)

Primers 12335/12336 were used on a pCR2.1-WWP1 template for PCR amplification of a 646 bp long nucleotide fragment corresponding to amino acids 140-345 in mouse WWP1. The fragment was directly subcloned in pCRII-TOPO, further excised with EcoRI/XhoI (restriction sites introduced via the primers) and ligated into the corresponding sites of pGEX-4T-1.

pGEX-WWP1 (335-582 aa)

Primers 9339/9340 were used on a pCR2.1-WWP1 template for PCR amplification of a 744 bp long nucleotide fragment corresponding to amino acids 335-582 in mouse WWP1. The fragment was directly subcloned in pCRII-TOPO, further excised with EcoRI/SalI (restriction sites introduced via the primers) and ligated into the corresponding sites of pGEX-4T-1.

pGEX-WWP2 (1-150 aa)

Primers 12325/12326 were used on a pCR2.1-WWP1 template for PCR amplification of a 475 bp long nucleotide fragment corresponding to amino acids 1-150 in mouse WWP2. The fragment was directly subcloned in pCRII-TOPO, further excised with EcoRI/XhoI (restriction sites introduced via the primers) and ligated into the corresponding sites of pGEX-4T-1.

pGEX-WWP2 (140-300 aa)

Primers 12327/12328 were used on a pCR2.1-WWP1 template for PCR amplification of a

505 bp long nucleotide fragment corresponding to amino acids 140-300 in mouse WWP2. The fragment was directly subcloned in in pCRII-TOPO, further excised with EcoRI/XhoI (restriction sites introduced via the primers) and ligated into the corresponding sites of pGEX-4T-1.

#### pGEX-WWP2 (290-533aa)

Primers 9343/9346 were used on a pCR2.1-WWP1 template for PCR amplification of a 732 bp long nucleotide fragment corresponding to amino acids 290-533 in mouse WWP2. The fragment was directly subcloned in in pCRII-TOPO, further excised with EcoRI/XhoI (restriction sites introduced via the primers) and ligated into the corresponding sites of pGEX-4T-1.

#### pF(syn)W-RBN-EGFP-WWP1

The 3.5 kbp long fragment coding EGFP-WWP1wt was excised from pEGFP-WWP1 WT with NheI/SmaI, and ligated in the NheI/SmaI restriction sites on pF(syn)W-RBN vector.

#### pF(syn)W-RBN-EGFP-WWP2

The 3.4 kbp long fragment coding EGFP-WWP2wt was excised from pEGFP-WWP2 WT with NheI/SmaI, and ligated in the NheI/SmaI restriction sites on pF(syn)W-RBN vector.

## **2.4 Yeast two-hybrid (YTH) screening**

Screening the mouse brain cDNA library and the rat brain cDNA library was performed by GAL4-based yeast two-hybrid (YTH) system using PJ69-4A yeast strain.

### **2.4.1 Media, buffers, and stock Solutions used in YTH screening**

#### **Yeast complete media and yeast selective media**

The following media were prepared with ddH<sub>2</sub>O and autoclaved. To make culture plates, 2% (w/v) agarose was added to media before autoclave.

#### YPAD (per 1 L)

10 g yeast extract, 20 g bacto peptone, 0.4 g adenine, 20 g glucose (dextrose).

SC –W (per 1 L)

6.7 g yeast nitrogen base without amino acids, 20 g glucose, 5 g casamino acids, 0.2 g adenine, and 0.2 g uracil.

SC –WL (per 1L)

6.7 g yeast nitrogen base without amino acids, 20 g glucose, 50 ml 20x –WL mix.

SC –WLH (per 1L)

6.7 g yeast nitrogen base without amino acids, 20 g glucose, 50 ml 20x –WLH mix.

SC –WLH(+3AT) (per 1L)

Add 1 ml of 1M 3-amino-1,2,4 triazol (3AT, sterilized by 0.22 µm filter) to 100 ml of SC-WLH media after autoclave.

SC –WLA (per 1L)

6.7 g yeast nitrogen base without amino acids, 20 g glucose, 50 ml 20x –WLA mix.

20x complete amino acids mix (per 1L)

0.4 g adenine, 0.4 g uracil, 0.4 g L-tryptophan, 0.4 g L-histidine HCl, 0.4 g L-arginine, 0.4 g L-methionine, 0.6 g L-tyrosine, 0.6 g L-isoleucine, 0.6 g L-lysine HCl, 1.2 g L-phenylalanine, and 0.6 g L-leucine.

20x –WL mix

As above with the following amino acids omitted: L-tryptophan and L-leucine.

20x –WLH mix

As above with the following amino acids omitted: L-tryptophan, L-leucine, and L-histidineHCl.

20x –WLA mix

As above with the following amino acids omitted: L-tryptophan, L-leucine, and adenine.

20x –LA mix

As above with the following amino acids omitted: L-leucine and adenine.

**Buffers and M9 medium**



1 M Lithium Acetate (LiAc)

10.2 g Lithium Acetate, adjusted the pH to 7.5 with diluted acetic acid and brought volume up to 100 ml with ddH<sub>2</sub>O.

Yeast lysis buffer

1% SDS, 100 mM NaCl, 10 mM Tris-HCl (pH8.0), 1 mM EDTA, 2% TritonX-100.

10x M9 mix

29.0 g Na<sub>2</sub>HPO<sub>4</sub>, 15.0 g KH<sub>2</sub>PO<sub>4</sub>, 25.0 g NaCl, and 5.0 g NH<sub>4</sub>Cl, adjusted to 500 ml with ddH<sub>2</sub>O and autoclaved

M9 plate (per 600 ml)

1.2 g glucose, 24 mg L-proline, 60 mg thiamine hydrochloride, 12 g agarose, and 510 ml ddH<sub>2</sub>O were mixed and autoclaved, then 60 ml 10x M9 mix, 30 ml 20x -LA mix, 0.6 ml 1M MgSO<sub>4</sub>, and 0.6 ml 0.1 M CaCl<sub>2</sub> are added and stirred. 0.6 ml of 100 mg/ml ampicillin was supplied before making plates.

**2.4.2 Generation of bait constructs for YTH screening**

Eight bait cDNA constructs were generated by PCR using the following sets of primers and pCR2.1-WWP1 or pCR2.1-WWP2 as templates. The amplified cDNA was cloned into pCRII-TOPO vector, and error-free cDNA clone was subcloned into pGBD-C2 bait vector. All bait constructs were sequenced to confirm the proper reading frame between the pGBD-C2 vector and the cDNA.

Bait construct	5' primer #	3' primer #
WWP1 1- 344aa	12929	12938
WWP1 336-451aa	12930	12937
WWP1 410-581aa	12931	12935
WWP1 571-918aa	12933	12934
WWP2 1-287aa	12919	12928

WWP2 285-404aa	12920	12927
WWP2 400-534aa	12921	12925
WWP2 535-870aa	12923	12924

### 2.4.3 Transformation of DNA into yeast

In this experiment, PJ69-4A yeast was transformed using a heat shock procedure with DMSO and salmon sperm carrier DNA. 10 ml of YPAD medium was inoculated with a single colony of yeast and the yeast was grown overnight at 30 °C. The culture was then diluted to an OD<sub>660</sub> of 0.2 in 100 ml of YPAD medium and allowed to grow for an additional 3 hours. Cultured yeast cells were pelleted by centrifugation for 5 minutes at 2,000 x g and resuspended in 1 ml of 100 mM LiAc/ TE. Cells were centrifuged again, resuspended in 0.5 ml of 100 mM LiAc/ TE and incubated at room temperature for 10 minutes. The following was dispensed to tubes: 1 µg of each plasmid DNA, 5 µl of denatured sheared salmon sperm DNA (10 mg/ml), 100 µl of the cell suspension in TE/LiAc, 600 µl of 40% PEG/ 100 mM LiAc/ TE. This mixture was then incubated at 30 °C with shaking for 30 minutes. 70 µl of DMSO was added, and the mixture was heat-shocked at 42 °C for 15 minutes. Cells were harvested by centrifugation, resuspended in 1 ml of YPAD medium, and incubated at 30°C for 1 hour. Cells were washed with autoclaved ddH<sub>2</sub>O, cultured with the appropriated selective medium, and then plated onto the appropriate selective plate. To determine the transformation efficiency, the aliquot of transformed yeast was streaked on YPAD plate. The transformation efficiency with a single plasmid DNA was about 10<sup>4</sup> to 10<sup>5</sup> colonies per microgram DNA.

### 2.4.4 Selection of bait constructs for screening

To determine optimal bait constructs for library screening, the auto-activation of each bait construct was examined. Yeast was transformed as above with the following three combinations for each bait constructs: a bait plasmid alone; the bait plasmid and the pVP16-3 vector; the bait plasmid and the pGAD424-HA vector. The transformed yeast was streaked on

selective plates, SC-WL, SC-WLH(+3AT), and SC-WLA, and allowed to grow for 3 days.

#### **2.4.5 Screening**

Yeast clones containing bait constructs were transformed with the rat brain pVP16-3 prey library or the mouse brain pGAD prey library to perform screening. The transformed yeast clones were cultured by the SC-WL media overnight, streaked onto the SC-WLH(+3AT) plates, and allowed to grow for 2-3 days. The yeast colonies growing on the SC-WLH(+3AT) plate were picked up and transferred onto the SC-WLA plate, and allowed to grow for 2-3 days. The colonies on SC-WLA plate were selected as positive interacting clones.

#### **2.4.6 Extraction of plasmid DNA from yeast**

Plasmid DNA of positive interacting clones was extracted from yeast. The yeast was put into an eppendorf 1.5 ml tube with 0.3 µg of glass beads and suspended with 200 µl of ddH<sub>2</sub>O. The yeast with glass beads was spin downed by centrifugation at 3,000 rpm for 5 minutes at room temperature and suspend with 200 µl of yeast extraction buffer. 200 µl of phenol/ CH<sub>3</sub>Cl was added to the tube. After incubation for 20 minutes at room temperature with shaking, the extracted plasmid DNA was isolated into aqueous phase separated by centrifugation at 15,000 rpm for 5 minutes at room temperature. The plasmid DNA was purified and concentrated by the ethanol precipitation method.

#### **2.4.7 Identification of the interacting cDNA clones**

HB101 *E.coli* competent cells were transformed with recovered plasmid DNA by electroporation. The transformed cells were spread on M9 plates and incubated at 37°C for 1-2 days. The colonies were picked up and inoculated in 3 ml LB (+Amp). The plasmid DNA was amplified and purified by the mini-prep method. Sequence of the purified plasmid DNA was analyzed and the interacting bait clones were identified. To verify interactions of bait and prey clones, yeast was re-transformed with the recovered plasmid and grown on the selective media plates.

## **2.5 *In situ* hybridization (ISH)**

DIG-labeled single strand RNA probes were used for *in situ* hybridization (ISH) analysis.

### **2.5.1 Molecular cloning for ISH probes**

To generate ISH probes, the 3'UTR of WWP1 (565 bp) and WWP2 (300 bp) were amplified by PCR from mouse brain cDNA library (Clontech) using oligonucleotide primers 14587/14588 and 14574/14575, respectively, and subcloned into the pCRII-TOPO vector.

### **2.5.2 PCR reaction to generate template DNAs for ISH probe synthesis**

Linerized DNA template for *in vitro* transcription was amplified by PCR using oligo primers #89/#91 from the pCRII-TOPO plasmid DNA containing the sequence of the ISH probe. The PCR product was separated on an agarose gel and purified using the PureLink Quick gel extraction kit (Invitrogen) according to the protocol supplied by the manufacturer. The linerized DNA templates contain SP6 promoter and P7 promoter on either side of the ISH probe sequence.

### **2.5.3 Transcriptional labeling of RNA probes**

RNA probes were generated and labeled in an *in vitro* transcription reaction with digoxigenin-UTP (DIG) using MEGAscript (SP6 or T7) transcription kit (Ambion) and DIG RNA Labeling Mix with an optimized Transcription Buffer (Roche) according to protocols supplied by manufacturers. Linerized DNA templates were removed by DNaseI (RNase free, Roche), and then DIG labeled RNA transcripts were purified by ethanol precipitation. The quality and quantify of DIG labeled RNA transcripts were analyzed by non-denaturing agarose gel electrophoresis and ethidium bromide staining.

### **2.5.4 Tissue preparation**

*In situ* hybridization was carried out on C57BL/6 adult male mice. 20  $\mu$ m sagittal sections were cut from the fresh frozen brain using cryostat (Leica) and placed on the

microscope slide glass (SUPERFROST® PLUS, MENZEL-GLASER). The sections were kept at -80°C until use.

### **2.5.5 Hybridization and Detection**

The sections were fixed with 4% PFA/PBS at 4°C for 20 minutes, washed with PBS three times (5 minutes each), incubated in 100% Ethanol for 5 minutes, and dried up at room temperature. Then the sections were incubated in the pre-hybridization buffer at least 10 minutes. DIG-labeled RNA probes were diluted to approximately 2 µg/µl in the hybridization buffer just before use. The hybridization was carried out for 36 hours at 37°C in the humid chamber. After the hybridization, the slides were washed with pre-warmed 0.2x SSC buffer at 37°C for 10 min, washed twice with 1x SSC buffer at room temperature for 20 minutes each. To detect the DIG-labeled probes, the slices were incubated with 1:1000 diluted anti-DIG antibody conjugated with alkali phosphatase (Roche) in the blocking buffer at 4 °C overnight, followed by 2 hours blocking reaction. After washing with 1xSSC for 10 min three times, the slides were incubated with pre-warmed BM Purple (Roche) at room temperature for approximately 30 minutes to develop the conjugated alkali phosphatase.

#### 20x SSC buffer

3 M Sodium chloride, 300 mM tri-Sodium citrate dihydrate, pH 7.0.

#### Pre-hybridization buffer

4x SSC, 50% dionized formamide.

#### Hybridization buffer

4x SSC, 40% dionized formamide, 10% dextran sulfate, 1x denhardts solution.

## **2.6 Biochemical experiments**

### **2.6.1 Protein assay**

BCA assay kit (Thermo, Pierce) was used for the BCA method. The absorbance of developed sample was analyzed by DU®650 Spectrophotometer (Beckman, USA).

## 2.6.2 Sodium dodecyl sulfate polyacrylamide gel electrophoresis (SDS-PAGE)

To separate proteins based on their molecular size and post-translational modification, for example, phosphorylation, glycosylation, and ubiquitination, protein samples were subjected to sodium dodecyl sulfate polyacrylamide gel electrophoresis (SDS-PAGE) under denaturing condition. Generally, the protein samples were dissolved in SDS-sample buffer and boiled at 95°C for 5 minutes. A two-layer Tris-Glycine gel: upper stacking gel and lower separating gel (Laemmli, 1970) was set up with Bio-Rad Mini-PROTEAN II casting system. The gel was set up onto a Bio-Rad mini gel electrophoresis system filled with running buffer. The protein sample was loaded onto the gel and the electrophoresis was performed with 20 mA for stacking and 30 mA for resolving.

### SDS-sample buffer

10% Glycerol, 50 mM Tris-HCl (pH 6.8), 2 mM EDTA, 2% SDS, 100 mM DTT, 0.05% Bromophenol blue.

### upper stacking gel

5% acrylamide/N,N'-Methylene-bis-Acrylamide (29:1) Solution (AMBA), 125 mM Tris-HCl (pH 6.8), 0.1% SDS, 0.05% ammonium persulfate (APS), 0.005 % TEMED.

### lower resolving gel

8-15% AMBA, 325 mM Tris-HCl (pH 8.8), 0.1% SDS, 0.05% APS, 0.005 % TEMED.

### running buffer

25 mM Tris-HCl, 250 mM Glycine, 0.1% SDS, pH 8.8.

## 2.6.3 Western blotting

Proteins separated on SDS-PAGE were electrophoretically transferred onto a PVDF membrane (Millipore, Immobilon-P-Membrane, 0.45 µm pore size) at 200 mA for 10 hours using a tank blotting system (Hoefer, TE22 Mighty Small tank transfer). The PVDF membrane blot was rinsed with TBS to remove gel debris and then incubated in the blocking

buffer for 1 hour with gentle agitation at room temperature. The blot was incubated with diluted primary antibodies (Table xx, antibody list) for 2 hour at room temperature or overnight at 4°C. After washing with wash buffer, the blot was incubated with diluted secondary antibodies conjugated to HRP for 1 hour at room temperature. The blot was visualized with an enhanced chemi-luminescence (ECL) detection system (Amersham).

#### Transfer buffer

25 mM Tris Base, 190 mM Glycine, 20% Methanol.

#### TBS

10 mM Tris-HCl, 150 mM NaCl, pH 7.5.

#### Blocking buffer

5% skin milk, 5% goat serum, 0.1% Tween 20, TBS.

#### Washing buffer

0.1% Tween 20, TBS.

### **2.6.4 Purification of recombinant GST-fusion proteins**

The GST Gene Fusion System (GE Healthcare Life Sciences) was used for the bacterial expression of GST-fused proteins. pGEX-4T-1 plasmids carrying different constructs were transformed by electroporation into *E. coli* BL21DE3 strain. Single colonies were transferred into 5 ml of LB medium supplied with ampicillin and incubated with vigorous shaking overnight at 37°C. This preculture was diluted in 50 ml of LB medium supplied with ampicillin and incubated further at 37°C until the optical density of the culture at 660 nm reached to 0.6. The bacterial culture was let to cool down to room temperature, 0.1 mM isopropyl -D-1-thiogalactopyranoside (IPTG) was added for the induction of protein expression and the culture was shaken for 4 hours at room temperature. The bacteria were sedimented for 20 min by centrifugation (4500 x g, 4°C) and the pellet was washed with 5 ml PBS and resuspended in buffer A supplied with the protease inhibitors 0.1 mM PMSF, 0.1

mM aprotinin, 0.1 mM leupeptin and 0.1 mM DTT. The cells were lysed by sonification using the Macro-tip from the Labsonic U Sonifiers (Braun) (5 pulses x 10 seconds). Triton X-100 (0.1%) was added to the suspension to solubilize the protein and it was shaken for 20 minutes on ice. The clear supernatant containing the soluble GST-fusion proteins was collected by ultracentrifugation (100,000 xg, 30 minutes, 4°C). The GST-fusion proteins were purified by butch purification using reduced glutathione (GSH) covalently coupled to Sepharose 4B (GE Healthcare) according to the instruction supplied by the manufacturer.

### 2.6.5 Antibodies against WWP1 and WWP2 generated in this study

The rabbit polyclonal antisera against WWP1 and WWP2 were raised by Eurogentec S.A. (Bergium, <http://www.eurogentec.com>) and purified using affinity column. The following recombinant proteins and synthetic peptides were used as antigen. Two rabbits were used to raise antisera for each antigen. The antiserum was affinity purified by the antigen using an affinity column, HiTrap NHS-activated HP (1 ml, GE Healthcare, 17-0716-01) according to the manufacture's instructions. Among these, affinity purified antibodies, 0221 and 0217 were used for Western blotting to detect WWP1 and WWP2, respectively.

Antibody #		Antigen
0219	WWP1	GST-WWP1 (1-150 aa)
0220		
0221	WWP1	GST-WWP1 (140-345 aa)
0222		
0215	WWP2	GST-WWP2 (1-150 aa)
0216		
0217	WWP2	GST-WWP2 (140-300 aa)
0218		
2240	WWP1	H <sub>2</sub> N- <u>VGPEARSLIDPDS</u> SR-CONH <sub>2</sub> (302-317 aa of mouse WWP1)
2241		
0287	WWP2	H <sub>2</sub> N- <u>CEQSPGARNRHRQPVK</u> -CONH <sub>2</sub>



0288		(209-223 aa of mouse WWP2)
2782	WWP2	H <sub>2</sub> N- <u>CTAEYVRNYEQWQSQR</u> -CONH <sub>2</sub>
2783		(362-376 aa of mouse WWP2)

### 2.6.6 Subcellular fractionation of rat brains

Subcellular fractionation of rat brains was performed based on published protocols [Huttner et al., 1983; Mizoguchi et al., 1989]. 10 male Sprague-Dawley rats (200-250 g) were anaesthetized, decapitated, and cortices were isolated in 0.32 M sucrose. After homogenization with a Teflon-glass homogenizer, debris and the nuclear fraction (P1) were centrifuged at 1,400 x g for 10 min. The supernatant (S1) was further centrifuged at 13,800 x g for 15 min and the pellet and the supernatant were harvested as the crude membrane fraction (P2) and the cytosol fraction (S2). The P2 fraction in 0.32M sucrose solution was further fractionated by discontinuous sucrose density gradient centrifugation (0.85 M, 1.0 M, and 1.2 M sucrose layers) at 82,500 x g for 2 h. The interface between 0.32 M and 0.85 M sucrose was harvested as the P2A fraction (myelin-enriched fraction), the one between 0.85 M and 1.0 M sucrose as the P2B fraction (ER-, Golgi-, and microsome-enriched fraction), the one between 1.0 M and 1.2 M sucrose as the P2C fraction (synaptosome fraction), and the bottom fraction as the P2D fraction (mitochondria-enriched fraction). The P2C fraction was lysed by suspending it in 6 mM Tris/HCl pH8.0 and centrifuged at 32,800 x g for 20 min. The pellet was harvested as the crude synaptic membrane (CSM) fraction. The supernatant was further centrifuged at 200,000 x g for 2 h and the supernatant was harvested as the synaptic soluble cytoplasm (SS) fraction and the pellet as the crude synaptic vesicle (CSV) fraction. The CSM fraction was suspended in a buffer containing 6 mM Tris/HCl pH8.0, 0.32 M sucrose, and 0.5% TritonX100. After incubation for 15 min on ice, the sample was centrifuged at 32,800 g for 20 min. The pellet fraction was harvested as the PSD fraction and the supernatant as the Triton-Sup fraction. All procedures were performed at 0-4°C

### **2.6.7 Affinity purification of GST-WWP1/2 binding proteins**

Recombinant GST-WWP1 (residues 335-582) and GST-WWP2 (residues 290-533) were purified and 40 µg of protein were immobilized on 50 µl glutathione Sepharose 4B beads (GE Healthcare Life Sciences). After washing the beads with five bed volumes of A-buffer (20 mM Tris/Cl pH 7.5 at 4°C, 1 mM EDTA, 1 mM DTT, and 1% Triton X-100, 150 mM NaCl, 0.2 mM PMSF, 1 µg/ml Aprotinin, 0.5 µg/ml Leupeptin), a Triton X-100 extract (A-Buffer) of rat brain synaptosomes (containing 80 mg protein) was loaded. Beads were washed with five bed volumes of A-buffer, and GST-WWP1/2 binding proteins were eluted with B-buffer (same buffer as A-buffer except with 1 M NaCl).

### **2.6.8 Protein identification by mass spectrometry**

Proteins eluted from the GST-WWP1/2 beads were separated under reducing conditions by SDS-PAGE on pre-cast NuPAGE 10% Bis-Tris gels (Invitrogen) using a MOPS buffer system recommended by the manufacturer. Eluates from GST beads were used as controls. After colloidal Coomassie staining of gels, gel plugs were excised manually from bands representing specifically enriched proteins indicative of putative WWP1/2 binding partners. Gel plugs were subjected to an automated platform for the identification of gel-separated proteins [Jahn et al., 2006] as described previously [Reumann et al., 2007; Werner et al., 2007]. An Ultraflex MALDI-TOF-mass spectrometer (Bruker Daltonics) was used to acquire both peptide mass fingerprint and fragment ion spectra, resulting in confident protein identifications based on peptide mass and sequence information. Database searches in the NCBI non-redundant primary sequence database restricted to the taxonomy *Rat* were performed using the Mascot Software 2.0 (Matrix Science) with parameter settings described earlier [Reumann et al., 2007; Werner et al., 2007]. The minimal requirement for accepting a protein as identified was at least one peptide sequence match above homology threshold in coincidence with at least four peptide masses assigned in the peptide mass fingerprints.

### **2.6.9 *In Vitro* ubiquitination assays**

Mammalian expression vectors for FLAG-tagged SAD-A, FLAG-tagged liprin- $\alpha$ 3, or Shank1a were co-transfected in HEK cells with EGFP-tagged WWP1 (WT), EGFP-tagged WWP1 C886S, EGFP-tagged WWP2 (WT), or EGFP-tagged WWP2 C838S and HA-tagged ubiquitin expression vectors using Lipofectamine2000 (Invitrogen). Recombinant proteins were extracted in RIPA buffer in the presence of 20 mM NEM with 20  $\mu$ M MG132. FLAG-tagged proteins were immunoprecipitated using anti-FLAG M2 agarose beads (Sigma-Aldrich). Immunoprecipitation of FLAG-tagged proteins were confirmed by Western blotting using anti-FLAG M2 monoclonal antibody. Shank1a was pull-downed using GKAP beads [Brendel et al., 2004]. Pull-down of shank1a was confirmed by Western blotting using anti-shank antibody. Ubiquitination was detected by Western blotting using an anti-ubiquitin antibody (Dako).

#### RIPA buffer

50 mM Tris-HCl (pH 8.0), 150 mM NaCl, 1% NP40, 0.5% Sodium deoxycholate, 0.1% SDS, 5 mM EDTA, 0.2  $\mu$ M Aprotinin, 20  $\mu$ M Leupeptin, 1 mM PMSF.

Ubiquitination assay under a denaturing condition was performed following a previously published protocol [Lu et al., 2007]. Ubiquitination status of FLAG-tagged protein was analyzed using 1.0 mg total protein, which were boiled in 1.0% SDS for 5 minutes at 95 °C (to dissociate coprecipitated proteins), diluted 10 $\times$  in lysis buffer to neutralize the SDS and immunoprecipitated with anti-FLAG M2 agarose beads. After overnight incubation, precipitated proteins (on beads) were washed twice with lysis buffer and twice with HNTG.

#### Lysis buffer

50 mM HEPES (pH7.5), 150 mM NaCl, 10% Glycerol, 1.5 mM MgCl<sub>2</sub>, 1% TritonX/100, 20 mM NEM, 0.2  $\mu$ M Aprotinin, 20  $\mu$ M Leupeptin, 1 mM PMSF.

#### HNTG

20 mM HEPES (pH 7.5), 150 mM NaCl, 0.1% Triton-X-100, 10% Glycerol.

## **2.7 Cell cultures**

### **2.7.1 Media and solutions**

#### Solution 1

0.2 mg/ml Cystein, 1 mM CaCl<sub>2</sub>, and 0.5 mM EDTA in D'MEM

#### Papain Solution

20-25 units of Papain per 1 ml of solution 1 were mixed and bubbled with carbogen (95% oxygen, 5% carbon dioxide) for 10-20 minutes (until the solution turned to be clear). The papain solution was sterilized by filtration through a 0.2 µm filter.

#### Stop Solution

2.5 mg/ml BSA, 2.5 mg/ml trypsin inhibitor, and 10% FCS in D'MEM

The solution was kept in a water bath at 37°C until use.

#### 10% FCS/D'MEM

500 ml DMEM, 50 ml FCS, 5 ml GlutaMAX I (Invitrogen), 5 ml Penicillin/Streptomycin (100x, Invitrogen)

#### Complete Neurobasal Medium

500 ml Neurobasal A, 5 ml GlutaMAX I (Invitrogen), 10 ml B-27 supplement (Invitrogen), 5 ml Penicillin/Streptomycin (100x, Invitrogen)

### **2.7.2 Treatment of coverslips for culturing primary neurons**

To attain direct adhesion of cultured neurons, the surface of glass coverslips was coated with Poly-L-Lysine (PLL, Sigma) in a sterile atmosphere. The cover slips were incubated with 1:12 diluted PLL in PBS for at least three hours (usually overnight) at 37°C. The cover slips were then rinsed twice with PBS and once with HBSS, and then incubated with the Complete Neurobasal Medium at 37°C until plating the cell.

### **2.7.3 Mouse neuronal cultures**

Primary dissociated mouse neurons were isolated from neonatal (P0) mice. The

individual brains were quickly removed from newborn pups and collected in HBSS at room temperature. Hippocampi or cortex were dissected out and transferred immediately to 0.5 ml of pre-warmed Papain Solution and incubated for approximately 1 hour at 37°C with gentle agitation. The Papain Solution was carefully discarded, 0.5 ml of the pre-warmed Stop Solution was added, and the tissue were incubated for 15-20 minutes at 37°C with gentle agitation. All the supernatant was removed and 200 µl pre-warmed Complete Neurobasal Medium was added. The tissue were gently triturated 10-20 times with a plastic pipett tip for P-200 Pippetman, and after leaving the tubes to stand for 1-2 minutes the supernatant was transferred to 1 ml of pre-warmed Complete Neurobasal Medium. A second trituration step was used to increase the yield of the preparation, if necessary. Cells were counted using the Naubauer Counting Chamber (4x4 grid x 1000 cells/ml) and approximately 60.000-120.000 cells were plated out per well in 24 well plate. The medium was changed after confirming that the plated cells were settled and attached onto the coverslips. The neurons were cultured in the 37°C/5% CO<sub>2</sub> incubator.

#### **2.7.4 Rat neuronal cultures**

Forebrains from rat embryos (E18) were dissected out and collected in a 6-cm sterile plastic dish with HBSS, and the hippocampi were dissected and pooled in a 15 ml Falcon tube. Hippocampi were washed three times with HBSS and incubated in 1800 µl of HBSS supplemented with 200 µl of 0.05% Trypsin-EDTA (GIBCO) for 20 min in the 37°C waterbath . After incubation, the hippocampi were washed 5 times with HBSS and transferred to a 2 ml sterile Eppendorf tube, where 1600 µl HBSS supplemented with 400 µl DNase I (0.01% final) was added. Hippocampi were triturated slowly with a plastic pipett tip for P-200 Pippetman. The triturated cells were then filtered through a cell strainer (40 µm) into a 50 ml Falcon tube, and complemented to a volume of 20 ml with 10% FCS/D'MEM. Cells were plated at a density of 60.000 cells per well in 24 well plates. The media was exchanged to the

Complete Neurobasal Medium after the overnight culture. Neurons were cultured in the 37°C/5% CO<sub>2</sub> incubator.

### **2.7.5 HEK 293FT cell line**

Human embryonic kidney (HEK) 293FT cells were used for production of the lentivirus and *in vitro* ubiquitination assay. HEK293FT cells were maintained in tissue culture dishes with 10% FBS/D'MEM in the 37°C/5% CO<sub>2</sub> incubator.

### **2.7.6 Transfection**

Mouse and rat neurons were transfected at DIV1-5 by the calcium phosphate method. The transfection efficiency was 5-20%. The culture medium in each well of the 24-well plate was replaced to 500 µl of pre-warmed Opti-MEM I (Invitrogen) 30 minutes before transfection. Transfection mixture was prepared in a 1.5 ml eppendorf sample tube. 37.9 µl of ddH<sub>2</sub>O was added to 1.5 µl of 2mg/ml DNA and 5.6 µl of 2M CaCl<sub>2</sub> in the tube, and then 45 µl of 2xHBS was added to the mixture stepwise with shaking on a Vortex mixer. After incubation at room temperature for 20 minutes, 10-30µl of the mixture was applied into each well of the 24-well plate, and incubated in the 37°C/5% CO<sub>2</sub> incubator. Then the neurons were washed with pre-warmed Neurobasal A (Invitrogen) and cultured with the Complete Neurobasal Medium.

#### **2xHBS**

274 mM NaCl, 10 mM KCl, 1.4 mM Na<sub>2</sub>HPO<sub>4</sub>, 15 mM glucose, 42 mM HEPES (Sigma, H3375, pH 7.08 adjusted by NaOH). The aliquots of optimized buffer were stored at -20°C.

### **2.7.7 Lenti-virus production and infection**

To produce transduction component viral particles, semiconfluent HEK293FT cells cultured in 2% FCS/D'MEM were co-transfected with the vector plasmid (pFUGW, pFUGW-iCre, pF(syn)-EGFP (pL21), pF(syn)-EGFP-WWP1 or pF(syn)-EGFP-WWP2) together with

a packaging plasmid (PACK) and an envelope plasmid (ENV) using Lipofectamine 2000 (Invitrogen) according to the manufacture's instructions. 1/50 volume of 500 mM sodium butyrate (pH 7.0 at RT) was added to the culture medium in 4-6 hours after transfection. Then 48 hours after transfection, the supernatant was harvested, filtered through 0.45  $\mu\text{m}$  pores (Millipore) in order to remove the aggregate of the virus and cell debris. The virus in the supernatant was concentrated using an Amicon filter system (Millipore) to 1/20 volume by centrifugation at 3500 rpm for 20-100 min at 4°C and washed with pre-cold Neurobasal A. The concentrated viral solution was dialyzed against TBS (pH 7.5) for overnight at 4°C and stored in small aliquots at -80°C before use. The viral solution was added to the neuron culture medium at DIV1-3. The medium was changed 16-24 hours after infection. The viral titer was determined by expression level of EGFP in neuron.

## **2.8 *In utero* electroporation**

The plasmid DNA prepared with the EndoFree Plasmid Maxi Kit (QIAGEN) was used for *in utero* electroporation. The DNA was mixed with 1/10 volume of 0.1% Fast Green solution. The micropipettes for injection were made with a puller and 1-mm diameter glass capillary tubes (Kimble, Kimax-51 Melting Point Capillaries). The tip of the micropipettes was cut obliquely with a fine forceps under a dissecting microscope. The micropipettes were attached to the aspirator tube assembly. A pregnant mouse was deeply anesthetized with isoflurane in oxygen carrier and placed on the warm pad (31-32°C) by holding its limbs with surgical tapes. After shaving the fur over the abdomen using a shaver and disinfecting the abdominal skin with 70% ethanol and batisodona, an approximately 2-cm midline skin incision was made extending anteriorly from the level of the mid point between the most posterior two pairs of nipples. A 2-cm midline incision was then made in the abdominal wall along the linea alba. Uterine horns were drawn out through the incision and moistened with warmed PBS containing antibiotics. After observing the orientation of the embryos through the wall of

uterine bone, a micropipette was inserted into the lateral ventricle, and 1-2  $\mu$ l of plasmid DNA solution was injected by expiratory pressure using the aspirator tube assembly. Fast Green enabled visualizing the distribution of the DNA solution through uterine wall. After soaking the uterine horn with warmed PBS containing antibiotics, the head of embryo was pinched with a forceps-type electrode (CUY650P1, Nepa gene, Chiba, Japan), and electronic pulses (the voltage: 30-35 V, the actual current: 50 mA, the duration of square pulse: 50 ms, the interval between pulses: 950 ms, 6 pulses per embryo) were applied with an ECM830 electro square porator (BTX HARVARD APARATUS, USA). When the procedures on the both uterine bones had been completed, the uterine bones were placed back into its original location, the abdominal cavity was filled with warmed PBS containing antibiotics, the abdominal wall was closed with suture, and then skin was closed with 9-mm Autocrip (ROBOZ). The animal was kept warm on the warm pad (31-32°C) until recovery from anesthesia.

## **2.9 Immunocytochemistry (ICC)**

After washing with PBS, cells cultured on coverslip were fixed with 4% paraformaldehyde (PFA) in PBS for 20 minutes at 4°C. After washing with PBS three times, the cells were incubated with blocking buffer (5% goat serum and 0.1% TritonX-100 in PBS) at room temperature for 30 minutes. The cells were incubated with primary antibodies at room temperature for 2 hours or at 4°C overnight, washed three times with PBS, and incubated with secondary antibodies conjugated fluorescence dye at room temperature for 1 hour. The cells were washed with PBS after incubation with secondary antibodies and mounted on the microscope glass slide (MENZEL-GLASER) with mounting medium (Immunount, Thermo Scientific Shandon).

## **2.10 Immunohistochemistry (IHC)**

After intracardiac perfusion with 4% PFA in PBS, mouse brains were removed from



the skulls and kept in 4% PFA in PBS at 4 °C for 24 hour. The brains were embedded in 2% agarose, cut into 50-100 µm sections with a vibratome (Leica) and floated in PBS. The floating section was incubated with blocking buffer (5% goat serum and 0.3% Triton X-100 in PBS) for 2 hours, followed by incubated with primary antibodies at 4°C or room temperature for 1-2 days. The sections were washed with PBS and incubated with secondary antibodies conjugated fluorescence dye at room temperature for 4-6 hours. After washing with PBS, the sections were attached onto microscope glass slides (SUPERFROST PLUS, MENZEL-GLASER) and mounted with cover glass (MENZEL-GLASER) and mounting medium with DAPI (VECTOR SHILD H1500, vector).

### **2.11 Nissl staining**

Vibratome sections were mounted on microscope glass slides (SUPERFROST PLUS, MENZEL-GLASER) and air dried at 37°C overnight. The sections were rehydrated, incubated in 0.1% Cresyl violet solution (Merck) for 0.5-5 minutes, destained in 95% ethanol containing 0.5% acetic acid, dehydrated with isopropanol, cleared in xylene, and mounted with the mounting medium (D.P.X., Sigma-Ardrich).

### **2.12 Image analysis and statistics**

Images were obtained using a fluorescence stereomicroscope (Leica MZ16 F), a fluorescence microscope (Olympus BX-61), or a confocal laser scanning microscope (Leica SP2). ImageJ software (<http://rsbweb.nih.gov/ij>) was used for image analysis. Statistical analyses were performed using the InStat software (GraphPad Software, Inc.). Colocalization analysis was carried out by the Pearson's correlation coefficient using ImageJ plug-in Mander's coefficient. Low (close to zero) values for coefficient for fluorescent images indicate exclusion and a value close to 1 indicates reliable colocalisation. All results are presented as mean  $\pm$  standard error of the mean (SEM). Student's-t test was applied for comparison of two groups. Neuronal polarity phenotypes were categorized into three groups

(single axon, two axon, and more than two axons). An axon was defined as a neurite whose length is longer than 100  $\mu\text{m}$  at DIV7 and is also immunoreactive for axonal markers (Tau-1 or Ankyrin G). Cells were then scored in a blinded manner. Statistical analysis of neuronal polarity defects in neuron was carried out by the  $\chi^2$  test. To examine polarity defects of mouse cortical neurons, images from serial z-stacks of cortical sections immunostained with Ankyrin G was collected using a Leica SP2 confocal laser scanning microscope, and projected using LSM software. The morphology of individual neurons in the layer IV of the cortex was categorized into three groups based on the orientation of their processes. A main dendritic shaft oriented within  $15^\circ$  from a line orthogonal to the pial surface was considered normal. A dendritic main shaft orientated more than  $15^\circ$  was grouped into either lateral or basal. A  $\chi^2$  test was used for the statistical analysis.



## 3 Results

### 3.1 Largely overlapping distribution of WWP1 and WWP2 in the brain

To determine WWP1 and WWP2 gene expression patterns, I first analyzed their mRNA expression patterns in the mouse brain by in situ hybridization (Fig. 3-1A). Both mRNAs are widely expressed throughout the brain and are strongly and largely overlappingly expressed in many brain regions, including the olfactory bulb, the hippocampus, the cortex, and the cerebellar granule cell layer. These expression patterns are similar to those of many key neuron specific proteins, i.e., PSD95, Neuroligins, or Shanks [Fukaya et al., 1999; Fukaya and Watanabe, 2000; Varoqueaux et al., 2006; Lim et. al., 1999].

To study protein expression profiles of WWP1 and WWP2 in the rodent brain, homogenates of several regions of the adult rat brain, including the cerebellum, the brainstem, the olfactory bulb, the striatum, the hippocampus, the cerebral cortex, and the basal brain were analyzed by Western blotting using antibodies specific for each protein (Fig. 3-1B). Both WWP proteins are widely expressed in the adult brain, consistent with the result of in situ hybridization (Fig. 3-1A). These results indicate general and shared roles of WWP1 and WWP2 proteins in various types of neurons in the brain.

I next studied the developmental expression profiles of WWP1 and WWP2 proteins in the mouse brain by Western blotting (Fig. 3-1C). WWP2 protein was most strongly expressed in the embryonic (E13) brain, while expression of WWP1 protein in the E13 brain was relatively low. Both proteins were developmentally up-regulated in the postnatal brain, indicating their roles in the regulation of the function of mature neurons as well as in the development of the brain.

In order to study the subcellular distribution of WWP1, WWP2, and the third member

of the WWP subfamily, Itch, subcellular fractions of the adult rat cerebrum were separated biochemically [Huttner et al., 1983; Mizoguchi et al., 1989], and equal amounts of proteins from each fraction were subjected to SDS-PAGE, followed by Western blotting (Fig. 3-1D). The fidelity of fractionation was confirmed by Western blotting using antibodies to RabGDI, PSD95, and Synaptophysin as protein markers for the synaptic soluble cytoplasm (SS), the postsynaptic density (PSD), and the crude synaptic vesicle (CSV) fractions, respectively. Both WWP1 and WWP2 are partially enriched in the crude synaptic vesicle fraction (CSV), the synaptic membrane fraction (CSM), and the postsynaptic density fraction (PSD). Itch showed a different distribution pattern from WWP1 and WWP2. It was enriched in the synaptic soluble cytoplasm (SS) and the P2A fractions. Given that myelin proteins are enriched in the P2A fraction, Itch may have a distinct function from WWP1 and WWP2 in glial formation or function.

Taken together, these results indicate that WWP1 and WWP2 are expressed dominantly in neurons and play multiple roles in the regulation of the differentiation, development, or function of neurons.

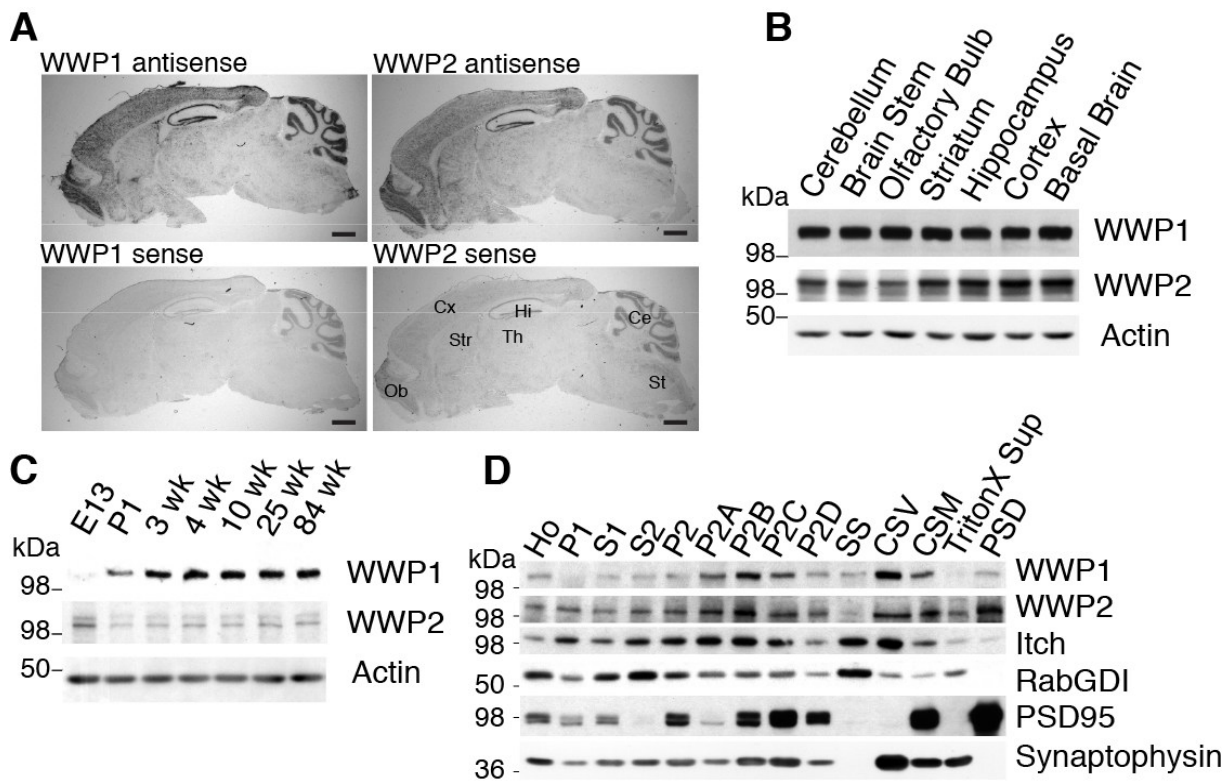


**Figure 3-1 Gene expression profiles of WWP1 and WWP2 in the brain**

(A) *In situ* hybridization analyses of WWP1 and WWP2 mRNA in the mouse brain. Sagittal sections of the adult mouse at 10 weeks of age were hybridized with *antisense* and *sense* RNA probes to WWP1 and WWP2. Both mRNAs are widely expressed throughout the brain and their expression patterns are almost identical. Highest signals for both mRNAs were detected in the olfactory bulb, the hippocampus, the cerebral cortex and the cerebellar granule cell layer. *Ce*, cerebellum; *Cx*, cerebral cortex; *Hi*, hippocampus; *Ob*, olfactory bulb; *St*, brainstem; *Str*, striatum; *Th*, thalamus. Scale bar = 2 mm. (B) WWP1 and WWP2 protein expression in the adult rat brain. 10  $\mu$ g of the homogenate from indicated brain regions were analyzed by Western blotting using specific antibodies to WWP1 or WWP2 proteins. (C) Developmental expression profiles of WWP1 and WWP2 proteins in the mouse forebrain. 10  $\mu$ g of the homogenate of hemispheres from mice at developmental stages from E13 to postnatal 84 weeks were analyzed by Western blotting using antibodies to the indicated proteins. (D) Enrichment of WWP1, WWP2, and Itch proteins in the crude synaptic vesicle fraction of the adult rat cerebrum. Antibodies to Rab-GDI, PSD-95, and Synaptophysin were used to show the fidelity of the biochemical subcellular fractionation as markers for synaptic soluble cytoplasm (SS), postsynaptic density (PSD), and crude synaptic vesicle (CSV) fractions. Ho, homogenate; P1, debris and nuclear fraction; S1, supernatant of Ho excluding P1; S2, cytosol fraction; P2, crude membrane fraction; P2A, myelin-enriched fraction; P2B, ER- Golgi- and microsome-enriched fraction; P2C, synaptosome

fraction; P2D, mitochondria-enriched fraction; SS, synaptic soluble cytoplasm fraction; CSV, crude synaptic vesicle fraction; CSM, crude synaptic membrane fraction; TritonX sup, TritonX 100 soluble-synaptic membrane fraction; PSD, post synaptic density (PSD) fraction.

### **3.2 Subcellular localization of WWP1 and WWP2 in neurons**

The loss of function mutant of *wwp-1* in *C.elegans* shows severe defects in axonal guidance and presynaptic synaptogenesis [Sieburth et al., 2005, and Schmitz et al., 2007]. These results indicate that *wwp-1* is dominantly expressed in neurons. However, the subcellular distribution of WWP1 family proteins in the mammalian neuron has never been explored. In order to address this question, I studied the localization of WWP1 and WWP1 in developing and mature neurons by immunofluorescence microscopy.

#### **3.2.1 Axonal localization of WWP1 and WWP2 in developing neurons**

To study subcellular localization of WWP1 and WWP2 during neuronal development, expression vectors for enhanced green fluorescence protein (EGFP)-fusion proteins of WWP1 (EGFP-WWP1) and WWP2 (EGFP-WWP2), and control EGFP were transfected to wild type rat hippocampal neurons in culture at day in vitro 1 (DIV1) using the calcium phosphate transfection method. The relatively low transfection efficiency with this method allows the tracing of entire neurites projecting from an EGFP-expressing neuron at DIV4. EGFP-WWP1 was enriched at the distal region of the axon, especially at the growth cone, and EGFP-WWP2 was enriched at both the proximal and distal regions of the axon, while control EGFP was evenly and diffusely distributed throughout the neuron (Fig. 3-2). The polarized distributions of these ligases are similar to those of proteins that exert functions in neuronal polarity, i.e., SAD-A/B, LKB1 kinases, Tsc1/2, and TGF $\beta$  Receptors1/2 [Kishi et al., 2005; Barnes et al., 2007; Shelly et al., 2007; Choi, et al., 2008; Yi et al., 2010]. These results indicate that WWP1 and WWP2 may play roles in neuronal polarity formation or axon specification in the developing neuron.

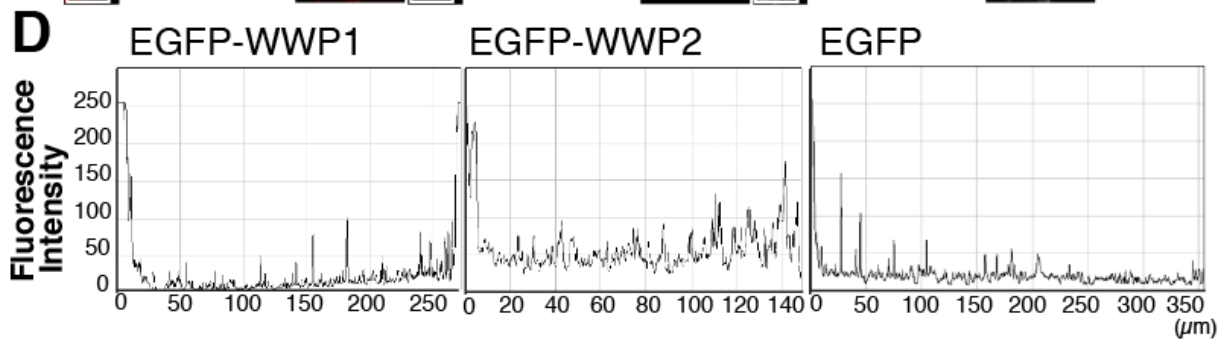
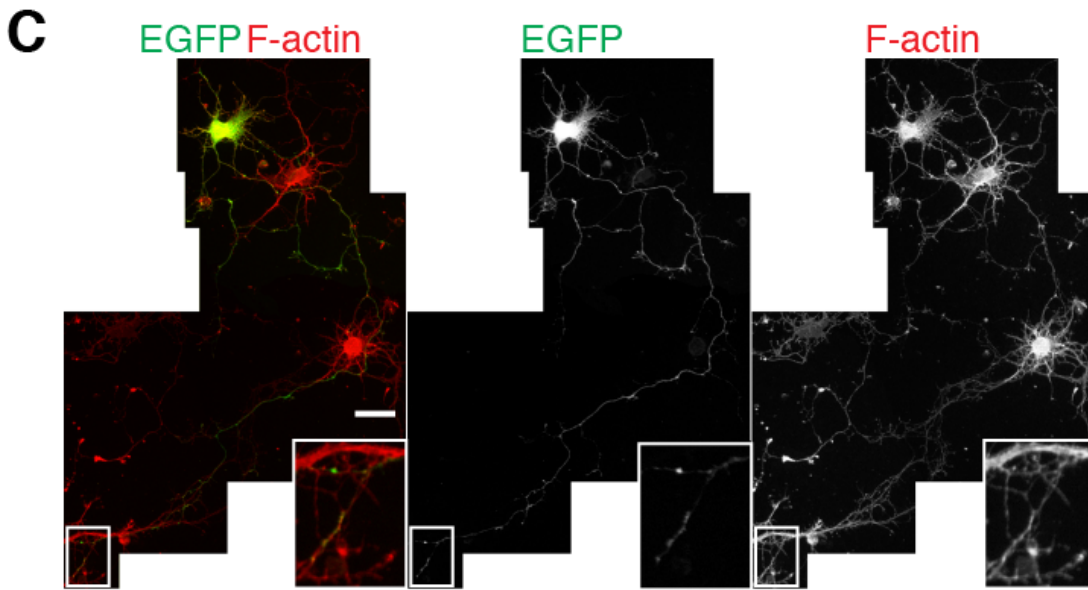
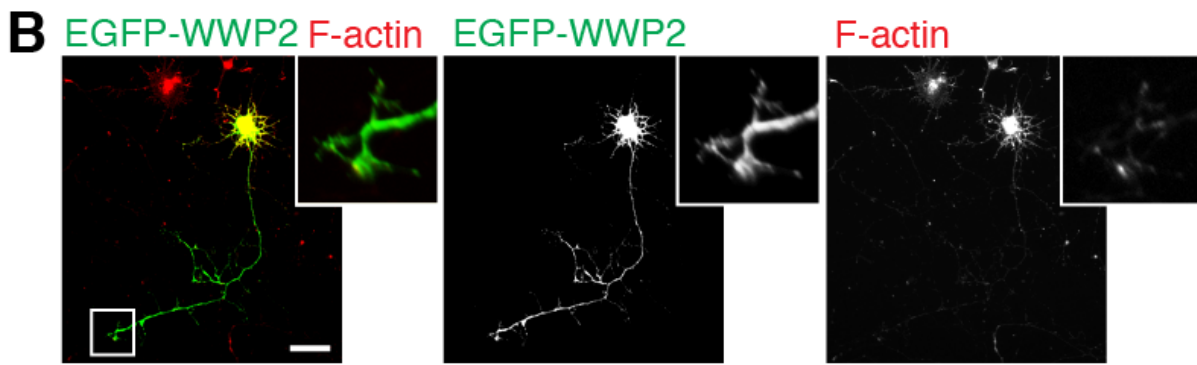
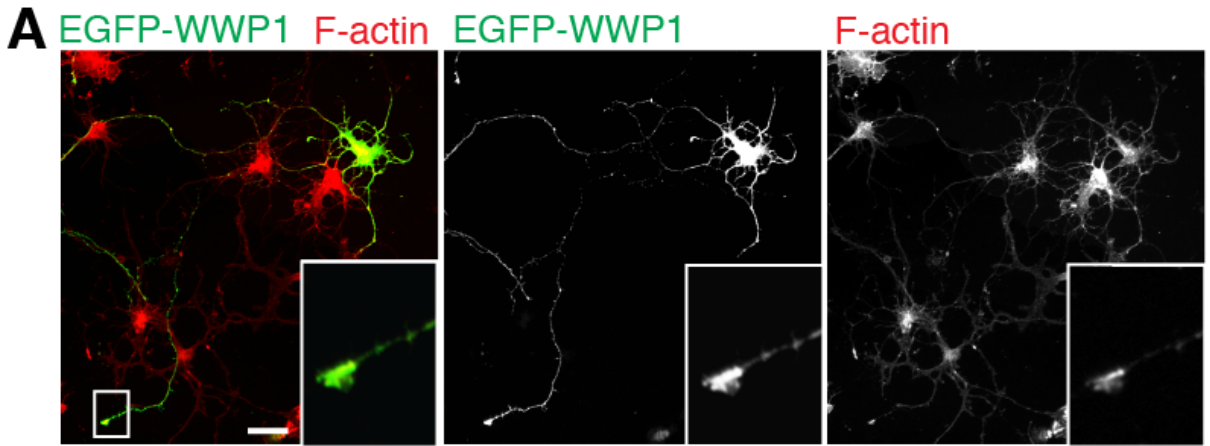




**Figure 3-2 Axonal localization of WWP1 and WWP2 in developing neurons**

(A, B, C) Wild type rat hippocampal neurons were transfected with expression vectors for EGFP-WWP1 (A), EGFP-WWP2 (B), or control EGFP (C) by the calcium phosphate method at DIV1. Neurons were fixed at DIV4 and labeled for F-actin using rhodamine phalloidin. (D) Fluorescence intensity profiles of EGFP-WWP1, EGFP-WWP2, and control EGFP along the axon (the longest neurite in A, B, and C, respectively.) Note that EGFP-WWP1 and -WWP2 are enriched in the axon. Enlargements of the indicated white rectangular regions are shown as insets in each panel. Scale bar = 20  $\mu$ m.

**3.2.2 Synaptic localization of WWP1 and WWP2 in neurons**

In the next set of experiments, I studied the subcellular localization of WWP1 and WWP2 in the mature neuron. EGFP-WWP1 and EGFP-WWP2 were expressed in cultured hippocampal neurons by the lentivirus system. In mature neurons, EGFP-WWP1 and -WWP2 showed punctate signals along neurites, partially colocalizing with the presynaptic active zone protein Bassoon [Dieck et al., 1998] (Fig. 3-3A, B). To test if WWP1 and WWP2 localize to postsynapses, I transfected the expression vectors for EGFP-WWP1, EGFP-WWP2, or EGFP to hippocampal neurons by the calcium phosphate method at DIV4. The neurons were fixed at DIV21 and immunostained with an antibody to PSD-95 as a marker of the postsynaptic density (PSD) [Kornau et al., 1995; Okabe et al., 2001]. Punctate signals for EGFP-WWP1 and -WWP2 colocalized almost perfectly with PSD95, while control EGFP showed a diffuse distribution (Fig. 3-3C-E). The extent of colocalization was quantified by deriving the Pearson's correlation coefficient for the two fluorophores (see Materials and Methods). On average, the Pearson's correlation coefficient was  $0.80 \pm 0.020$  (mean  $\pm$ SEM) for EGFP-WWP1 and PSD95, and  $0.67 \pm 0.025$  for EGFP-WWP2 and PSD95. These values were significantly higher than that for EGFP and PSD-95 ( $0.34 \pm 0.024$ ), indicating that EGFP-WWP1 and -WWP2 co-localize strongly with PSD95 at dendritic spines (Fig. 3-3F).

These results are consistent with biochemical subcellular fractionation analyses (Fig. 3-1D) and indicate that WWP1 and WWP2 are localized at pre- and postsynapses in mature neurons, where they may be involved in synaptic transmission and synaptogenesis in the mammalian brain.

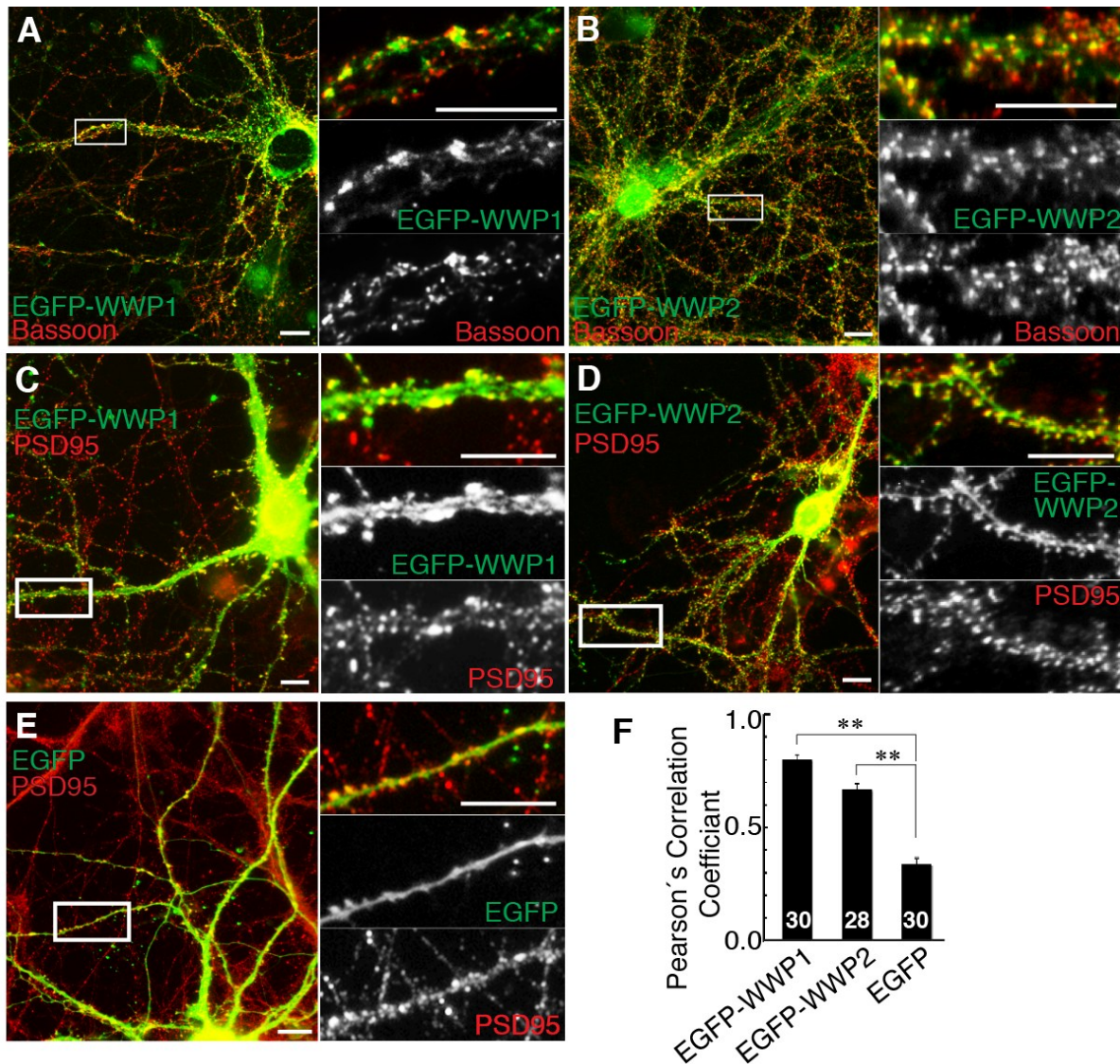


**Figure 3-3 Synaptic localization of WWP1 and WWP2**

(A, B) Wild type rat hippocampal neurons were infected with lentiviruses containing Synapsin promoter-driven expression cassettes for EGFP-WWP1 (A) or EGFP-WWP2 (B). Neurons were fixed at DIV21, and immunostained for Bassoon as a marker for the presynaptic active zone. EGFP-WWP1 and EGFP-WWP2 (green) partially colocalized with Bassoon (red). (C-E) Wild type rat hippocampal neurons were transfected with expression vectors for EGFP-WWP1 (C), EGFP-WWP2 (D), or EGFP

(E) by the calcium phosphate method at DIV4. Neurons were fixed at DIV21 and immunostained for PSD95 as a marker for the postsynaptic density. Note that EGFP-WWP1 and -WWP2 (green) show punctate signals, colocalizing with PSD95 (red) at dendritic spines, while control EGFP is distributed diffusely. (F) Pearson's correlation coefficients between EGFP-WWP1 and PSD95 ( $0.80 \pm 0.020$ ), between EGFP-WWP2 and PSD95 ( $0.67 \pm 0.025$ ), and between EGFP and PSD95 ( $0.34 \pm 0.024$ ), with the number of dendritic fields studied at the bottom of the bars. EGFP-WWP1 and EGFP-WWP2 are specifically colocalized with PSD95, while colocalization of EGFP and PSD95 is not specific. Scale bar = 20  $\mu\text{m}$ .

### 3.3 Generation of neuron specific WWP1 and WWP2 conditional KO mouse lines

In order to inactivate both *WWP1* and *WWP2* genes brain-specifically, we generated WWP1 and WWP2 conditional knockout mouse lines using the Cre/loxP recombination system. The Cre/loxP system is a powerful tool for activation and inactivation of specific genes in a spatially and temporally restricted manner [Sauer and Henderson, 1989; Rajewsky et al., 1996; reviewed by Kwan, 2002]. This allows biological questions to be addressed with exquisite accuracy and also helps circumventing early lethal phenotypes. Two mouse lines are required for conditional gene inactivation; first, a mouse strain with a mutation at the target gene flanked by two loxP sites ("floxed gene"), and second, conventional transgenic or knockin mouse lines with the Cre recombinase expression cassette targeted to specific cell types. Recombination (excision and consequently inactivation of the target gene) takes place only in cell types expressing Cre recombinase. Hence, the target gene remains active in all cell types that do not express Cre recombinase.

In preparation of the present study, Dr. Hiroshi Kawabe and Prof. Dr. Nils Brose generated two floxed mouse strains: floxed WWP1 and WWP2 mouse lines (Fig 3-4A-H). The exon 6 of WWP1 that encodes amino acid (aa) 180-216 and the exon 5 of WWP2 that encodes aa 160-191 were flanked by loxP sites. I verified that WWP1 and WWP2 protein expression was eliminated by overexpression of Cre recombinase in primary cultured neurons prepared from WWP1<sup>flox/flox</sup> and WWP2<sup>flox/flox</sup> mice (Fig. 3-4E, H).

I crossed these two mutant lines and obtained a double floxed WWP1 and WWP2 mouse line (WWP1<sup>f/f</sup>; WWP2<sup>f/f</sup>). Subsequently, the WWP1<sup>f/f</sup>; WWP2<sup>f/f</sup> line was crossed with two different Cre deleter lines, the Emx1-Cre line [Gorski *et al.*, 2002] and the NEX-Cre line [Goebbels *et al.*, 2006]. The Emx1-Cre line expresses Cre recombinase only in dorsal

telencephalic neuronal/glial precursors starting at around embryonic day 9.5 (E9.5) while the NEX-Cre line expresses Cre recombinase in dorsal telencephalic postmitotic neurons starting at E11.5 (Fig. 3-4I). Thus, the NEX-Cre line limits Cre expression to glutamatergic neurons while the Emx1-Cre line expresses Cre recombinase in both neurons and glia. I established two conditional WWP mutant lines, WWP1<sup>ff</sup>, WWP2<sup>ff</sup>; Emx1-Cre and WWP1<sup>ff</sup>, WWP2<sup>ff</sup>; NEX-Cre. Both of these conditional KO mice were born normally and remained viable and fertile.

To determine the efficiency of elimination of WWP proteins, I prepared crude postnuclear membrane fractions of the mouse cerebral cortex, and proteins in these fractions were separated by SDS-PAGE and analyzed by Western blotting. Protein expression of WWP1 and WWP2 were efficiently suppressed in both WWP1<sup>ff</sup>, WWP2<sup>ff</sup>; NEX-Cre and WWP1<sup>ff</sup>, WWP2<sup>ff</sup>; Emx1-Cre mice (Fig. 3-4J). Residual WWP1 and WWP2 expression in the WWP1<sup>ff</sup>, WWP2<sup>ff</sup>; NEX-Cre cortex was higher than those in the WWP1<sup>ff</sup>, WWP2<sup>ff</sup>; Emx1-Cre cortex probably because of expression of WWP proteins in GABA-ergic neurons and/or glia cells in the NEX-Cre recombined mouse.

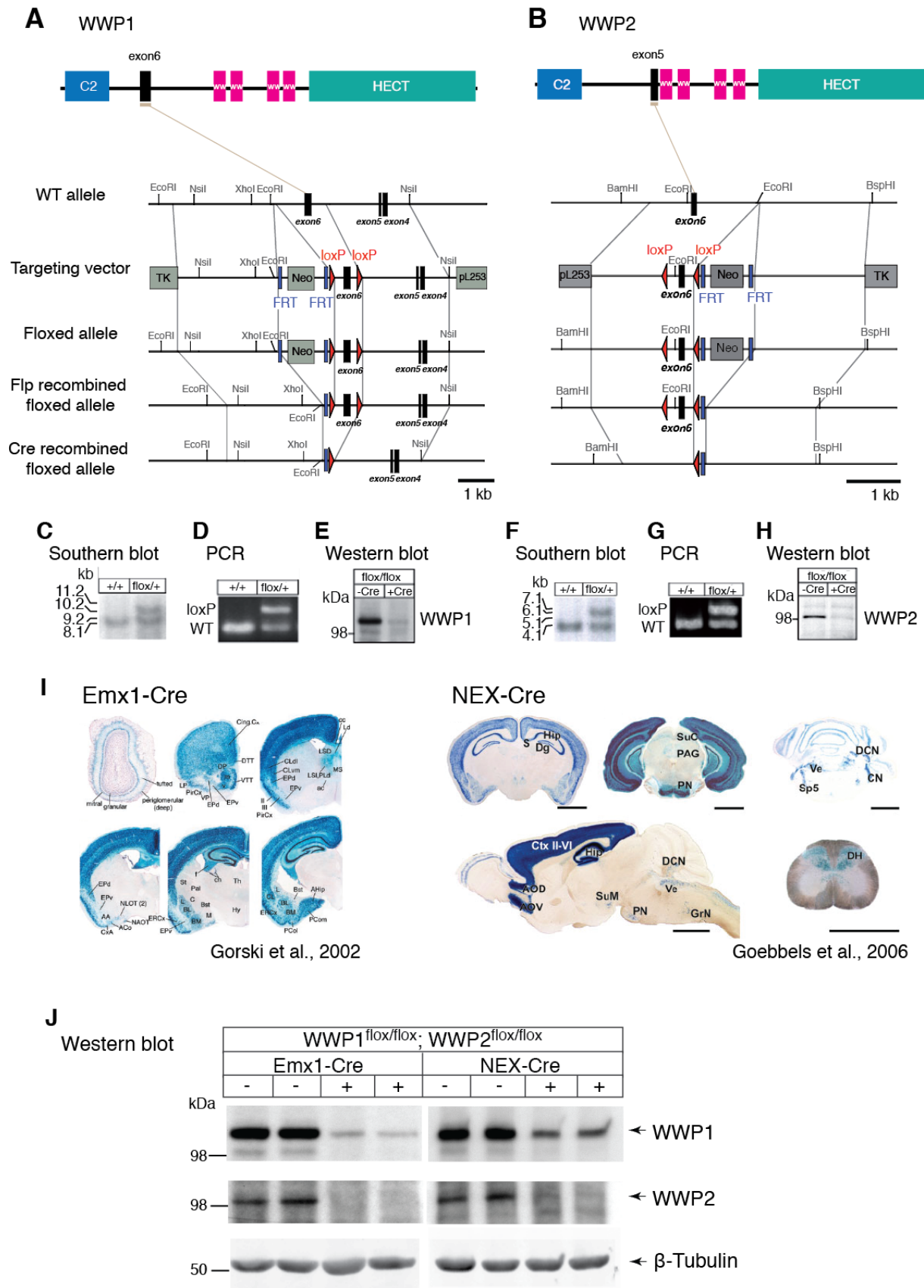


**Figure 3-4 Generation and basic characterization of WWP1 and WWP2 conditional knockout (KO) mouse lines**

(A, B) Targeting strategies for *WWP1* (A) and *WWP2* (B) genes. Domain structures of WWP1 and WWP2 proteins (top schemes), structures of the wild type (WT) *WWP1* and *WWP2* alleles (WT allele), *WWP1*<sup>flox</sup> and *WWP2*<sup>flox</sup> targeting vectors (Targeting vector), floxed mutant alleles (floxed allele, Flp recombined floxed allele, and Cre recombined floxed allele) of *WWP1* and *WWP2*. Exons are represented as black boxes. Flp recombinase targets (FRT) and loxP sites are represented as blue rectangles and red triangles, respectively. After homologous recombination and germ line transmission of mutant alleles, *WWP1*<sup>flox/+</sup> and *WWP2*<sup>flox/+</sup> mice were crossed with the FLP deleter line to delete the Neomycin resistance cassettes by Flp recombination. Subsequently, exons flanked by loxP sites in mutant alleles were floxed-out by Cre recombination. pL253, pL253 gene targeting vector; Neo, Neomycin resistance cassette; TK, herpes simplex virus thymidine kinase expression cassette. (C-H) Verification for gene targeting. (C, F) Southern blot analyses of genomic DNA samples of the WT (+/+) and targeted (flox/+) embryonic stem cells. BsrGI and NcoI were used for digestion of the genomic DNA purified from cloned embryonic stem cells of *WWP1*<sup>flox/+</sup> line (C) and *WWP2*<sup>flox/+</sup> line (F), respectively. 8.7 kb and 10.7 kb bands represent WT and *WWP1* floxed alleles in (C), 4.0 kb and 6.0 kb bands represent WT and *WWP2* floxed alleles in (F). (D, G) PCR analyses of genomic DNA samples from WT (+/+) and heterozygous (flox/+) mice. (E, H) Western blotting of lysates of primary cultured neurons prepared from the newborn homozygous (flox/flox, Flp recombined) mutants. The neurons were infected with lentiviruses for expression of the Cre recombinase (+Cre) or the negative control EGFP (-Cre) at day in vitro 1 (DIV1). The neurons were harvested at DIV21 and expression of endogenous WWP1 or WWP2 proteins was studied using custom made antibodies against WWP1 and WWP2. (I) X-gal staining of *Emx1*<sup>IRE5</sup> Cre;R26R (adapted from Gorski et al., 2002), and NEX-Cre; R26R or NEX-Cre; floxLacZ mice (adapted from Goebbeles et al., 2006). Blue signals in the images represent the Cre recombinase activity in each Cre driver mouse line. In the *Emx1*-Cre mouse, Cre is expressed exclusively in neocortical progenitors from E9.5, whereas in the NEX-Cre mouse, Cre is expressed almost exclusively in postmitotic neurons and not in progenitor cells from E11.5. (J) Western blotting of brain lysates of different genotypes. Crude postnuclear membrane fractions were prepared from the littermate with indicated genotypes at P5 and analyzed by Western blotting using antibodies against WWP1, WWP2, and  $\beta$ -Tubulin. Note that expression levels of WWP1 and WWP2 are drastically reduced when the Cre recombinase is expressed under the control of *Emx1* or NEX promoters.

### 3.4 The effect of WWP1 and WWP2 deficiency on axon specification

Considering the axonal localizations of WWP1 and WWP2 (Fig. 3-2), I first tested whether WWP1 and WWP2 play roles in axon specification during nerve cell development. For this purpose, I prepared cortical neuron cultures from newborn WWP1/2 conditional DKO (WWP1<sup>ff</sup>; WWP2<sup>ff</sup>; Emx1-Cre) and littermate controls (WWP1<sup>+/+</sup>; WWP2<sup>+/+</sup>; Emx1-Cre) and studied the morphologies of individual neurons at DIV7. At this stage of the culture, wild type neurons show a polarized shape with a single axon and multiple dendrites. The axon and dendrites are differentially labeled by microtubule associated proteins, phosphorylated Tau-1 and MAP2. Phospho-Tau-1 is abundant in the axon, whereas MAP2 decorates only dendritic microtubules [Dotti, et al., 1988; Kaech and Banker, 2006]. Neurons were transfected with an EGFP expression vector to visualize individual neurons using the calcium phosphate transfection method and immunostained for phospho-Tau-1 and MAP2 (Fig. 3-5A). Most control neurons (WWP1<sup>+/+</sup>; WWP2<sup>+/+</sup>; Emx1-Cre) possessed a single long Tau-positive, MAP2-negative axon (86.4 ±4.0%). In contrast, neurons lacking WWP1 and WWP2 (WWP1<sup>ff</sup>; WWP2<sup>ff</sup>; Emx1-Cre) extended multiple Tau-1-positive, MAP2-negative axons (45.7 ±0.6%). This striking result indicates that deletion of WWP1 and WWP2 induces multiple axons in the developing neuron.

Expression of Cre recombinase in the Emx1-Cre driver line starts around E9.5. Because of the early onset of expression of Cre recombinase in the Emx-Cre driver line, expression of WWP1 and WWP2 proteins in the WWP1<sup>ff</sup>; WWP2<sup>ff</sup>; Emx1-Cre mouse are significantly reduced at P0 when I dissected the hippocampus for primary culture of the neuron (Fig. 3-5A). The cultured neuron starts extending multiple neurites in twenty-four hours after settling on the glass coverslip and one of neurites acquire the specific features as the axon [i.e. excess speed of extension of the neurite and polarized distribution of the axon specific motor protein KIF3A [Nishimura et al, 2004] around DIV2 to DIV4. In order to

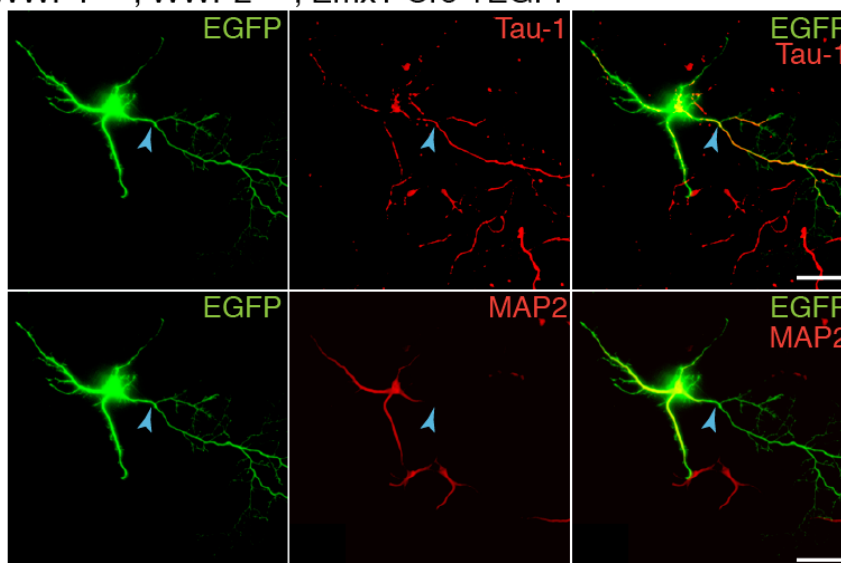


achieve later onset of downregulation of WWP1 and WWP2 during or after axon acquisition, I transfected WWP1<sup>f/f</sup>; WWP2<sup>f/f</sup> hippocampal neurons with the expression vector for Cre recombinase and EGFP by the calcium phosphate method at DIV1, and analyzed neurons at DIV7 (Fig 3-5B). With calcium phosphate transfection at DIV1, one can expect the onset of expression of recombinant proteins around DIV2 to DIV3 when the neurons start polarizing. Deletion of WWP1 and WWP2 in cultured neuron by overexpression of Cre recombinase caused the same multiple-axons phenotype as observed in WWP1<sup>f/f</sup>; WWP2<sup>f/f</sup>;Emx-Cre neurons. 85.7 ±2.8% of WWP1/WWP2 double KO neurons (WWP1<sup>f/f</sup>; WWP2<sup>f/f</sup> +EGFP +Cre) projected multiple neurites colocalizing with the axonal marker, whereas 82.8 ±6.8% of negative control neurons expressing only EGFP (WWP1<sup>f/f</sup>; WWP2<sup>f/f</sup> +EGFP) had a single axon. These results indicate that WWP1 and WWP2 are required for axon specification during neuritogenesis.

### **Figure 3-5 WWP1 and WWP2 are required for axon specification**

(A) Loss of function of WWP1 and WWP2 induces excess axon acquisition of neurites in cultured neurons. WWP1<sup>+/+</sup>; WWP2<sup>+/+</sup>; Emx1-Cre (upper panels) and WWP1<sup>ff</sup>; WWP2<sup>ff</sup>; Emx1-Cre (lower panels) cortical neurons were transfected with the expression vector for EGFP (pFUGW) at DIV4 by the calcium phosphate method and fixed at DIV7. (B) WWP1<sup>ff</sup>; WWP2<sup>ff</sup> hippocampal neurons were transfected with the expression vector for EGFP as a control (pFUGW, upper panels) or the expression vector for EGFP and Cre recombinase (pFUGW-iCre, lower panels) at DIV1 by the calcium phosphate method and fixed at DIV7. Subsequently, the neurons were immunostained with antibodies to Tau-1 (a marker for axons) and MAP2 (a marker for dendrites). The neurites from individual neurons were visualized by the EGFP signal. Blue arrowheads indicate axons (Tau-1-positive/MAP2-negative neurites) of EGFP-expressing neurons. Note that WWP1 and WWP2 deficient neurons project multiple axons. Neuronal polarities were categorized into three groups: one axon (red), two axons (blue), and  $\geq 3$  axons (yellow). P0 brain homogenates from each mouse were analyzed by Western blotting using antibodies for WWP1 and WWP2 in (A). \*p < 0.01 by Fisher's test. Scale bar = 20  $\mu$ m.

**A** WWP1<sup>+/+</sup>; WWP2<sup>+/+</sup>; Emx1-Cre +EGFP



WWP1<sup>ff</sup>; WWP2<sup>ff</sup>; Emx1-Cre +EGFP

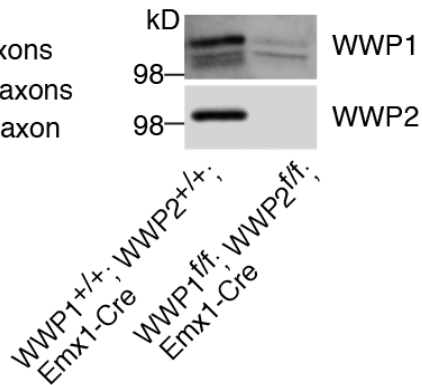
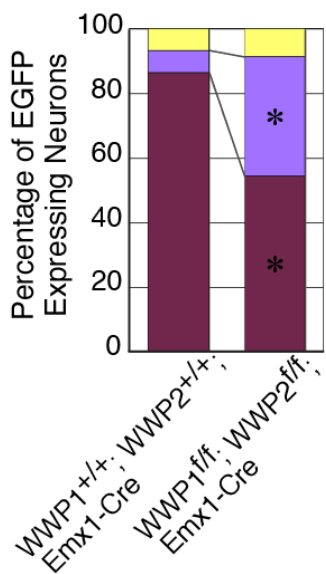
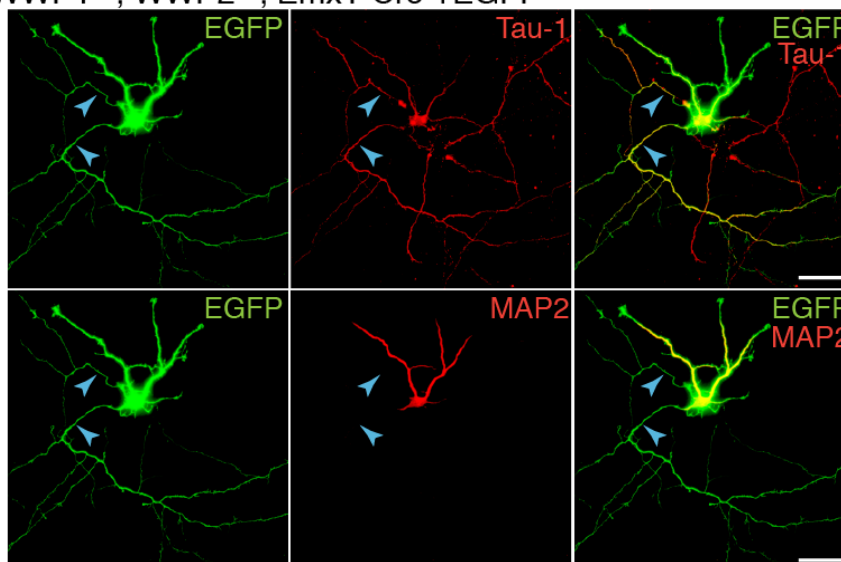
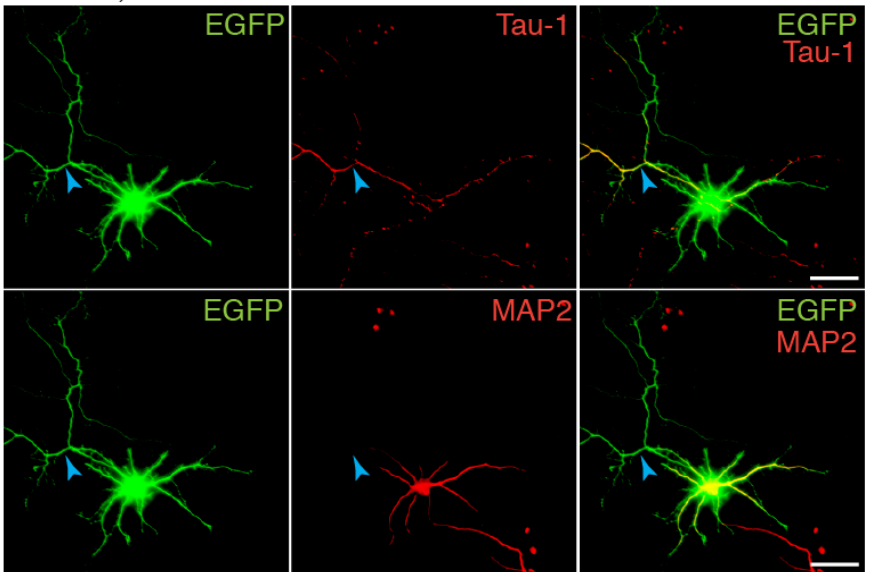


Figure 3-5

**B** WWP1<sup>ff</sup>; WWP2<sup>ff</sup> +EGFP



WWP1<sup>ff</sup>; WWP2<sup>ff</sup> +EGFP +Cre

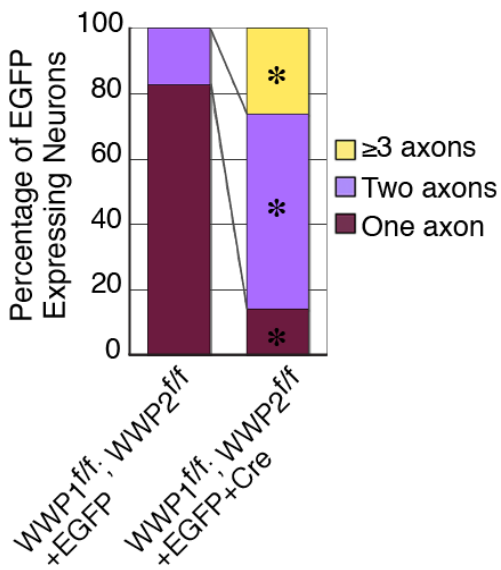
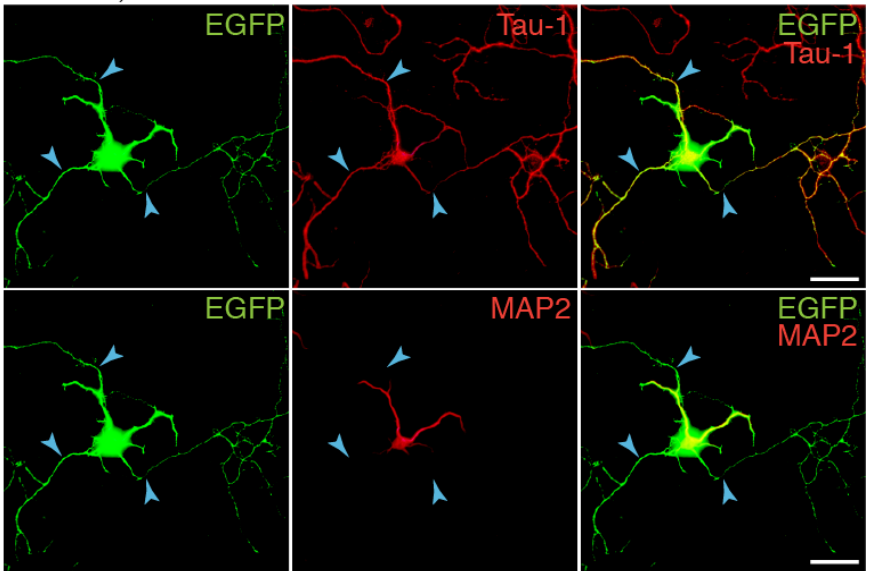
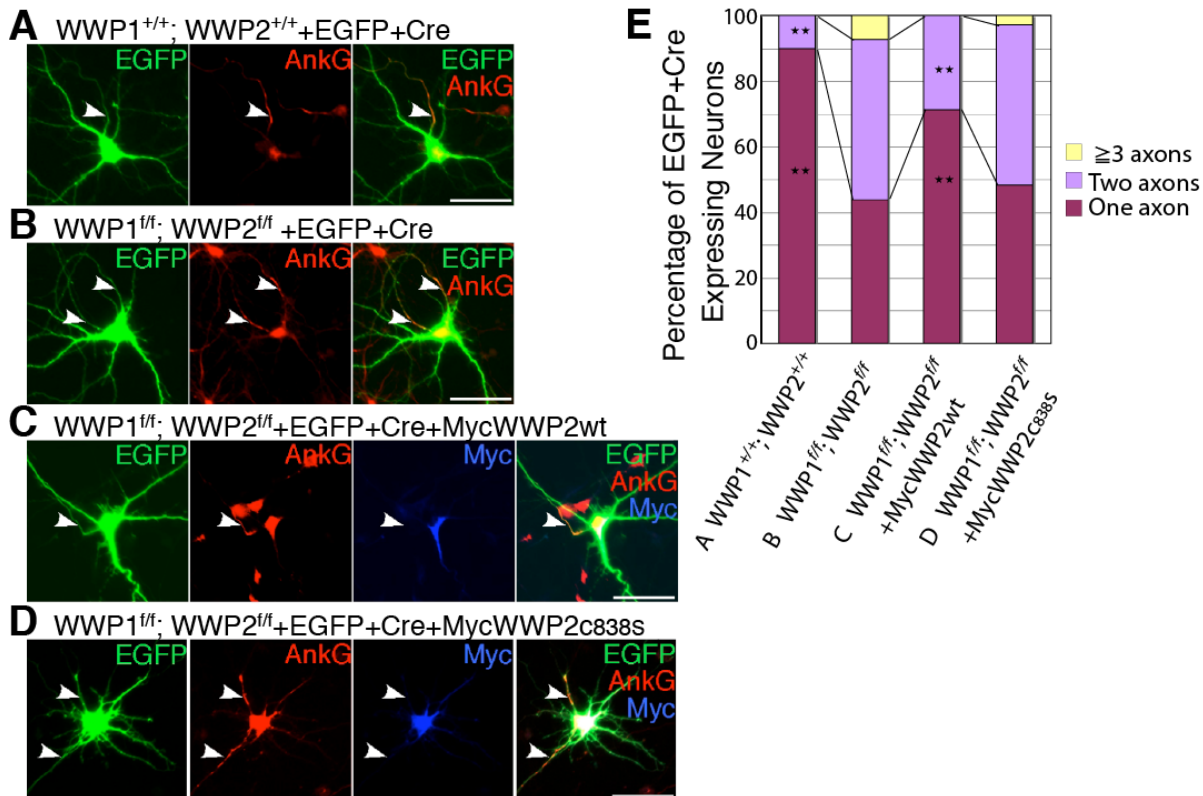


Figure 3-5

In order to verify this result, I immunostained WWP1/WWP2 double KO neurons with antibodies to an axon initial segment (AIS) marker, ankyrin G (AnkG), [Jenkins and Bennett, 2001]. Axons of EGFP and Cre expressing WT (WWP1<sup>+/+</sup>; WWP2<sup>+/+</sup>) or WWP1/2-floxed (WWP1<sup>f/f</sup>; WWP2<sup>f/f</sup>) neurons were identified as AnkG-positive, MAP2-negative neurites (Fig. 3-5B, b). Quantification of AnkG-positive, MAP2-negative axons showed that  $61.4 \pm 6.1\%$  of Cre expressing WWP1/2-floxed neurons projected multiple axons, while only 10% of control WT neurons had multiple axons (Fig. 3-5B). This result is consistent with the result obtained using anti-phospho-Tau antibody as a marker for the axon.

To test if the misregulation of axon acquisition in WWP1/WWP2 double KO neurons is a specific consequence of WWP1/2 loss, an expression vector for Myc-tagged wild type WWP2 (Myc-WWP2wt) was transfected in WWP1/2-floxed neurons together with the Cre expression vector (Fig. 3-6C). Transfected neurons were fixed at DIV7 and immunostained for Myc-WWP2wt and AnkG (Fig. 3-6C). Re-expression of Myc-WWP2wt rescued the multiple-axon phenotype as shown in Fig. 3-6C. In order to study whether the axon specification is dependent on the enzymatic activity of WWP2, a Myc-tagged catalytically inactive point mutant of WWP2 (Myc-WWP2C838S) was overexpressed in WWP1/WWP2 double KO neurons instead of Myc-WWP2wt. Although the expression level of Myc-WWP2C838S was comparable to that of Myc-WWP2wt (see the second panels from the right in Figs. 3-6C and D), overexpressed Myc-WWP2C838S failed to rescue the multiple-axon phenotype (Fig. 3-6D). From these results, I concluded that the cell-autonomous enzymatic activity of WWP E3 ligases is essential for formation of proper neuronal cell polarity by suppressing axon acquisition by multiple neurites during the neuronal development.



### Figure 3-6 Quantification of polarity defects and rescue experiments

(A-D) WWP1<sup>+/+</sup>; WWP2<sup>+/+</sup> or WWP1<sup>fl/fl</sup>; WWP2<sup>fl/fl</sup> hippocampal neurons were transfected with the expression vector for EGFP and Cre recombinase at DIV1 by the calcium phosphate method and fixed at DIV7. Individual neurons were visualized the EGFP signal. Axon initial segments (AIS) and dendrites were detected by immunostaining with anti-Ankyrin G antibody (AnkG, red) and anti-MAP2 antibody (data not shown), respectively. For rescue experiments, Myc-tagged wild type WWP2 (MycWWP2wt) or the catalytically inactive point mutant of WWP2 (MycWWP2c838s) were co-expressed with EGFP and Cre recombinase, and analyzed by immunostaining with the anti-Myc antibody. White arrows show AnkG positive- and MAP2 negative-axons. Scale bar = 20  $\mu$ m.

(E) Quantification of neuronal cell polarities. Note that the multiple-axon phenotype was rescued by MycWWP2wt overexpression, while MycWWP2c838s overexpression failed to rescue the phenotype.

\*\*p < 0.0001 by chi-squared test comparison with WWP1/2-KO condition (B).

### 3.5 WWP1 and WWP2 are required for polarity formation in developing cortical neurons *in vivo*

To explore the role of WWP1 and WWP2 in neuronal polarity formation *in vivo*, I analyzed the brain-specific WWP1/2 double conditional knockout mouse. As shown in Fig. 3-7, the WWP1<sup>ff</sup>;WWP2<sup>ff</sup>;Emx1-Cre mouse showed a slight hypertrophy at the caudal region of the forebrain as compared with the control WWP1<sup>ff</sup>;WWP2<sup>ff</sup> mouse at postnatal day 7 (P7). Given the slow turnover of WWP1 and WWP2 proteins, it is likely that both WWP1 and WWP2 proteins remain expressed in the radial glial cells during the neurogenic phase in the WWP1<sup>ff</sup>;WWP2<sup>ff</sup>;Emx1-Cre mouse. Thus, the increased thickness of the cortex in the WWP1<sup>ff</sup>;WWP2<sup>ff</sup>;Emx1-Cre mouse does not seem to be due to the upregulation of neurogenesis but rather seems to be due to developmental misregulation of post-mitotic neurons.

In order to study the impact of WWP1 and WWP2 loss-of-function on neuronal development *in vivo*, the morphology of individual neurons was visualized by over-expressing the membrane-anchored variant of Venus. For this purpose, I employed the *in utero* electroporation method as shown in Fig. 3-8A [Nagai et al., 2002; Rhee et al, 2006]. pCX-myrVenus was injected into the lateral ventricle at E14–E15 (Fig. 3-8A[a]) and transfected into a subpopulation of neuronal progenitor cells by applying electrical pulses (Fig. 3-8A[b]). Brain sections were prepared at postnatal day 0 (P0) or at P7, and then immunostained for the axon initial segment marker, Ankyrin G (AnkG).

I acquired confocal images of cortical neurons expressing myr-Venus with serial z-stacks to reconstitute neurites projecting directly from the cell body. In the P0 cortex, WWP1<sup>ff</sup>;WWP2<sup>ff</sup>;Emx1-Cre neurons were similar in morphology to WWP1<sup>ff</sup>;WWP2<sup>ff</sup> neurons, exhibiting normal migration and polarization (Fig. 3-8B). However, at P7, neurons showed a severe defect in migration in the somatosensory cortex of the

WWP1<sup>ff</sup>;WWP2<sup>ff</sup>;Emx1-Cre mouse. In the WWP1<sup>ff</sup>;WWP2<sup>ff</sup> control mouse, Venus-positive neurons were mostly located in layer II/III, which is the normal destination for cortical pyramidal neurons derived from progenitor cells transfected at E14–15 [Saito and Nakatsuji, 2001]. In contrast, nearly half of the Venus-positive neurons in the P7 WWP1<sup>ff</sup>;WWP2<sup>ff</sup>;Emx1-Cre cortex were located in layer IV–VI and in the intermediate/subventricular zone (IZ/SVZ) (Fig. 3-8C, left panels). These neurons in the WWP1<sup>ff</sup>;WWP2<sup>ff</sup>;Emx1-Cre cortex showed complex morphology with long processes that ran diagonally or tangentially rather than radially. Analyzing the orientation of the dendritic main shaft of Venus-positive neurons in Layer IV revealed that 87% of WWP1<sup>ff</sup>;WWP2<sup>ff</sup> control neurons extended thick apical dendrites toward the marginal zone, while 43% of WWP1<sup>ff</sup>;WWP2<sup>ff</sup>;Emx1-Cre neurons displayed aberrant dendrite orientation (Figs. 18D-a and 18F-a).

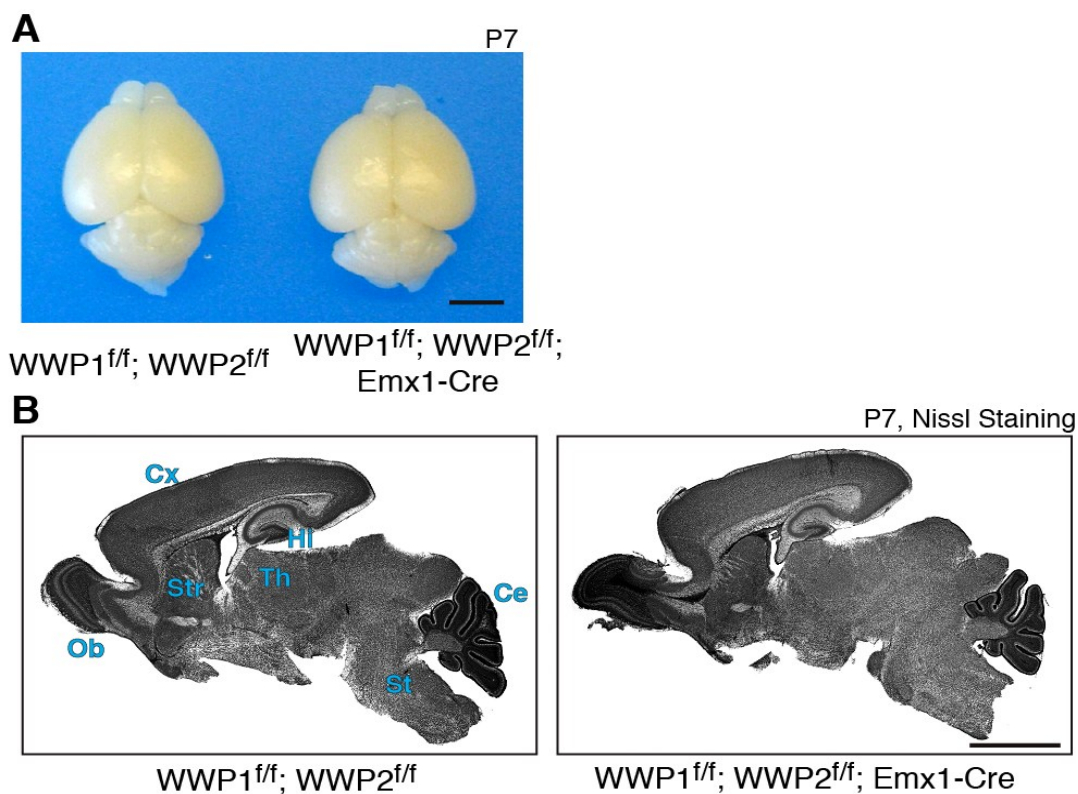


**Figure 3-7 WWP1/2 conditional KO mouse exhibits a slight hypertrophy in cortical and hippocampal architectures**



Appearances (A) and nissl stained sagittal sections (B) of brains from P7 control (WWP1<sup>ff</sup>;WWP2<sup>ff</sup>) and WWP1/2 conditional KO (WWP1<sup>ff</sup>;WWP2<sup>ff</sup>;Emx1-Cre) littermates. Note that the thickness of the cortex is slightly increased in the conditional KO. *Ce*, cerebellum; *Cx*, cerebral cortex; *Hi*, hippocampus; *Ob*, olfactory bulb; *St*, brainstem; *Str*, striatum; *Th*, thalamus. Scale bar = 5 mm.

---

Given that Cre expression is not limited to the postmitotic neurons in the EmxCre driver mouse line, this neuronal phenotype could be due to the misregulation of surrounding cell types, astrocytes, or oligodendrocytes. To study this possibility, I analyzed neurons lacking WWP1/2 proteins in the normal cortical surrounding. I introduced pFUGW-iCre, the expression vector for Cre recombinase, into cortical progenitors of WWP1<sup>+/+</sup>;WWP2<sup>+/+</sup> or WWP1<sup>ff</sup>;WWP2<sup>ff</sup> mouse embryos with pCX-myrVenus by *in utero* electroporation at E13.5. It has been reported that EGFP-labeled neurons stop migration earlier, and mostly stay in deeper layers, layers II/III–IV, at P7 when EGFP expression vectors are transfected by *in utero* electroporation at E13.5 instead of E14.5 [Langevin et al., 2007]. Cre-expressing cells were detected by immunostaining using an anti-Cre antibody at P7 (data not shown), and neurons co-expressing Cre and Venus were analyzed. In both genotypes, most neurons localized at layers II–IV while some neurons still showed severe migration delay in the WWP1<sup>ff</sup>;WWP2<sup>ff</sup> mouse (Fig. 3-8C). In layer IV of the WWP1<sup>+/+</sup>;WWP2<sup>+/+</sup> cortex, 90% of Cre- and Venus-co-expressing neurons showed the typical morphology of pyramidal neurons with a thick apical dendrite pointing toward the marginal zone and a thin long axon projected radially toward the intermediate zone. In contrast, 48% of Cre- and Venus-co-expressing WWP1<sup>ff</sup>;WWP2<sup>ff</sup> neurons displayed an abnormal axon-dendrite orientation. Dendritic shafts were oriented laterally or basally, and AnkG-positive axons orientated laterally or apically in such neurons (Fig. 3-8D). Some of these neurons possessed axons projecting toward the pia from the cell body and turning toward the intermediate zone (Fig. 3-8D). These results indicate that WWP1 and WWP2 are required for cell-autonomous neuronal morphogenesis and polarity formation.

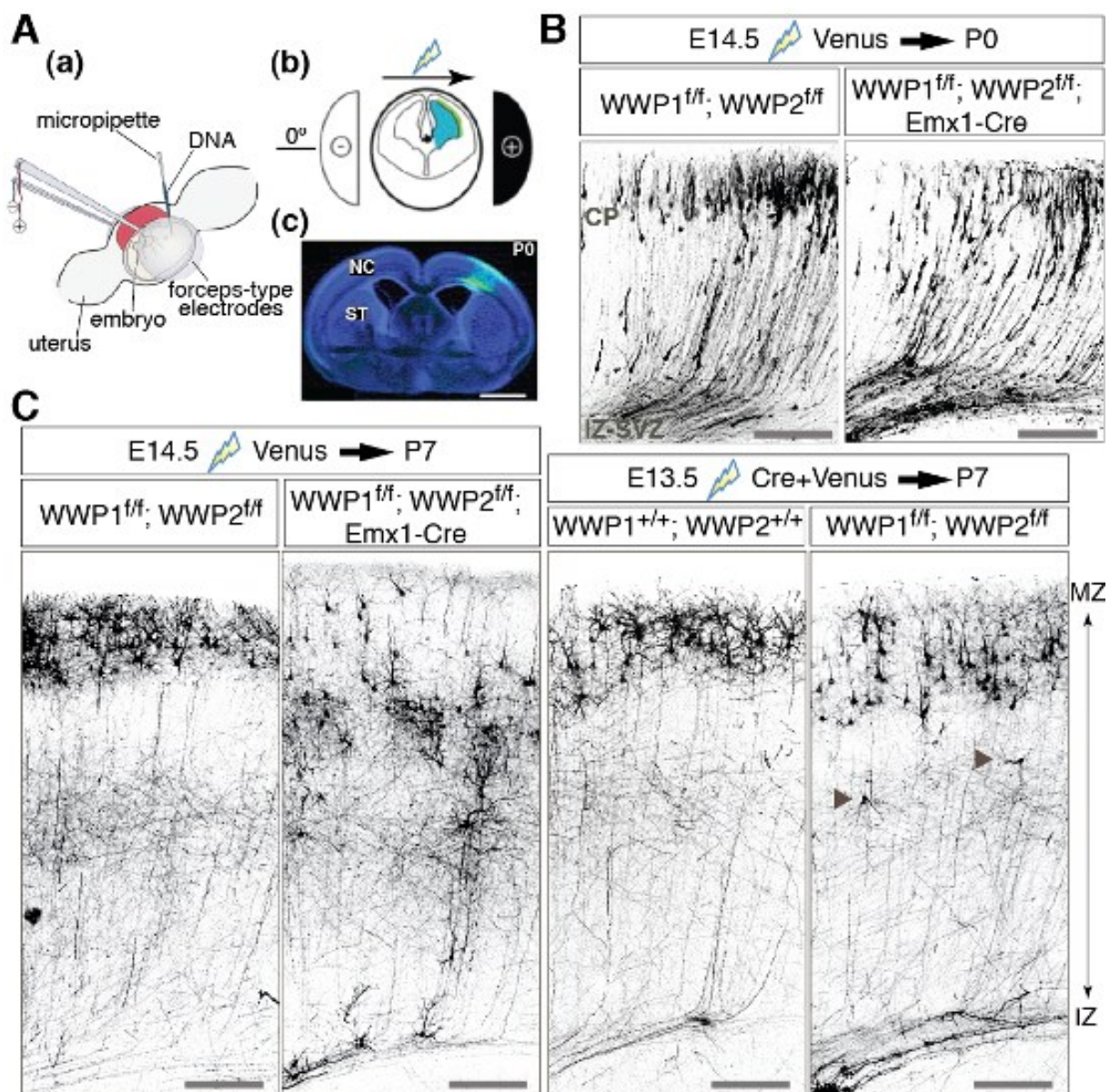
I further examined whether neurons lacking WWP1/2 proteins possess multiple axons *in vivo*. In the WWP1<sup>ff</sup>;WWP2<sup>ff</sup>;Emx1-Cre cortex, in which Cre is expressed from E9–10, 10% of neurons (4/40 neurons in low density regions of transfected cells) displayed multiple AnkG-positive axons (Fig. 3-8F). Although the number of neurons showing multiple axon phenotypes is smaller as compared to the *in vitro* culture experiment shown in Fig. 3-5, these results indicate that WWP1 and WWP2 have important roles for establishing neuronal polarity *in vivo*. Considering the timing of Cre recombinase expression, it is likely that WWP1 and WWP2 have different roles in various stages of neuronal development, i.e. axon acquisition, neuronal migration, and orientation of dendrites and the axon.

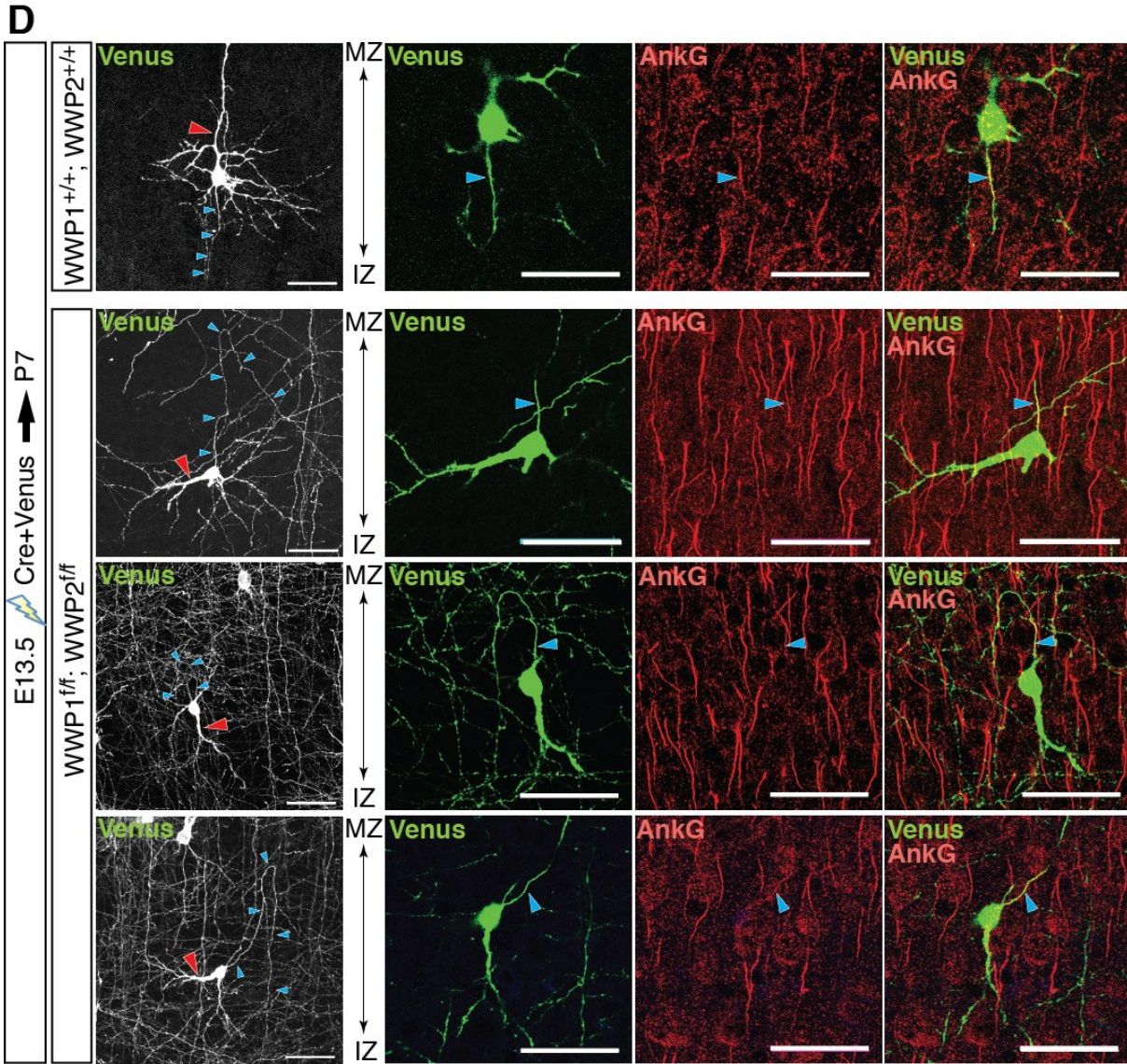
**Figure 3-8 WWP1 and WWP2 are required for polarity formation in developing cortical neurons *in vivo***

(A) Schematic illustration of *in utero* electroporation. (a) Plasmid DNA containing Fast Green was injected into the lateral ventricle of embryos through the uterine wall using a micropipette. Electronic pulses were then applied to the brain from outside the uterine wall using forceps-type electrodes. (b) When the electrodes are placed at 0° from the brain's horizontal plane, the DNA injected into the lateral ventricle (blue) is transferred into the ventricular zone cells (green) of the adjacent neocortex (NC). (c) A coronal section of P0 brain electroporated with an expression vector for GFP at E14.5 as illustrated in (b). GFP fluorescence (green) was observed in the ventricular zone and the upper cortical plate of the NC. These images are modified from Borrell et al. (2005). ST, striatum. Scale bar = 1 mm.

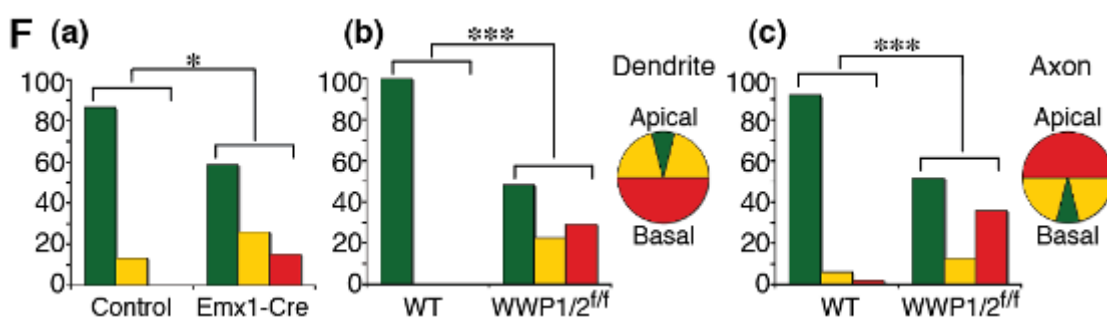
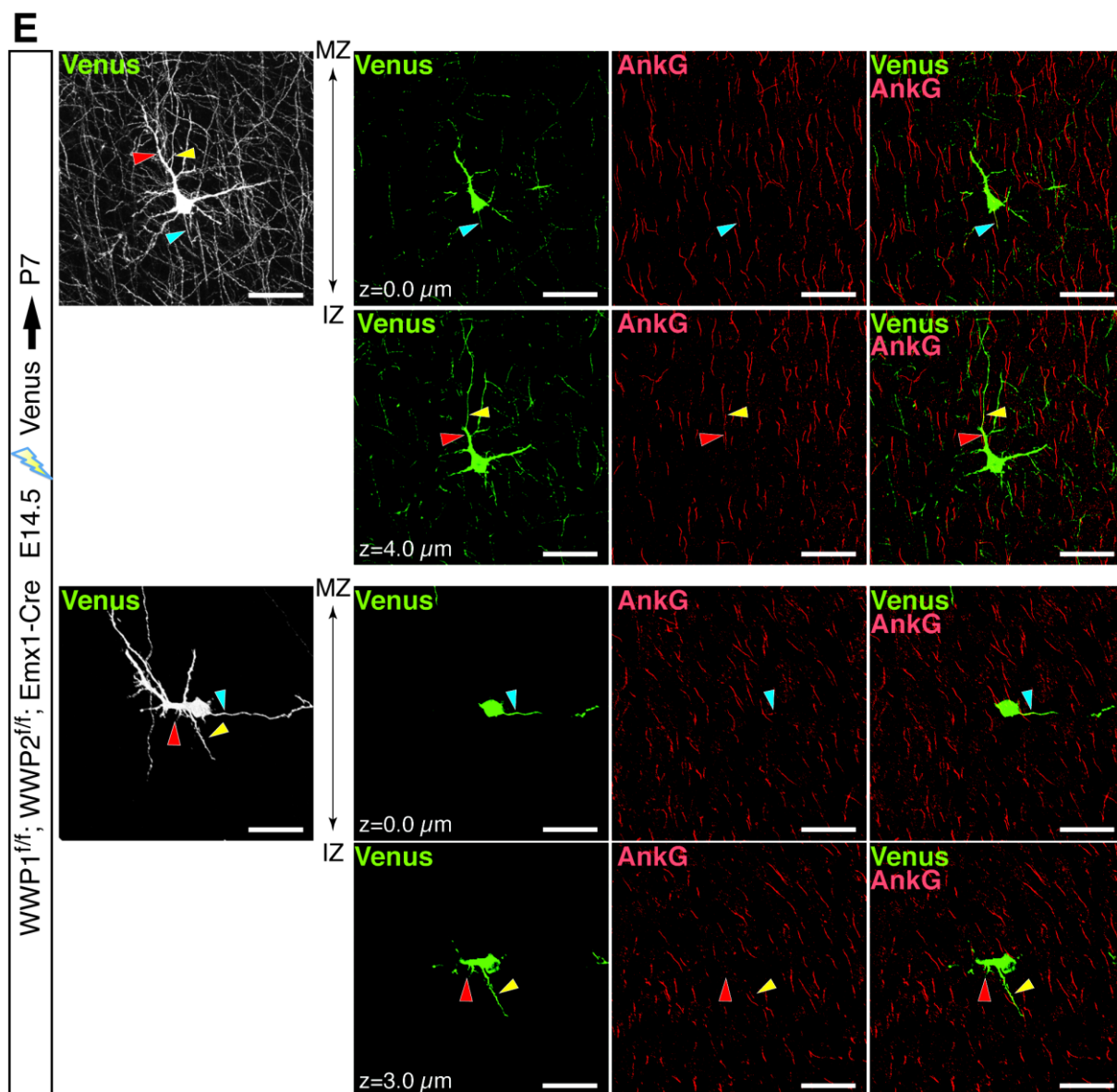
(B) Venus fluorescence of P0 WWP1<sup>ff</sup>;WWP2<sup>ff</sup> or WWP1<sup>ff</sup>;WWP2<sup>ff</sup>;Emx1-Cre mouse cortices transfected with the Venus expression vector by *in utero* electroporation at E14.5. CP, cortical plate; IZ, intermediate zone; SVZ, subventricular zone. Scale bar = 200 μm.

(C) (Left panels) Venus fluorescence of P7 WWP1<sup>ff</sup>;WWP2<sup>ff</sup> or WWP1<sup>ff</sup>;WWP2<sup>ff</sup>;Emx1-Cre mouse cortices transfected with the Venus expression vector by *in utero* electroporation at E14.5. Note that in the WWP1<sup>ff</sup>;WWP2<sup>ff</sup>;Emx1-Cre mouse cortex, transfected neurons show retarded migration. (Right panels) Venus fluorescence of P7 WWP1<sup>+/+</sup>;WWP2<sup>+/+</sup> or WWP1<sup>ff</sup>;WWP2<sup>ff</sup> mouse cortices cotransfected with the expression vectors for Cre recombinase and Venus by *in utero* electroporation at E13.5. Arrowheads indicate neurons with apparent abnormal dendrite-axon projections in layer IV. MZ, marginal zone; IZ, intermediate zone. Scale bar = 200 μm.





(D, E) 2D projection of serial z-stack confocal images (gray scale images at left panels) and each confocal image (RBG color images at right panels) of individual neurons in (C). The brain section with myrVenus-expressing neurons was counterstained with Ankyrin G (AnkG) to label the axon initial segment. (D) The axons projecting from the WWP1/2 double KO neuron (blue arrowheads) are directed toward the marginal zone (MZ) first and then turn toward the intermediate zone (IZ). Blue and red arrowheads indicate the axonal process and dendritic main shaft, respectively. (E) Neurons with multiple axons (blue and yellow arrowheads) in the WWP1<sup>fl/fl</sup>; WWP2<sup>fl/fl</sup>; Emx1-Cre mouse cortex. Note that a second AnkG-positive axon (yellow arrowheads) is projecting from dendritic shafts. Scale bar = 50  $\mu$ m. (F) Quantification of polarity defects of WWP1/2 double knockout neurons at P7 in layer IV. Phenotypes were categorized into three groups based on the orientation of the dendritic main shaft (a, b) or orientation of the axon (c); (a, b) apical orientation within 15° (green), lateral orientation 15 and 90° (yellow) and basal orientation with >90° (red); (c) basal orientation within 15°



(green), lateral orientation between 15 and 90° (yellow), and apical orientation with >90° (red). The main shaft of the dendrite (a, b) or the axon (c) were largely rotated from the vertical axis upon between 15 and 90° (yellow) and basal orientation with >90° (red); (c) basal orientation within 15° (green), lateral orientation between 15 and 90° (yellow), and apical orientation with >90° (red). expression of Cre under the control of the endogenous Emx promoter (a) or exogenous over-expression of Cre (b, c). Neurons in regions with low transfection efficiency were analyzed in order to trace all neurites projecting from individual neurons.

## 3.6 Identification of WWP1 and WWP2 interacting proteins in the mammalian brain

### 3.6.1 Affinity purification of WWP1- and WWP2-binding proteins from synaptosomes

In order to identify the physiological targets of WWP1 and WWP2, I purified WWP1- and WWP2-binding proteins by affinity chromatography. Purified GST-fused WW domains of WWP1 (residues 335–582, GST-WWP1) or WWP2 (residues 290–533, GST-WWP2) were immobilized on glutathione-Sepharose beads and a Triton X-100 extract of rat brain synaptosomes (P2 fraction) was loaded. After washing nonspecifically bound proteins from the beads with the TritonX-100 extraction buffer, bound proteins were eluted from the affinity columns with 1 M NaCl and subjected to SDS-PAGE. Protein bands enriched in the eluate from the GST-WWP1 and GST-WWP2 columns were analyzed by mass spectrometry and 10 proteins bound to GST-WWP1 or GST-WWP2 were identified.

Among these, liprin- $\alpha$ 3 was identified as a WWP1-binding protein (Fig. 3-9A). Liprin- $\alpha$ 3 is a synaptic scaffolding protein and a member of the evolutionarily conserved liprin- $\alpha$  protein family. Liprin- $\alpha$  proteins were originally identified by their interaction with the leukocyte-common antigen-related family of receptor protein tyrosine phosphatases [Serra-Pages et al., 1995]. Four mammalian liprin- $\alpha$  isoforms, liprin- $\alpha$ 1, - $\alpha$ 2, - $\alpha$ 3 and - $\alpha$ 4, have been identified and cloned [Serra-Pages et al., 1998]. Both *C. elegans* and *Drosophila* only have a single copy of the liprin- $\alpha$  gene, *syd-2* (synapse defective-2) in *C. elegans* and Dliprin (*Drosophila* liprin) in *Drosophila* [Zhen et al., 1999, Kaufmann et al., 2002]. While the synaptic function of liprin- $\alpha$  in vertebrates is largely unknown, *syd-2* and Dliprin play important roles in invertebrate synapse development, neurotransmitter release and synaptic protein trafficking. Given that *syd-2* is functionally related to *wwp-1* in *C. elegans* synaptogenesis and synaptic transmission [Ch'ng et al., 2008], it should be important to investigate whether WWP1 and WWP2 interact with mammalian Liprin- $\alpha$  and are required

for synaptic functions.

### 3.6.2 Liprin- $\alpha$ 3 is a specific ubiquitination substrate of WWP1 and WWP2

I first verified the results from the mass spectrometry analysis by Western blotting using an antibody specific for liprin- $\alpha$ 3 (Fig. 3-9B), which does not cross-react with other liprin family members, liprin- $\alpha$ 1,  $\alpha$ 2 or  $\alpha$ 4. Liprin- $\alpha$ 3 was present in the affinity-purified material that eluted from the GST-WWP1 column with 1M NaCl (Fig. 3-9B right panel). I further eluted GST-WWP1 and GST-WWP2 with their bound proteins from the glutathione-sepharose beads with 40 mM glutathione and subjected the eluate to Western blot analysis. Liprin- $\alpha$ 3 was detected in the eluate from both GST-WWP1 and GST-WWP2 columns (Fig. 3-9B left panel), indicating that interaction between liprin- $\alpha$ 3 and WWP1 or WWP2 is strong and partially resistant to 1M NaCl.

In order to examine whether the interaction with WWP1 and WWP2 leads to ubiquitination of liprin- $\alpha$ 3, I performed an ubiquitination assay in heterologous cells. Expression vectors for FLAG-tagged liprin- $\alpha$ 3 (FLAG-liprin- $\alpha$ 3), HA-tagged ubiquitin, and EGFP-tagged WWP1wt or WWP2wt were cotransfected into HEK293FT cells. FLAG-liprin- $\alpha$ 3 was then immunoprecipitated from cell extracts using an anti-FLAG antibody. Ubiquitination of immunoprecipitated proteins was detected by Western blotting with an anti-HA antibody. Although endogenous WWP1 and WWP2 in HEK293FT cells might ubiquitinate FLAG-liprin- $\alpha$ 3, smear patterns of ubiquitin-reactive bands in immunoprecipitates were enhanced by overexpressed EGFP-WWP1wt and -WWP2wt (Fig. 3-9C). EGFP-WWP1 and -WWP2 were also co-immunoprecipitated with FLAG-liprin- $\alpha$ 3, indicating that they may form a complex. These results are consistent with the affinity purification data and indicate that liprin- $\alpha$ 3 is ubiquitinated by WWP1 and WWP2.

### 3.6.3 Ubiquitination of SAD kinase by WWP1 and WWP2

In *C. elegans* *wwp-1*/Wwp1 and 2, *syd-2*/Liprin- $\alpha$  and *sad-1*/SAD kinases are

functionally related in presynaptic synaptogenesis [Ch'ng et al., 2007]. SAD-1 plays a role both in establishing neuronal polarity at an early developmental stage and in maintaining synaptic vesicle clustering at a later stage [Crump et al., 2001; Kim et al., 2008]. *sad-1* has two mammalian orthologs, SAD-A and SAD-B. SAD-B regulates the release of neurotransmitters while being associated to the presynaptic cytomatrix and synaptic vesicles in rats [Inoue et al., 2006]. Neurons in double knockout mice of both *Sad-A* and *Sad-B* genes fail to develop axons in the brain, indicating that SAD kinases regulate neuronal polarity [Kishi et al., 2005]. Considering the polarity defects in neurons lacking WWP1 and WWP2 in the developing neuron (Fig. 3-4–7) and synaptic localization of WWP1 and WWP2 in the mature neuron (Fig. 3-1D and 3-3), it is likely that the functional correlation between Wwp-1/WWP1 and WWP2 E3 ligases, and *Sad-1/SAD-A* and *SAD-B* kinases is evolutionarily conserved.

To examine the ubiquitination of SAD kinases by WWP1 and WWP2, FLAG-tagged SAD-A (FLAG-SAD-A), HA-tagged ubiquitin, and EGFP-tagged WWP1wt, WWP2wt, WWP1C886S or WWP2C838S were coexpressed in HEK293FT cells. FLAG-SAD-A was immunoprecipitated using an anti-FLAG antibody. Immunoprecipitates from FLAG-SAD-A-expressing cell lysates showed a ladder of protein bands detected by anti-ubiquitin and anti-FLAG antibodies (Fig. 3-9D, upper panels). EGFP-WWP1wt, -WWP2wt, -WWP1C886S and -WWP2C838S were co-immunoprecipitated with FLAG-SAD-A. These results indicate that WWP1 and WWP2 interact with SAD-A and that SAD-A or its binding proteins may be ubiquitinated in HEK cells.

In order to test if SAD-A itself is ubiquitinated by WWP1 and WWP2, FLAG-SAD-A was extracted from HEK cells under denaturing conditions (95°C, 1% SDS) and immunoprecipitated using an anti-FLAG antibody. Anti-ubiquitin antibody crossreactive bands were detected only in the immunoprecipitates from EGFP-WWP1 and -WWP2 over-expressing HEK cells. This indicated that SAD-A itself, but not associated proteins, is



ubiquitinated by WWP1 and WWP2 (Fig. 3-9D, lower panels). The ubiquitination of FLAG-SAD-A was abolished when catalytically inactive mutants, WWP1C886S and WWP2C838S, were used instead of WWP1wt and WWP2wt. These results indicate that SAD-A kinase is a specific ubiquitination substrate of WWP1 and WWP2.

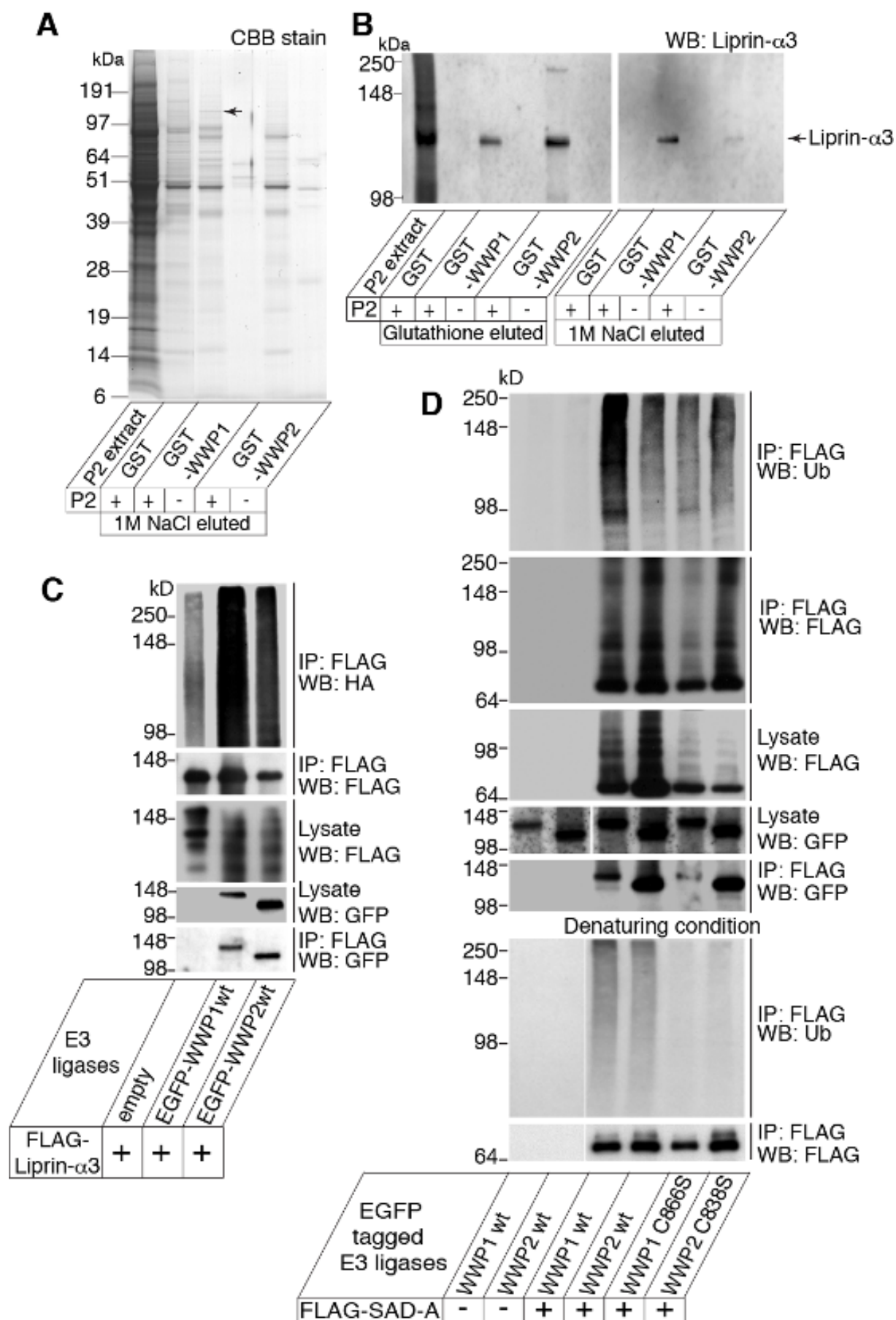


**Figure 3-9 Liprin- $\alpha$ 3 and SAD-A are ubiquitination substrates of WWP1 and WWP2**

(A) 40  $\mu$ g of GST, GST-WWP1 (residues 217–549) or GST-WWP2 (residues 217–549) were immobilized on glutathione-sepharose beads. A Triton X-100 extract of rat brain synaptosomes (P2 extract, +) or buffer (-) was loaded. After washing the beads, bound proteins were eluted with 1 M NaCl. The P2 extract and the 1 M NaCl eluate were separated by SDS-PAGE and stained with CBB. Protein bands enriched in the eluate from the GST-WWP1 or GST-WWP2 beads were analyzed by mass spectrometry. Liprin- $\alpha$ 3 was identified as a binding protein of GST-WWP1.

(B) Western blot analysis using an anti-Liprin- $\alpha$ 3 antibody on the same samples as (A). Liprin- $\alpha$ 3 was present in the P2 extract and in the eluate from GST-WWP1 and GST-WWP2 beads. Liprin- $\alpha$ 3 was bound to both GST-WWP1 and GST-WWP2.

(C) FLAG-tagged liprin- $\alpha$ 3 (FLAG-liprin- $\alpha$ 3) and HA-tagged ubiquitin were coexpressed in HEK293FT cells with EGFP-tagged WWP1wt, WWP1C886S, WWP2wt or WWP2C838S. FLAG-liprin- $\alpha$ 3 was immunoprecipitated using an anti-FLAG antibody. Immunoprecipitates (IP) were analyzed by Western blotting using anti-ubiquitin (Ub), anti-FLAG and anti-GFP antibodies. Note that liprin- $\alpha$ 3 was ubiquitinated by EGFP-WWP1wt and EGFP-WWP2wt.

(D) EGFP-tagged WWP1wt, WWP1C886S, WWP2wt or WWP2C838S and HA-tagged ubiquitin were coexpressed in HEK293FT cells with or without FLAG-tagged SAD-A kinase (FLAG-SAD-A). (Upper panels) FLAG-SAD-A was immunoprecipitated using an anti-FLAG antibody. Immunoprecipitates (IP) were analyzed by Western blotting using anti-Ub, anti-FLAG and anti-GFP antibodies. (Lower panels) For analysis of ubiquitinated FLAG-SAD-A after purification under denaturing conditions, FLAG-SAD-A was extracted from HEK293FT cells in the presence of 1% SDS and boiled for 5 min. FLAG-SAD-A was immunoprecipitated using an anti-FLAG antibody after dilution of the SDS extract with 10 volumes of a buffer containing 1% Triton X-100. Note that specific ubiquitination of purified FLAG-SAD-A by WWP1 and WWP2 was detected under denaturing conditions.

### 3.6.4 Yeast two-hybrid screening for proteins interacting with WWP1 and WWP2

To systematically identify proteins that physically interact with WWP1 and WWP2, I performed yeast two-hybrid (YTH) screening using rat and mouse brain cDNA libraries. I cloned eight bait vectors covering the entire sequences of WWP1 and WWP2 as listed below (see also Table 3-1 and Fig. 3-10A).

- 1) pGBDC2-WWP1<sub>1-344</sub>, covering 1–344 aa of WWP1, containing the C2 domain
- 2) pGBDC2-WWP1<sub>336-451</sub>, covering 336–451 aa of WWP1, containing the 1<sup>st</sup> and 2<sup>nd</sup> WW domains
- 3) pGBDC2-WWP1<sub>410-581</sub>, covering 410–581 aa of WWP1, containing the 3<sup>rd</sup> and 4<sup>th</sup> WW domains
- 4) pGBDC2-WWP1<sub>571-918</sub>, covering 571–918 aa of WWP1, containing the HECT domain
- 5) pGBDC2-WWP2<sub>1-287</sub>, covering 1–287 aa of WWP2, containing the C2 domain
- 6) pGBDC2-WWP2<sub>285-404</sub>, covering 285–404 aa of WWP2, containing the 1<sup>st</sup> and 2<sup>nd</sup> WW domains
- 7) pGBDC2-WWP2<sub>400-534</sub>, covering 400–534 aa of WWP2, containing the 3<sup>rd</sup> and 4<sup>th</sup> WW domains
- 8) pGBDC2-WWP2<sub>535-870</sub>, covering 535–870 aa of WWP2, containing the HECT domain

Subsequently, I examined the auto-activity of each bait vector by transforming PJ69-4A with each bait vector together with an empty prey vector. Only pGBDC2-WWP2<sub>285-404</sub> showed a strong auto-activity while the other seven vectors did not. These seven bait vectors were used for screening using rat or mouse brain libraries. 3–48 positive interacting clones were isolated from each screening (Table 3-1). After confirming the interaction by retransforming PJ69-4A with each individual bait vector and isolated and purified prey vectors, the prey vectors were sequenced. Eleven positive clones were found to encode open reading frames of rat or mouse cDNAs (Table 3-2).

	Bait constructs			Rat brain library		Mouse brain library	
	Bait vectors	Amino acid residues (aa)	Domain structure	Screening clone size ( $\times 10^6$ )	Number of positive interactive clones	Screening clone size ( $\times 10^6$ )	Number of positive interactive clones
1	pGBDC2-WWP1 <sub>1-344</sub>	1-344	C2	1.05	15	1.19	24
2	pGBDC2-WWP1 <sub>336-451</sub>	336-451	1 <sup>st</sup> and 2 <sup>nd</sup> WW	0.82	7	0.61	21
3	pGBDC2-WWP1 <sub>410-581</sub>	410-581	3 <sup>rd</sup> and 4 <sup>th</sup> WW	0.55	17	0.53	40
4	pGBDC2-WWP1 <sub>571-918</sub>	571-918	HECT	0.90	14	1.00	24
5	pGBDC2-WWP2 <sub>1-287</sub>	1-287	C2	0.95	3	1.00	7
6	pGBDC2-WWP2 <sub>285-404</sub>	285-404	1 <sup>st</sup> and 2 <sup>nd</sup> WW	-	-	-	-
7	pGBDC2-WWP2 <sub>400-534</sub>	400-534	3 <sup>rd</sup> and 4 <sup>th</sup> WW	1.20	19	0.75	48
8	pGBDC2-WWP2 <sub>535-870</sub>	535-870	HECT	1.34	48	1.03	24

**Table 3-1 Bait constructs used for YTH screening**

Amino acid residues and the domain structures of WWP1 and WWP2 covered by the bait constructs (see Fig. 3-10), the estimated numbers of the screened clones and the numbers of the positive interactive clones.

Proteins encoded by prey cDNAs of the positive interactive clones	GenBank accession number	Prey library	Number of positive interactive clones	Bait construct
solute carrier family 26, member 6	NP_001137289	rat	1	WWP1 <sub>336-451</sub>
Shank1a	AAD29417	rat	2	WWP1 <sub>410-581</sub>
amyloid beta precursor protein (cytoplasmic tail) binding protein 2	NP_001094439	rat	3	WWP1 <sub>410-581</sub>
glyceraldehyde 3-phosphate dehydrogenase, NAD binding domain.	XP_988596	mouse	1	WWP1 <sub>410-581</sub>
NADH dehydrogenase subunit K	NP_038400.2	mouse	1	WWP1 <sub>571-918</sub>
transthyretin	NP_038725	mouse	1	WWP2 <sub>1-287</sub>
ring-box 1, isoform CRA_a	EDL04571	mouse	1	WWP2 <sub>1-287</sub>
activating transcription factor 7 interacting protein (predicted), isoform CRA_a	EDM01611	rat	1	WWP2 <sub>535-870</sub>

**Table 3-2 Proteins encoded by the prey cDNAs of positive interacting clones**

### 3.6.5 Shank1a is identified as a WWP1 binding protein

Among these, the two independent prey clones that interact with the bait clone coding the 3<sup>rd</sup> and 4<sup>th</sup> WW domains of WWP1 overlapped with the amino acid residues 201–905 of rat Shank1a. Shank1a is an alternative splicing variant of Shank1, a member of a scaffold protein family comprising Shank1, Shank2 and Shank3, all of which are core components of the PSD in excitatory synapses of the CNS.

Shank proteins have two main functions in the CNS. First, they play roles as scaffolding molecules at the PSD by directly or indirectly interacting with AMPA receptors [Boeckers et al., 1999, Bruckner et al., 1999, Dong et al., 1997, and Wyszynski et al., 1999], NMDA receptors [Naisbitt et al., 1999] and metabotropic glutamate receptors [Tu et al., 1999]. It has been reported that these protein interactions are critical for the maturation of glutamatergic synapses, triggering the recruitment of synaptic AMPA receptors and increasing synaptic strength [Sala et al., 2001]. Second, Shank proteins interact with cortactin and regulate reorganization of the actin cytoskeleton, which is critical for dendritic spine morphogenesis and the subsequent synaptogenesis in response to repetitive stimuli of the mature postsynaptic neuron [Sala et al., 2001 and Hering et al., 2003]. Full-length Shank consists of multiple ankyrin repeats near the N-terminus followed by an SH3 domain, a PDZ domain, a long proline-rich region and a sterile alpha motif (SAM) at the C-terminus (Fig. 3-10B) [Boeckers et al., 1999; Du et al., 1998; Ehlers, 1999; Lim et al., 1999; Naisbitt et al., 1999; Sheng and Kim, 2000; Tu *et al.*, 1999; Zitzer *et al.*]. Each domain is responsible for a specific protein-protein interaction that is important for the formation and maintenance of the PSD. The region covered by the two prey clones contains some ankyrin repeats, the SH3 domain, the PDZ domain and a part of the proline-rich region. The partial proline rich region contained some proline-rich motifs (PPxY, PxxP, or PY motif, where P denotes proline, Y represents tyrosine, and x denotes any amino acid) that commonly act as binding sites for the WW domain. In biochemical preparations of the PSD, WWP1 and WWP2 are enriched and

resistant to extraction by Triton X-100 (Fig. 3-1D). Taken together with the postsynaptic localization of WWP1 and WWP2 (Fig. 3-3), these results indicate that the PSD scaffold proteins of the Shank family are potential binding partners of WWP1 and WWP2. I therefore analyzed these two prey clones encoding Shank1a further.

### **3.6.6 Shank1a is a ubiquitination substrate of WWP1 and WWP2**

To test if Shank1a is ubiquitinated by WWP1 and WWP2, I transfected expression vectors for Shank1a, HA-tagged ubiquitin, and EGFP-tagged WWP1wt, WWP1C886S, WWP2wt, WWP2C838S or EGFP into HEK293FT cells. Then, Shank1a was selectively pulled down using GKAP beads, sepharose beads covalently coupled with the C-terminal amino acids PEAQTRL of the GKAP protein, which have a high affinity for the PDZ domain of Shank proteins [Brendel et al., 2004]. Ubiquitination of Shank1a pulled down from cell lysates was determined by Western blotting using an anti-ubiquitin antibody. Anti-ubiquitin antibody crossreactive signals were enhanced in the presence of EGFP-WWP1wt and -WWP2wt, but not in the presence of EGFP-WWPC886S, -WWP2C838S or EGFP. These results indicate that Shank1a is a ubiquitination substrate of WWP1 and WWP2.

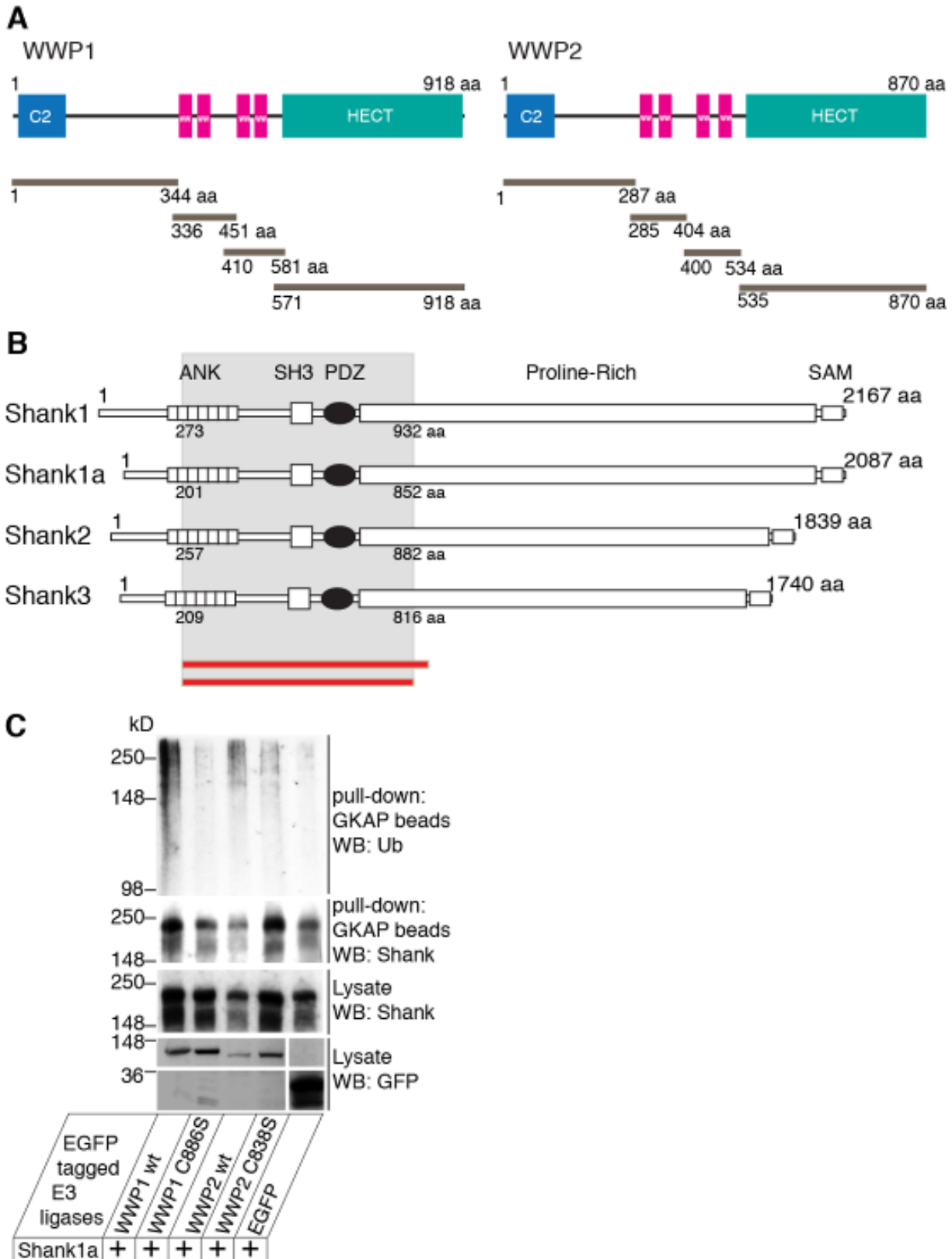


**Figure 3-10 Shank1a was isolated as a binding protein of WWP1 by YTH screening**

(A) Schematic diagram of the WWP1 and WWP2 bait proteins used in this study. Eight bait constructs covering amino acid residues 1–344, 336–451, 410–581 and 571–918 of WWP1, and 1–287, 285–404,



400–534 and 535–870 of WWP2 were cloned into a pGBDC2 YTH bait vector. C2, a C2 domain; WW, multiple WW domains; HECT, HECT domain.

(B) The domain organization of Shank family proteins and the relative location of rat Shank1a prey inserts (shown as red bars) isolated in the YTH screening. The common region of the two prey clones is indicated in light gray. Shank1 (GenBank Accession No. NP\_113939), Shank1a (an alternative splicing variant of Shank1, AAD29417.1), Shank2 (NP\_958738) and Shank3 (NP\_067708) are shown. ANK, multiple Ankyrin repeats; SH3, Src Homology domain 3; PDZ, PSD-95/Dig/ZO-1 domain; Proline-Rich, proline-rich region; SAM, a sterile alpha motif.

(C) Ubiquitination of Shank1a by WWP1 and WWP2. EGFP-tagged WWP1wt, WWP1C886S, WWP2wt, WWP2C838S or EGFP were coexpressed in HEK293FT cells with Shank1a and HA-tagged ubiquitin. Shank1a was pulled down using sepharose beads coupled with C-terminal amino acid peptides of GKAP (GKAP beads). The pull-down precipitates were analyzed by Western blotting using anti-ubiquitin (Ub), anti-Shank and anti-GFP antibodies. Note that ubiquitination of Shank1a was enhanced by coexpression of EGFP-WWP1wt and EGFP-WWP2wt.

	EGFP-WWP1	EGFP-WWP2	EGFP
$R_{(r)}$	0.80 ±0.020	0.67 ±0.025	0.34 ±0.024
	(n= 30)	(n= 28)	(n= 30)
	p< 0.0001	p< 0.0001	

**Table S1 Postsynaptic localization of EGFP-WWP1 and -WWP2**

Pearson's correlation coefficient ( $R_{(r)}$ ) between expression patterns of the EGFP tagged constructs and PSD95 in DIV21 neurons (related to Figure 3-3). The  $R_{(r)}$  values represent mean ±SEM. Comparison of  $R_{(r)}$  values between EGFP tagged constructs was determined by the unpaired t-test with Welch correction. The two-tailed P values show significant difference compared with the  $R_{(r)}$  value of control EGFP.

Number of axons	WWP1 <sup>+/+</sup> , WWP2 <sup>+/+</sup> , Emx1-Cre (n= 44)		WWP1 <sup>fl/fl</sup> , WWP2 <sup>fl/fl</sup> , Emx1-Cre (n= 46)		p= 0.0012
One	38	86.4 %	25	54.3 %	
Two	3	13.6 %	17	45.7 %	
≥3	3		4		

Number of axons	WWP1 <sup>fl/fl</sup> , WWP2 <sup>fl/fl</sup> +EGFP (n= 29)		WWP1 <sup>fl/fl</sup> , WWP2 <sup>fl/fl</sup> +EGFP +Cre (n= 42)		p< 0.0001
One	24	82.8 %	6	54.3 %	
Two	5	17.2 %	27	85.7 %	
≥3	0		9		

**Table S2 The effect of WWP1 and WWP2 deficiency on axon specification**

Number of neurons with one, two, or ≥3 axons, percentage of one-axon and multiple-axons neurons, and the two-sided P values from Fisher's exact test are represented (Related to Figure 3-5). Each condition is quantified from three independent experiments. The axon was detected by Tau-1 staining. Images of neurons were acquired and scored in a blind manner.

Number of axon	WWP1 <sup>+/+</sup> ; WWP2 <sup>+/+</sup> +EGFP +Cre (n=110)	WWP1 <sup>fl/fl</sup> ; WWP2 <sup>fl/fl</sup> +EGFP +Cre (n=274)	WWP1 <sup>fl/fl</sup> ; WWP2 <sup>fl/fl</sup> +EGFP +Cre +MycWWP2wt (n=188)	WWP1 <sup>fl/fl</sup> ; WWP2 <sup>fl/fl</sup> +EGFP +Cre +MycWWP2C838S (n=108)
One	99 (90.0%)	120 (43.7%)	134 (71.2%)	52 (48.1%)
Two	11 (10.0%)	134 (48.9%)	54 (28.7%)	53 (49.0%)
≥3	0 (0.00%)	20 (7.29%)	0 (0.00%)	3 (2.78%)
	p< 0.0001	-	p< 0.0001	p= 0.2280

**Table S3 Rescue of WWP1/2-KO phenotype by re-expression of MycWWP2**

Number and percentage of neurons with one, two, or ≥3 axons in each condition are represented (Related to Figure 3-6). Each condition is quantified from three independent experiments. The P values for each condition are determined by chi-squared test comparison with the WWP1/2-KO (WWP1<sup>fl/fl</sup>; WWP2<sup>fl/fl</sup>+EGFP +Cre) condition. The axon was detected by AnkG staining. Images of neurons were acquired and scored in a blind manner.

Angle of dendritic main shaft	WWP1 <sup>fl/fl</sup> ; WWP2 <sup>fl/fl</sup> ; (n= 30)		WWP1 <sup>fl/fl</sup> ; WWP2 <sup>fl/fl</sup> ; Emx1-Cre (n= 46)		p= 0.0012
0°-15°	26	86.7 %	27	58.7 %	
15°-90°	4	13.3%	12	26.1%	
>90°	0	0.0%	7	15.2%	

Angle of dendritic main shaft	WWP1 <sup>+/+</sup> ; WWP2 <sup>+/+</sup> +Cre (n= 50)		WWP1 <sup>fl/fl</sup> ; WWP2 <sup>fl/fl</sup> +Cre (n= 64)		p< 0.0001
0°-15°	46	92.0 %	33	51.5%	
15°-90°	3	6.0%	8	1.8%	
>90°	1	2.0%	23	35.9%	

Angle of axon	WWP1 <sup>+/+</sup> ; WWP2 <sup>+/+</sup> +Cre (n= 20)		WWP1 <sup>fl/fl</sup> ; WWP2 <sup>fl/fl</sup> +Cre (n= 62)		p< 0.0001
0°-15°	20	100.0 %	30	48.4%	
15°-90°	0	0.0%	14	22.6%	
>90°	0	0.0%	18	29.0%	

**Table S4 Neuronal polarity defects of the WWP1/2-KO neuron *in vivo***

Quantification of polarity defects of the WWP1/2-KO neuron *in vivo* (related to Figure 3-8). Number and percentage of neurons categorized into three groups and the two-sided P values from Fisher's exact test are represented. Each condition is quantified from three animals.

## 4 Discussion

### 4.1 WWP1 and WWP2 regulate axon specification and neuronal polarity formation

Recent studies have shown that ubiquitination can directly regulate mammalian nerve cell development. The HECT type E3 ubiquitin ligase Nedd4-1 acts as a positive regulator of dendrite extension and arborization. Ubiquitination by Nedd4-1 inhibits Rap2A function, reducing the activity of Rap2 effector kinases of the TNIK family and promoting dendrite growth [Kawabe et al., 2010]. The Nedd4 family E3 ligase Smurf1 contributes to axon initiation and promotes axon extension by regulating polarity protein PAR6 and growth-inhibiting RhoA [Cheng et al., 2011]. In addition to these HECT type E3 ligases, the RING Finger type E3 ligase APC and its adaptor protein Cdc20 promote dendrite growth by ubiquitinating the centrosomal protein Id1 [Kim et al., 2009]. In the present study, I demonstrated that WWP1 and WWP2 are required for proper neuronal morphogenesis during *in vitro* and *in vivo* development. WWP1/2 KO leads to the development of multiple axons in cultured neurons (Fig. 3-5). The cellular KO phenotype is rescued by re-expression of recombinant WWP2 (Fig. 3-6), indicating that this is due to the loss of cell-autonomous WWP1/2 function and not to secondary effects. This conclusion is supported by the fact that WWP1/2 KO neurons show related morphological changes, multiple axon formation and axon/dendrite misorientation in the developing cortex (Fig. 3-8). I conclude that WWP1 and WWP2 play a key role in neuronal polarization during development.

In the developing brain, neocortical pyramidal neurons polarize during migration (Fig. 1-3). Upon asymmetric cell division of radial glial progenitors, early unpolarized postmitotic neurons show a transient phase of unspecified neurite outgrowth in the subventricular zone. This occurs before adopting a bipolar morphology in the intermediate zone where cells

advance radial migration with a leading process directed toward the pial surface and a trailing process directed toward the ventricle. This leading process becomes the apical dendrite and the trailing process becomes the axon. After migration is complete, multiple dendrites are elaborated and the axon initial segment forms a diffusion barrier to maintain the distinct molecular composition of the axon [Nishimura et al., 2007]. Neuronal polarization can be regulated by intracellular and extracellular polarizing cues in each developmental step *in vivo*. A loss of WWP1/2 resulted in significant polarity defects in cortical neurons during development (Fig. 3-8). WWP1/2 KO neurons may fail to receive polarizing cues either directly from radial glial mother cells by inheritance or extracellular cues from contacting cells or elsewhere in the tissue.

#### **4.1.1 Molecular pathways involved in neuronal polarization *in vivo***

Using dissociated hippocampal neurons, many signaling molecules were found to be essential for neuronal polarization. These include the axon specific microtubule-associated protein CRMP-2 [Inagaki et al., 2001], the small GTPases Rap1B and Cdc42 [Schwamborn and Puschel, 2004], GSK3 $\beta$  and its upstream regulators PI3K and PTEN [Shi et al., 2003; Jing et al., 2005; Yoshimura et al., 2005], the plasma membrane ganglioside sialidase [Da Silva et al., 2005], the mammalian partitioning-defective (PAR) proteins PAR3 and PAR6 [Shi et al., 2003], PAR1-related SAD-A/B kinases and PAR4-related LKB1 kinase [Kishi et al., 2005; Barnes et al., 2007; Shelly et al., 2007], the tuberous sclerosis complex proteins Tsc1/2 [Choi et al., 2008], and the plus-end motor protein KIF3A [Nishimura et al., 2004]. Inactivation of these molecules abolishes axon differentiation or causes multiple axon formation *in vitro*.

Several *in vivo* studies have examined axon formation in the developing cortex and improved our understanding of molecular mechanisms underlying neuronal polarization. Loss

of the intracellular kinases SAD-A/B or LKB1 [Kishi et al., 2005; Barnes et al., 2007; Shelly et al., 2007] or the actin cytoskeleton regulatory Ena/VASP proteins [Kwiatkowski et al., 2007] results in failure of cortical neurons to develop a single axon. In corresponding knockout mice, neuronal migration is relatively normal despite the lack of axons. Loss of Tsc1/2 proteins also causes multiple axon formation [Choi et al., 2008]. Recently Cheng et al. (2011) demonstrated that depletion of the Nedd4 family E3 ligase Smurf1 by shRNA transfection causes neurons to accumulate in the IZ/SVZ and exhibit only short multiple processes. This indicates that neurons lacking Smurf1 fail to become bipolar and migrate radially [Cheng et al., 2011]. In addition to these intracellular signaling molecules, a recent study provided evidence that TGF $\beta$  signaling is required for both axon initiation and neuronal migration in the developing mouse neocortex. Loss of the TGF $\beta$  receptor type II (T $\beta$ R2) prevents axon formation and radial migration [Yi et al., 2010].

#### **4.1.2 LKB1-SAD pathway and WWP1/2**

Among these molecules involved in neuronal polarization, in this study I found that SAD-A kinase is ubiquitinated by WWP1/2. SAD-A/B kinases are the mammalian orthologues of PAR1 and required for creating neuronal polarity in the developing mouse brain [Kishi et al., 2005]. The entire signal pathway through SAD-A/B kinases in neuronal polarity formation has been studied in substantial detail (Fig. 4-1).

Among dozens of guidance cues, brain-derived neurotrophic factor (BDNF) [Shelly et al., 2007] and the class 3 secreted semaphorin, Sema3A, that is enriched in the most superficial part of the cortical wall at the top of the cortical plate, activate protein kinase A (PKA) [Collins et al., 2000] and p90RSK kinase [Sapkota et al., 2001]. These kinases phosphorylate the mammalian ortholog of PAR4, LKB1 kinase, at Ser431, which is critical for activation of this kinase. LKB1 is one of a few enzymes enriched at the axon. Activated

LKB1 phosphorylates and activates SAD kinases, which in turn phosphorylate the microtubule associated protein Tau at Ser262 [Barnes et al. 2007] that may promote axon specification and growth. Interestingly, phospho-SAD-A is enriched within the polarized axon preferentially [Barnes et al., 2007] while bulk SAD-A/B kinases localize to all neurites, i. e. axons and dendrites [Kishi et al., 2005]. Although it is still possible that phosphorylation of SAD-A/B takes place everywhere in the neuron and phospho-SAD-A/B is recruited by phospho-serine/threonine binding proteins enriched at the axon, it is more likely that axon-enriched LKB1 phosphorylates SAD-A/B in a spatially restricted manner and that this local activation of SAD-A/B is essential for establishment of the neuronal cell polarity.

Besides posttranslational regulation of the SAD kinase pathway by protein phosphorylation, translational regulation of SAD kinases is of critical importance for neuronal polarity formation. Tsc1 and Tsc2 form a protein complex and function as the GTPase activating protein (GAP) for the small GTPase Rheb. GTP-bound Rheb activates a protein kinase, mammalian target of rapamycin (mTOR), which is critical for translational regulation of a certain set of target genes. Loss of function of TSC1 or -2 in cultured neurons results in projection of the multiple axons, resembling the phenotype of the WWP1/2 double knockout neuron [Choi et al. 2008]. TSC2 deficient neurons exhibit increased levels of protein expression of SAD-A and -B while SAD mRNA levels are not changed. SAD-A protein level is not affected when proteasome-dependent protein degradation is blocked in either wild-type or Tsc2-deficient neurons, indicating that TSC1/2 suppress expression of SAD-A/B at the translation level, which is critical for regulation of this signal pathway for proper polarization of the neuron [Choi et al. 2008], (Fig. 4-1).

My biochemical data show that SAD-A itself, but not associated proteins including LKB1 or Tau, is ubiquitinated by WWP1 and -2 (Fig. 3-9D). Given that expression of SAD-A is not sensitive to proteasome inhibitors in cultured neurons [Choi et al. 2008], this ubiquitination may lead to non-proteasomal regulation of SAD-A, e.g. activation of the kinase

activity, recruitment of ubiquitin-interacting-motif (UIM) containing substrates, or subcellular compartmentalization of this kinase. Given that SAD-A itself has a putative UIM (see below) [Kishi et al., 2005] and that WWP1 has a strong biochemical activity to conjugate K63-linked polyubiquitin chains to substrates [Kim and Huibregtse, 2009], it is a possible scenario that K63-linked polyubiquitin chain conjugated to SAD-A interacts with its own UIM forming an intramolecular interaction that regulates the accessibility of the substrates or the enzymatic activity of this kinase.

#### **4.1.3 TGF $\beta$ signaling and WWP1/2**

Yi et al. (2010) reported recently that TGF $\beta$  is the dominant extracellular signaling molecule required for axon formation in the developing brain [Yi et al. 2010]. T $\beta$ R2 KO neurons show a bipolar morphology but fail to exhibit axonal growth at their trailing edges. TGF $\beta$  signaling for axon initiation depends on phosphorylation of the polarity protein PAR6. Over-expression of T $\beta$ R2 causes neurons to form multiple axons *in vitro*. Over-expression of a non-phosphorylatable PAR6 mutant blocks axon formation and prevents the induction of extra axons by over-expressed T $\beta$ R2. Over-expression of a phospho-mimetic PAR6 mutant in cortical slices, on the other hand, rescues axon formation in neurons lacking T $\beta$ R2, while this does not rescue the migration defect. This indicates that the signaling pathways for neuronal migration are separable from those for axon formation, even under control of the same extracellular cues [Yi et al., 2010]. Phosphorylated PAR6 might relocate phosphorylated Smurf1, which in turn promotes the proteasomal degradation of RhoA, altering local actin organization [Ozdamar et al., 2005; Cheng et al., 2011]. So far, such speculation connecting TGF $\beta$  signaling to the Smurf1 ubiquitination pathway has not been examined *in vivo*. Considering that the Smurf1 knockout mouse has no distinct neuronal phenotype as does the Smurf2 knockout mouse [Narimatsu et al., 2009], it is likely that other molecules including WWP1/2 might play a key role cooperatively with/without TGF $\beta$  signaling in neuronal



polarization *in vivo*. It would thus be important to understand molecular mechanisms for regulating TGF $\beta$  signaling in the developmental processes in neurons.

In human tumorigenesis, WWP1 participates in the regulation of TGF $\beta$  signaling [Kokumo et al., 2004]. TGF $\beta$  and related proteins, e.g., bone morphogenetic proteins (BMPs), bind to two types of serine/threonine kinase receptors, type I (T $\beta$ R1) and type II (T $\beta$ R2). This causes signal transduction through Smad proteins: receptor-regulated Smads (R-Smads)-Smad1, Smad2, Smad3, Smad5, Smad8/9, common-partner Smads (Co-Smads)-Smad4 and inhibitory Smads (I-Smads)-Smad6 and Smad7 [Heldin et al., 1997; Derzcnck et al., 1998; Attisano and Wrana, 2000; Kokumo et al., 2004]. Among these, R-Smads and C-Smad positively regulate TGF $\beta$  signaling. Upon phosphorylation by T $\beta$ R1, R-Smads form heteromeric complexes with Co-Smad, and translocate to the nucleus. Nuclear Smad complexes bind to transcription factors and coactivators/corepressors to regulate transcription of target genes [Mizayawa et al., 2002]. I-Smads are induced by transcriptional activation via TGF $\beta$  signaling, bind T $\beta$ R1 and prevent phosphorylation of R-Smads, resulting in the inhibition of TGF $\beta$  signaling [Imamura et al., 1999; Hanyu et al. 2001]. WWP1 interacts with Smad7 and negatively regulates TGF $\beta$  signaling in cooperation with Smad7, i.e., WWP1 binds to T $\beta$ R1 via Smad7 and induces ubiquitin-mediated degradation of T $\beta$ R1. Phosphorylation of Smad2 by T $\beta$ R1 is inhibited in the presence of WWP1 and inhibits transcriptional activity induced by TGF $\beta$  [Kokumo et al., 2004]. Considering that TGF $\beta$  signaling is critical for neuronal development [Yi et al., 2010], that WWP1/2 are expressed in the developing neuron and that T $\beta$ R2 KO neurons show an opposing phenotype to WWP1/2 KO neurons, I hypothesize that negative regulation of TGF $\beta$  signaling by WWP1/2 may contribute to neuronal polarization, normal axon specification and migration in the brain.

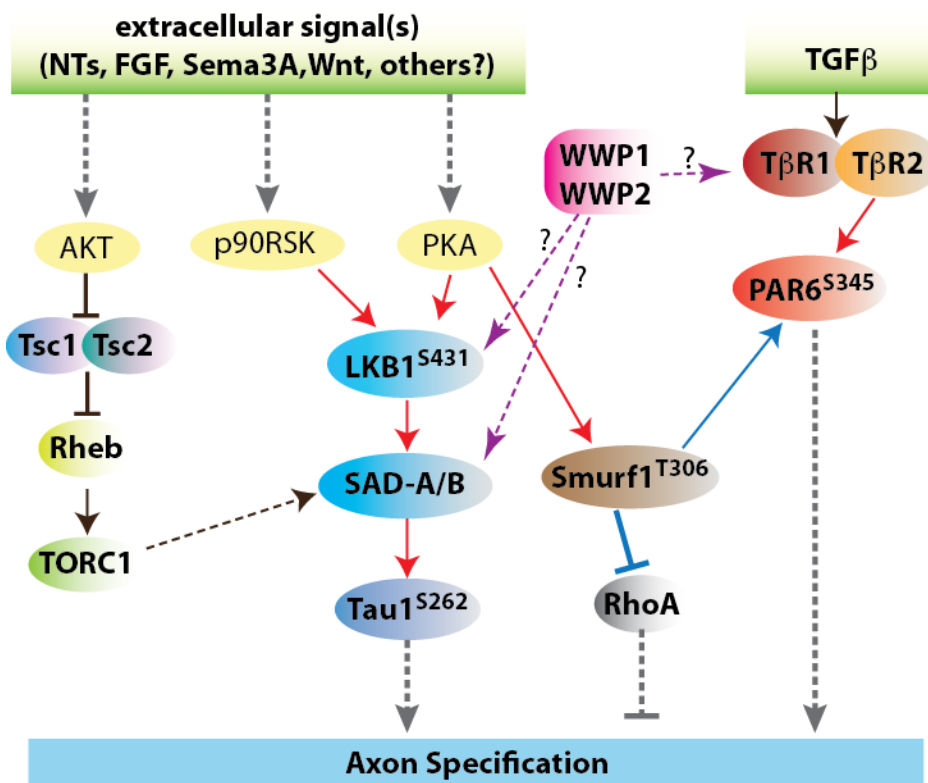


**Figure 4-1 Signaling pathways involved in axon specification in the mammalian brain**

Two pathways promote axon formation by regulating SAD kinase activity or SAD protein levels. SAD activity is positively regulated by LKB1 and is activated in response to extracellular signals such as BDNF [Barnes et al., 2007; Shelly et al., 2007]. In the absence of Tsc1-Tsc2 complex activity, the GTPase Rheb1 remains as a GTP-bound form and activates TORC1. TORC1 positively regulates translation of SAD-A/B kinases [Choi et al., 2008]. TGFβ signaling via PAR6 phosphorylation by TβR2 is required for axon formation [Yi et al., 2010]. Extracellular signals induce the phosphorylation of E3 ligase Smurf1 via activating PKA. The dendrite enriches unphosphorylated Smurf1 promoting polyubiquitination and degradation of PAR6 by the ubiquitin proteasome system (UPS) but not RhoA. This selective protein degradation leads to growth inhibition of the dendrites. Phosphorylated Smurf1 is enriched at the axon, where it targets RhoA for protein degradation by the UPS, while PAR6 becomes stabilized and promotes axon formation [Cheng et al., 2011]. WWP1 and WWP2 are required for axon specification, presumably by regulating LKB1-SAD signaling and/or TGFβ signaling.

## 4.2 Role of WWP1 and WWP2 in synaptic function

The molecular machinery underlying synaptic function consists of an intricate network of synaptic proteins. A synapse consists of a large number of proteins, of which at least 1500 exist in the human postsynapse density (PSD) [Bayes et al., 2011] and at least 410 proteins in the rat synaptic vesicle [Takamori et al., 2006]. Synaptic transmission involves large array of these synaptic proteins, which form the molecular machinery underlying transmitter release, activation and modulation of transmitter receptors, and signal transduction cascades. These processes are dynamically regulated and underlie the neuroplasticity crucial to learning and memory formation.

Neuroplasticity is mediated mainly by two ways; regulation of the efficacy of synaptic transmission or rearrangement the synaptic connectivity. Although the most basic aspects of synapse function, e.g., fusion of synaptic vesicles to the plasma membrane, have been studied extensively, the molecular basis of neuroplasticity remains largely unclear. Ube3A is the only E3 ligase reported to be critical for regulation of plasticity. Ube3A is involved in Angelman syndrome, which is characterized by mental retardation, stereotypical movement, and inappropriate laughter [Greer et al., 2010]. A recent study showed that Ube3A ubiquitinates a synaptic plasticity gene, *Arc/Arg3.1*, and that this ubiquitination cascade is critical for regulation of synaptic plasticity by modifying the surface expression of AMPA type glutamate receptors. Given the nature of protein ubiquitination in the regulation of multiple cellular functions, it is likely that more ubiquitination cascades are involved in neuroplasticity. In this study, I found that WWP1/2 E3 ligases localize to pre- and postsynapses (Fig. 3-1, 3) and that the synaptic proteins, *liprin- $\alpha$ 3*, *SAD-A* and *Shank1a*, are as specific ubiquitination substrates of WWP1/2 (Fig. 3-9, 10), indicating that WWP1/2 might also function in synaptic plasticity.

### 4.2.1 *Liprin- $\alpha$ 3* and WWP1/2

*Liprin- $\alpha$ 3*, a synaptic scaffold protein, was identified as a WWP1/2 binding protein

(Fig. 3-9). Mammalian liprin- $\alpha$  proteins localize at the axon, the dendrites and the synapse where they interact with various structural and motor proteins. These include the presynaptic active zone (AZ) proteins RIMs, CAST (ELKS) [Ko et al., 2003], CASK (calcium/calmodulin-dependent serine protein kinase), postsynaptic CaMKII (Ca<sup>2+</sup>/calmodulin-dependent protein kinase II), GRIP1 (glutamate receptor interacting protein) [Wyszynski et al., 2002], GIT1 (G protein-coupled receptor kinase interactor) [Ko et al., 2003] and the kinesin motor protein KIF1A (kinesin family member 1A) [Shin et al., 2003]. Through these interactions, liprin- $\alpha$  proteins play multiple roles in axon pathfinding, development of the AZ and the PSD, regulation of the synaptic vesicle (SV) pool, neurotransmitter release and vesicular trafficking. It was reported that the RING Finger type E3 ligase, the anaphase-promoting complex/cyclosome (APC/C) mediates polyubiquitination and subsequent proteasomal degradation of Dliprin, the *Drosophila* homolog of liprins, in the invertebrate synapse [van Roessel *et al.*, 2004]. However, regulation of the expression or the function of liprin- $\alpha$  proteins in the mammalian brain has never been explored. WWP1/2 dependent ubiquitination of liprins might alter synaptic functions in pre- and postsynapses.

#### **4.2.2 SAD-A and WWP1/2**

In addition to neuronal polarization [Kishi et al., 2005; Barnes et al., 2007], SAD kinases have multiple roles in synaptic functions. Mammalian SAD-B localizes to the presynapse, and associates with synaptic vesicles (SVs) and the AZ cytomatrix [Inoue et al., 2005]. SAD-B kinase regulates synaptic transmission at the presynapse and formation of the AZ, probably via phosphorylation of the vesicle priming factor RIM1 and other AZ proteins [Inoue et al., 2006]. SAD-A and SAD-B contain a conserved ubiquitin associated (UBA) domain. This is a commonly occurring sequence motif, composed of approximately 45 amino acid residues, that is found in diverse proteins involved in the ubiquitin/proteasome pathway, DNA excision-repair, and cell signaling via protein kinases [Kishi et al., 2005]. WWP1/2

show similar subcellular distributions as SAD-B, being enriched in the cytosolic vesicle (CSV) and PSD fractions in the adult brain (Fig. 3-1D) [Inoue et al., 2006]. In the present study, I demonstrated ubiquitination of SAD-A by WWP1 and -2. Because all lysine residues in SAD-A are conserved in SAD-B, it is likely that SAD-A is also ubiquitinated by WWP1 and -2. This ubiquitination does probably not occur via conjugation of K48-linked polyubiquitin chains that are recognized by the proteasome because expression levels of SAD kinases are not sensitive to proteasome inhibitors [Choi et al., 2011]. I assume ubiquitination is rather more important for functional modulation of SAD-A/B in neurotransmission. Injection of the C-terminal region of SAD-B into rat superior cervical ganglion neurons blocks neurotransmitter release, and overexpression of SAD-B in primary cultured rat hippocampal neurons increases neurotransmission [Inoue et al., 2006]. Although I have not identified target lysine residues for conjugation of ubiquitin chains in SAD-A, large polyubiquitin chains with their hydrophobic nature would impact on substrate recognition by or kinase activity of SAD-A during neurotransmitter release.

#### 4.2.3 Shank1a and WWP1/2

Assembly and stability of synapses are critical for establishing and maintaining functional neuronal circuits. Recent studies indicated that changes in synaptic architecture occur in part via post-translational modification through the ubiquitin pathway. For example, the RING Finger E3 ligase TRIM3 mediates turnover of the PSD scaffold protein GKAP and regulates dendritic spine morphology [Hung et al., 2010]. In this study, I demonstrated that WWP1 and WWP2 ubiquitinate the PSD scaffold protein Shank1a *in vitro* (Fig. 3-10). Ubiquitination of Shank by WWP1 and WWP2 could play an important role in synaptic function and plasticity.

Abnormalities in synaptic activity or plasticity, presumably underpinned by aberrant protein expression and/or protein-protein interactions, are known to occur in most psychiatric

disorders. It has been reported that more than 135 brain diseases including autism, chronic pain, schizophrenia and dementia are linked to defects in synaptic proteins [Bayes et al., 2011]. Although characterization of a gene that causes a particular disease is needed, it is also important to understand how the function of such genes is regulated posttranscriptionally. Autism spectrum disorder (ASD) is a common and heritable developmental disorder, affecting 0.6% of children. Mutations in members of the Shank family may contribute to ASD [Durand et al., 2006; Hung et al., 2008], indicating that proper regulation of Shank proteins is critical for normal cognitive functions. It has been reported that Shank is robustly polyubiquitinated in primary cultured neurons upon pharmacological activation of synapses although the E3 ligase that mediates this ubiquitination has not been reported yet [Ehlers, 2003]. In the present research, I showed that WWP1 and -2 ubiquitinate Shank1a and that both WWP proteins are recruited to the postsynapse in primary cultured neurons. How WWP1/2 might affect Shank function to coordinate various synaptic events in neuronal functions will be a fertile area for future research. Mouse models of human ASD due to post-transcriptional ubiquitin modification have not been created. The WWP1/2-flox conditional KO mouse, which I established in this study, is needed to examine whether they have morphological and behavioral features reminiscent of ASD, after breeding with fitting Cre deleter lines for analyses.

In summary, WWP1 and WWP2 are localized along the axon in the developing neuron, and a loss of WWP1 and WWP2 results in the failure of axon specification. Components of signaling pathways involved in neuronal polarization, including SAD kinases, might be regulated by WWP1 and WWP2 via ubiquitination during brain development. In mature neurons, on the other hand, WWP1 and WWP2 are localized at pre- and postsynapses, and both ubiquitinate synaptic scaffold proteins including liprin- $\beta$ 3 and Shank1. Ubiquitination of these synaptic proteins by WWP1 and WWP2 could modulate synaptic function and plasticity. Thus, WWP1 and WWP2 might contribute to various neuronal events, probably through ubiquitination of multiple targets and regulating multiple signaling pathways.





## 5 References

- Anthony TE, Klein C, Fishell G, Heintz N (2004) Radial Glia Serve as Neuronal Progenitors in All Regions of the Central Nervous System. *Neuron* **41**: 881-890
- Ashrafi K, Chang FY, Watts JL, Fraser AG, Kamath RS, Ahringer J, Ruvkun G (2003) Genome-wide RNAi analysis of *Caenorhabditis elegans* fat regulatory genes. *Nature* **421**: 268-272
- Attisano L, Wrana JL (2000) Smads as transcriptional co-modulators. *Current Opinion in Cell Biology* **12**: 235-243
- Atwood SX, Chabu C, Penkert RR, Doe CQ, Prehoda KE (2007) Cdc42 acts downstream of Bazooka to regulate neuroblast polarity through Par-6 aPKC. *Journal of Cell Science* **120**: 3200-3206
- Barnes AP, Lilley BN, Pan YA, Plummer LJ, Powell AW, Raines AN, Sanes JR, Polleux F (2007) LKB1 and SAD Kinases Define a Pathway Required for the Polarization of Cortical Neurons. *Cell* **129**: 549-563
- Barnes AP, Polleux F (2009) Establishment of Axon-Dendrite Polarity in Developing Neuron. *Annual Review of Neuroscience* **32**: 347-381
- Bayes A, Grabrucker AM, Knight MJ, Proepper C, Bockmann J, Joubert M, Rowan M, Durand CM, Betancur C, Boeckers TM, Chaste P, Fauchereau F, Nygren G, Rastam M, Gillberg IC, Anckarsater H, Sponheim E, Goubran-Botros H, Delorme R, Chabane N, Mouren-Simeoni M-C, de Mas P, Bieth E, Roge B, Heron D, Burglen L, Gillberg C, Leboyer M, Bourgeron T (2007) Mutations in the gene encoding the synaptic scaffolding protein SHANK3 are associated with autism spectrum disorders. *Nat Genet* **39**: 25-27
- Bayes A, Grabrucker AM, Knight MJ, Proepper C, Bockmann J, Joubert M, Rowan M, Nienhaus GU, Garner CC, Bowie JU, Kreutz MR, Gundelfinger ED, Boeckers TM (2011) Concerted action of zinc and ProSAP/Shank in synaptogenesis and synapse maturation. *EMBO J* **30**: 569-581
- Bayes A, van de Lagemaat LN, Collins MO, Croning MDR, Whittle IR, Choudhary JS, Grant SGN (2011) Characterization of the proteome, diseases and evolution of the human postsynaptic density. *Nat Neurosci* **14**: 19-21
- Boeckers TM, Kreutz MR, Winter C, Zuschratter W, Smalla K-H, Sanmarti-Vila L, Wex H, Langnaese K, Bockmann J, Garner CC, Gundelfinger ED (1999) Proline-Rich Synapse-Associated Protein-1/Cortactin Binding Protein 1 (ProSAP1/CortBP1) Is a PDZ-Domain Protein Highly Enriched in the Postsynaptic Density. *The Journal of Neuroscience* **19**: 6506-6518
- Borrell V, Yoshimura Y, Callaway EM (2005) Targeted gene delivery to telencephalic inhibitory neurons by directional in utero electroporation. *Journal of Neuroscience Methods* **143**: 151-158
- Bradke F, Dotti CG (2000) Differentiated neurons retain the capacity to generate axons from dendrites. *Current Biology* **10**: 1467-1470
- Brendel C, Rehbein M, Kreienkamp H-Jr, Buck F, Richter D, Kindler S (2004) Characterization of Staufen 1 ribonucleoprotein complexes. *Biochemical Journal* **384**: 239-246

- Brueckner K, Labrador JP, Scheiffele P, Herb A, Seeburg PH, Klein Rd (1999) EphrinB Ligands Recruit GRIP Family PDZ Adaptor Proteins into Raft Membrane Microdomains. *Neuron* **22**: 511-524
- Cao XR, Lill NL, Boase N, Shi PP, Croucher DR, Shan H, Qu J, Sweezer EM, Place T, Kirby PA, Daly RJ, Kumar S, Yang B (2008) Nedd4 Controls Animal Growth by Regulating IGF-1 Signaling. *Science Signaling* **1**: ra5
- Carrano AC, Liu Z, Dillin A, Hunter T (2009) A conserved ubiquitination pathway determines longevity in response to diet restriction. *Nature* **460**: 396-399
- Chen C, Sun X, Guo P, Dong X-Y, Sethi P, Cheng X, Zhou J, Ling J, Simons JW, Lingrel JB, Dong J-T (2005) Human Kruppel-like Factor 5 Is a Target of the E3 Ubiquitin Ligase WWP1 for Proteolysis in Epithelial Cells. *Journal of Biological Chemistry* **280**: 41553-41561
- Chen C, Sun X, Guo P, Dong XY, Sethi P, Zhou W, Zhou Z, Petros J, Frierson HF, Jr., Vessella RL, Atfi A, Dong JT (2006) Ubiquitin E3 ligase WWP1 as an oncogenic factor in human prostate cancer. *Oncogene* **26**: 2386-2394
- Chen C, Zhou Z, Ross JS, Zhou W, Dong J-T (2007) The amplified WWP1 gene is a potential molecular target in breast cancer. *International Journal of Cancer* **121**: 80-87
- Chen C-S, Bellier A, Kao C-Y, Yang Y-L, Chen H-D, Los FCO, Aroian RV (2010) WWP-1 Is a Novel Modulator of the DAF-2 Insulin-Like Signaling Network Involved in Pore-Forming Toxin Cellular Defenses in *Caenorhabditis elegans*. *PLoS ONE* **5**: e9494
- Chen HI, Sudol M (1995) The WW domain of Yes-associated protein binds a proline-rich ligand that differs from the consensus established for Src homology 3-binding modules. *Proceedings of the National Academy of Sciences of the United States of America* **92**: 7819-7823
- Cheng P-l, Lu H, Shelly M, Gao H, Poo M-m (2011) Phosphorylation of E3 Ligase Smurf1 Switches Its Substrate Preference in Support of Axon Development. *Neuron* **69**: 231-243
- Choi Y-J, Nardo AD, Kramvis I, Lynsey M, Kwiatkowski DJ, Sahin M, He X (2008) Tuberous sclerosis complex proteins control axon formation. *Genes Dev* **15**: 2485/2495
- Choi Y, Nardo A, Kramvis I, Meikle L, Kwiatkowski DJ, Sahin M, He X (2008) Tuberous sclerosis complex proteins control axon formation. *Genes Dev* **15**: 2485-2495
- Collins I, Rowley M, Davey WB, Emms F, Marwood R, Patel S, Patel S, Fletcher A, Ragan IC, Leeson PD, Scott AL, Broten T (1998) 3-(1-Piperazinyl)-4,5-dihydro-1H-benzo[g]indazoles: high affinity ligands for the human dopamine D4 receptor with improved selectivity over ion channels. *Bioorganic & Medicinal Chemistry* **6**: 743-753
- Collins SP, Reoma JL, Gamm DM, Uhler MD (2000) LKB1, a novel serine/threonine protein kinase and potential tumour suppressor, is phosphorylated by cAMP-dependent protein kinase (PKA) and prenylated in vivo. *Biochem J* **345**: 673-680
- Crump JG, Zhen M, Jin Y, Bargmann CI (2001) The SAD-1 Kinase Regulates Presynaptic Vesicle Clustering and Axon Termination. *Neuron* **29**: 115-129
- Da Silva J, Hasegawa T, Miyagi T, Dotti CG, Abad-Rodriguez J (2005) Asymmetric membrane ganglioside sialidase activity specifies axonal fate. *Nat Neurosci* **8**: 606-615

- Da Silva JS, Hasegawa T, Miyagi T, Dotti CG, Abad-Rodriguez J (2005) Asymmetric membrane ganglioside sialidase activity specifies axonal fate. *Nat Neurosci* **8**: 606-615
- Dieck S, Sanmarti-Vila L, Langnaese K, Richter K, Kindler S, Soyke A, Wex H, Smalla K-H, Kämpf U, Fränzer Jr-T, Stumm M, Garner CC, Gundelfinger ED (1998) Bassoon, a Novel Zinc-finger CAG/Glutamine-repeat Protein Selectively Localized at the Active Zone of Presynaptic Nerve Terminals. *The Journal of Cell Biology* **142**: 499-509
- Dong H, O'Brien RJ, Fung ET, Lanahan AA, Worley PF, Huganir RL (1997) GRIP: a synaptic PDZ domain-containing protein that interacts with AMPA receptors. *Nature* **386**: 279-284
- Dotti CG, Sullivan CA, Banker GA (1988) The establishment of polarity by hippocampal neurons in culture. *The Journal of Neuroscience* **8**: 1454-1468
- Drinjakovic J, Jung H, Campbell DS, Strohlic L, Dwivedy A, Holt CE (2010) E3 Ligase Nedd4 Promotes Axon Branching by Downregulating PTEN. *Neuron* **65**: 341-357
- Dunn R, Klos DA, Adler AS, Hicke L (2004) The C2 domain of the Rsp5 ubiquitin ligase binds membrane phosphoinositides and directs ubiquitination of endosomal cargo. *The Journal of Cell Biology* **165**: 135-144
- Durand CM, Betancur C, Boeckers TM, Bockmann J, Chaste P, Fauchereau F, Nygren G, Rastam M, Gillberg IC, Anckarsater H, Sponheim E, Goubran-Botros H, Delorme R, Chabane N, Mouren-Simeoni M-C, de Mas P, Bieth E, Roge B, Heron D, Burglen L, Gillberg C, Leboyer M, Bourgeron T (2007) Mutations in the gene encoding the synaptic scaffolding protein SHANK3 are associated with autism spectrum disorders. *Nat Genet* **39**: 25-27
- Fouladkou F, Landry T, Kawabe H, Neeb A, Lu C, Brose N, Stambolic V, Rotin D (2008) The ubiquitin ligase Nedd4-1 is dispensable for the regulation of PTEN stability and localization. *Proceedings of the National Academy of Sciences* **105**: 8585-8590
- Fukaya M, Ueda H, Yamauchi K, Inoue Y, Watanabe M (1999) Distinct spatiotemporal expression of mRNAs for the PSD-95/SAP90 protein family in the mouse brain. *Neuroscience Research* **33**: 111-118
- Fukaya M, Watanabe M (2000) Improved immunohistochemical detection of postsynaptically located PSD-95/SAP90 protein family by protease section pretreatment: A study in the adult mouse brain. *The Journal of Comparative Neurology* **426**: 572-586
- Gallagher E, Gao M, Liu Y-C, Karin M (2006) Activation of the E3 ubiquitin ligase Itch through a phosphorylation-induced conformational change. *Proceedings of the National Academy of Sciences of the United States of America* **103**: 1717-1722
- Goebbels S, Bormuth I, Bode U, Hermanson O, Schwab MH, Nave K-A (2006) Genetic targeting of principal neurons in neocortex and hippocampus of NEX-Cre mice. *Genesis* **44**: 611-621
- Gorski JA, Talley T, Qiu M, Puelles L, Rubenstein JLR, Jones KR (2002) Cortical Excitatory Neurons and Glia, But Not GABAergic Neurons, Are Produced in the Emx1-Expressing Lineage. *The Journal of Neuroscience* **22**: 6309-6314
- Greer PL, Hanayama R, Bloodgood BL, Mardinly AR, Lipton DM, Flavell SW, Kim T-K, Griffith EC, Waldon Z, Maehr R, Ploegh HL, Chowdhury S, Worley PF, Steen J, Greenberg ME (2010) The

- Angelman Syndrome Protein Ube3A Regulates Synapse Development by Ubiquitinating Arc. *Cell* **140**: 704-716
- Heldin N-E, Bergström D, Hermansson A, Bergenstråhle A, Nakao A, Westermark B, ten Dijke P (1999) Lack of responsiveness to TGF- $\beta$ 1 in a thyroid carcinoma cell line with functional type I and type II TGF- $\beta$  receptors and Smad proteins, suggests a novel mechanism for TGF- $\beta$  insensitivity in carcinoma cells. *Molecular and Cellular Endocrinology* **153**: 79-90
- Henrique D, Schweisguth F (2003) Cell polarity: the ups and downs of the Par6/aPKC complex. *Current Opinion in Genetics & Development* **13**: 341-350
- Hevner RF, Hodge RD, Daza RAM, Englund C (2006) Transcription factors in glutamatergic neurogenesis: Conserved programs in neocortex, cerebellum, and adult hippocampus. *Neuroscience Research* **55**: 223-233
- Hicke L (2001) Protein regulation by monoubiquitin. *Nat Rev Mol Cell Biol* **2**: 195-201
- Huang K, Johnson KD, Petcherski AG, Vandergon T, Mosser EA, Copeland NG, Jenkins NA, Kimble J, Bresnick EH (2000) A HECT domain ubiquitin ligase closely related to the mammalian protein WWP1 is essential for *Caenorhabditis elegans* embryogenesis. *Gene* **252**: 137-145
- Huibregtse JM, Scheffner M, Beaudenon S, Howley PM (1995) A family of proteins structurally and functionally related to the E6-AP ubiquitin-protein ligase. *Proceedings of the National Academy of Sciences of the United States of America* **92**: 2563-2567
- Hung A, Futai K, Sala C, Valtschanoff JG, Ryu J, Woodworth MA, Kidd FL, Sung CC, Miyakawa T, Bear MF, Weinberg RJ, Sheng M (2008) Smaller dendritic spines, weaker synaptic transmission, but enhanced spatial learning in mice lacking Shank1. *J Neurosci* **28**: 1697-1708
- Hung AY, Sung CC, Brito IL, Sheng M (2010) Degradation of Postsynaptic Scaffold GKAP and Regulation of Dendritic Spine Morphology by the TRIM3 Ubiquitin Ligase in Rat Hippocampal Neurons. *PLoS ONE* **5**: e9842
- Hunt-Newbury R, Viveiros R, Johnsen R, Mah A, Anastas D, Fang L, Halfnight E, Lee D, Lin J, Lorch A, McKay S, Okada HM, Pan J, Schulz AK, Tu D, Wong K, Zhao Z, Alexeyenko A, Burglin T, Sonnhammer E, Schnabel R, Jones SJ, Marra MA, Baillie DL, Moerman DG (2007) High-Throughput In Vivo Analysis of Gene Expression in *Caenorhabditis elegans*. *PLoS Biol* **5**: e237
- Hustad CM, Perry WL, Siracusa LD, Rasberry C, Cobb L, Cattanaach BM, Kovatch R, Copeland NG, Jenkins NA (1995) Molecular Genetic Characterization of Six Recessive Viable Alleles of the Mouse *agouti* Locus. *Genetics* **140**: 255-265
- Huttenlocher PR, de Courten C, Garey LJ, Van der Loos H (1982) Synaptogenesis in human visual cortex -- evidence for synapse elimination during normal development. *Neuroscience Letters* **33**: 247-252
- Huttner WB, Schiebler W, Greengard P, De Camilli P (1983) Synapsin I (protein I), a nerve terminal-specific phosphoprotein. III. Its association with synaptic vesicles studied in a highly purified synaptic vesicle preparation. *The Journal of Cell Biology* **96**: 1374-1388
- Inagaki N, Chihara K, Arimura N, Menager C, Kawano Y, Matsuo N, Nishimura T, Amano M,

- Kaibuchi K (2001) CRMP-2 induces axons in cultured hippocampal neurons. *Nat Neurosci* **4**: 781-782
- Ingham RJ, Colwill K, Howard C, Dettwiler S, Lim CSH, Yu J, Hersi K, Raaijmakers J, Gish G, Mbamalu G, Taylor L, Yeung B, Vassilovski G, Amin M, Chen F, Matskova L, Winberg G, Ernberg I, Linding R, O'Donnell P, Starostine A, Keller W, Metalnikov P, Stark C, Pawson T (2005) WW Domains Provide a Platform for the Assembly of Multiprotein Networks. *Molecular and Cellular Biology* **25**: 7092-7106
- Ingham RJ, Gish G, Pawson T (2004) The Nedd4 family of E3 ubiquitin ligases: functional diversity within a common modular architecture. *Oncogene* **23**: 1972-1984
- Inoue E, Mochida S, Takagi H, Higa S, Deguchi-Tawarada M, Takao-Rikitsu E, Inoue M, Yao I, Takeuchi K, Kitajima I, Setou M, Ohtsuka T, Takai Y (2006) SAD: A Presynaptic Kinase Associated with Synaptic Vesicles and the Active Zone Cytomatrix that Regulates Neurotransmitter Release. *Neuron* **50**: 261-275
- Inoue H, Imamura T, Ishidou Y, Takase M, Udagawa Y, Oka Y, Tsuneizumi K, Tabata T, Miyazono K, Kawabata M (1998) Interplay of Signal Mediators of Decapentaplegic (Dpp): Molecular Characterization of Mothers against dpp, Medea, and Daughters against dpp. *Molecular Biology of the Cell* **9**: 2145-2156
- Jahn O, Hesse D, Reinelt M, Kratzin H (2006) Technical innovations for the automated identification of gel-separated proteins by MALDI-TOF mass spectrometry. *Analytical and Bioanalytical Chemistry* **386**: 92-103-103
- James P, Halladay J, Craig EA (1996) Genomic Libraries and a Host Strain Designed for Highly Efficient Two-Hybrid Selection in Yeast. *Genetics* **144**: 1425-1436
- Jiang H, Guo W, Liang X, Rao Y (2005) Both the Establishment and the Maintenance of Neuronal Polarity Require Active Mechanisms: Critical Roles of GSK-3[beta] and Its Upstream Regulators. *Cell* **120**: 123-135
- Joberty G, Petersen C, Gao L, Macara IG (2000) The cell-polarity protein Par6 links Par3 and atypical protein kinase C to Cdc42. *Nat Cell Biol* **2**: 531-539
- Kaech S, Banker G (2006) Culturing hippocampal neurons. *Nat Protocols* **1**: 2406-2415
- Kaufmann N, DeProto J, Ranjan R, Wan H, Van Vactor D (2002) Drosophila Liprin-[alpha] and the Receptor Phosphatase Dlar Control Synapse Morphogenesis. *Neuron* **34**: 27-38
- Kawabe H, Neeb A, Dimova K, Young SM, Takeda M, Katsurabayashi S, Mitkovski M, Malakhova OA, Zhang D-E, Umikawa M, Kariya K-i, Goebbels S, Nave K-A, Rosenmund C, Jahn O, Rhee J, Brose N (2010) Regulation of Rap2A by the Ubiquitin Ligase Nedd4-1 Controls Neurite Development. *Neuron* **65**: 358-372
- Kent C, Clarke PJ (1991) The immunolocalisation of the neuroendocrine specific protein PGP9.5 during neurogenesis in the rat. *Brain Res Dev Brain Res* **58**: 147-150
- Kim AH, Puram SV, Bilimoria PM, Ikeuchi Y, Keough S, Wong M, Rowitch D, Bonni A (2009) A Centrosomal Cdc20-APC Pathway Controls Dendrite Morphogenesis in Postmitotic Neurons. *Cell* **136**: 322-336

- Kim HC, Huibregtse JM (2009) Polyubiquitination by HECT E3s and the Determinants of Chain Type Specificity. *Molecular and Cellular Biology* **29**: 3307-3318
- Kim J, Lilley B, Zhang C, Shokat K, Sanes J, Zhen M (2008) A chemical-genetic strategy reveals distinct temporal requirements for SAD-1 kinase in neuronal polarization and synapse formation. *Neural Development* **3**: 23
- Kishi M, Pan YA, Crump JG, Sanes JR (2005) Mammalian SAD Kinases Are Required for Neuronal Polarization. *Science* **307**: 929-932
- Ko J, Kim S, Valtschanoff JG, Shin H, Lee J-R, Sheng M, Premont RT, Weinberg RJ, Kim E (2003) Interaction between liprin-alpha and GIT1 is required for AMPA receptor targeting. *J Neurosci* **23**: 1667-1677
- Ko J, Na M, Kim S, Lee J-R, Kim E (2003) Interaction of the ERC family of RIM-binding proteins with the liprin-alpha family of multidomain proteins. *The Journal of biological chemistry* **278**: 42377-42385
- Komuro A, Imamura T, Saitoh M, Yoshida Y, Yamori T, Miyazono K, Miyazawa K (2004) Negative regulation of transforming growth factor-[beta] (TGF-[beta]) signaling by WW domain-containing protein 1 (WWP1). *Oncogene* **23**: 6914-6923
- Kornau HC, Schenker LT, Kennedy MB, Seeburg PH (1995) Domain interaction between NMDA receptor subunits and the postsynaptic density protein PSD-95. *Science* **269**: 1737-1740
- Kreienkamp HJ (2008) Scaffolding Proteins at the Postsynaptic Density: Shank as the Architectural Framework. In *Protein-Protein Interactions as New Drug Targets*, Klusmann E, Scott J (eds), Vol. 186, pp 365-380. Springer Berlin Heidelberg
- Kriegstein A, Noctor S, Martinez-Cerdeno V (2006) Patterns of neural stem and progenitor cell division may underlie evolutionary cortical expansion. *Nat Rev Neurosci* **7**: 883-890
- Kwan K-M (2002) Conditional alleles in mice: Practical considerations for tissue-specific knockouts. *Genesis* **32**: 49-62
- Kwiatkowski AV, Garner CC, Nelson WJ, Gertler FB (2009) Cell autonomous defects in cortical development revealed by two-color chimera analysis. *Molecular and Cellular Neuroscience* **41**: 44-50
- Kwiatkowski AV, Rubinson DA, Dent EW, Edward van Veen J, Leslie JD, Zhang J, Mebane LM, Philippart U, Pinheiro EM, Burds AA, Bronson RT, Mori S, F%ossler R, Gertler FB (2007) Ena/VASP Is Required for Neuritogenesis in the Developing Cortex. *Neuron* **56**: 441-455
- Kwon HJ, Ma S, Huang Z (2011) Radial glia regulate Cajal-Retzius cell positioning in the early embryonic cerebral cortex. *Developmental Biology* **351**: 25-34
- Laemmli UK (1970) Cleavage of Structural Proteins during the Assembly of the Head of Bacteriophage T4. *Nature* **227**: 680-685
- Laine A, Ronai Z (2006) Regulation of p53 localization and transcription by the HECT domain E3 ligase WWP1. *Oncogene* **26**: 1477-1483
- Lange W (1975) Cell number and cell density in the cerebellar cortex of man and some other mammals. *Cell Tissue Res* **157**: 115-124

- Langevin LM, Mattar P, Scardigli R, Roussigné M, Logan C, Blader P, Schuurmans C (2007) Validating in utero electroporation for the rapid analysis of gene regulatory elements in the murine telencephalon. *Developmental Dynamics* **236**: 1273-1286
- Langevin L, Mattar P, Scardigli R, Roussigne M, Logan C, Blader P, Schuurmans C (2007) Validating in utero electroporation for the rapid analysis of gene regulatory elements in the murine telencephalon. *Developmental Dynamics* **236**: 1273-1286
- Lee S-H, Choi J-H, Lee N, Lee H-R, Kim J-I, Yu N-K, Choi S-L, Lee S-H, Kim H, Kaang B-K (2008) Synaptic Protein Degradation Underlies Destabilization of Retrieved Fear Memory. *Science* **319**: 1253-1256
- Lennox G, Lowe J, Morrell K, Landon M, Mayer RJ (1988) Ubiquitin is a component of neurofibrillary tangles in a variety of neurodegenerative diseases. *Neuroscience Letters* **94**: 211-217
- Li H, Zhang Z, Wang B, Zhang J, Zhao Y, Jin Y (2007) Wwp2-Mediated Ubiquitination of the RNA Polymerase II Large Subunit in Mouse Embryonic Pluripotent Stem Cells. *Molecular and Cellular Biology* **27**: 5296-5305
- Li W, Bengtson MH, Ulbrich A, Matsuda A, Reddy VA, Orth A, Chanda SK, Batalov S, Joazeiro CAP (2008) Genome-Wide and Functional Annotation of Human E3 Ubiquitin Ligases Identifies MULAN, a Mitochondrial E3 that Regulates the Organelle's Dynamics and Signaling. *PLoS ONE* **3**: e1487
- Li X, Huang M, Zheng H, Wang Y, Ren F, Shang Y, Zhai Y, Irwin DM, Shi Y, Chen D, Chang Z (2008) CHIP promotes Runx2 degradation and negatively regulates osteoblast differentiation. *The Journal of Cell Biology* **181**: 959-972
- Liao B, Jin Y (2010) Wwp2 mediates Oct4 ubiquitination and its own auto-ubiquitination in a dosage-dependent manner. *Cell Res* **20**: 332-344
- Lim S, Naisbitt S, Yoon J, Hwang J-I, Suh P-G, Sheng M, Kim E (1999) Characterization of the Shank Family of Synaptic Proteins. *Journal of Biological Chemistry* **274**: 29510-29518
- Lu C, Pribanic S, Debonneville A, Jiang C, Rotin D (2007) The PY Motif of ENaC, Mutated in Liddle Syndrome, Regulates Channel Internalization, Sorting and Mobilization from Subapical Pool. *Traffic* **8**: 1246-1264
- Malbert-Colas L, Fay M, Cluzeaud F, Blot-Chabaud M, Farman N, Dhermy D, Lecomte M-C (2003) Differential expression and localisation of WWP1, a Nedd4-like protein, in epithelia. *Pflügers Archiv European Journal of Physiology* **447**: 35-43-43
- Margeta MA, Shen K (2010) Molecular mechanisms of synaptic specificity. *Molecular and Cellular Neuroscience* **43**: 261-267
- Marin O, Valiente M, Ge X, Tsai L-H (2010) Guiding Neuronal Cell Migrations. *Cold Spring Harbor Perspectives in Biology* **2**: a001834
- McKay SJ, Johnsen R, Khattra J, Asano J, Baillie DL, Chan S, Dube N, Fang L, Goszczynski B, Ha E, Halfnight E, Hollebakk R, Huang P, Hung K, Jensen V, Jones SJM, Kai H, Li D, Mah A, Marra M, McGhee J, Newbury R, Pouzyrev A, Riddle DL, Sonhammer E, Tian H, Tu D, Tyson

- JR, Vatcher G, Warner A, Wong K, Zhao Z, Moerman DG (2003) Gene expression profiling of cells, tissues, and developmental stages of the nematode *C. elegans*. *Cold Spring Harbor symposia on quantitative biology* **68**: 159-169.
- Miyazawa K, Shinozaki M, Hara T, Furuya T, Miyazono K (2002) Two major Smad pathways in TGF-beta superfamily signalling. *Genes to cells* **7**: 1191-1204
- Miyazono K (2000) Positive and negative regulation of TGF-beta signaling. *Journal of Cell Science* **113**: 1101-1109
- Mizoguchi A, Ueda T, Ikeda K, Shiku H, Mizoguti H, Takai Y (1989) Localization and subcellular distribution of cellular ras gene products in rat brain. *Brain Res Mol Brain Res* **5**: 31-44
- Morrione A, Plant P, Valentini B, Staub O, Kumar S, Rotin D, Baserga R (1999) mGrb10 Interacts with Nedd4. *Journal of Biological Chemistry* **274**: 24094-24099
- Nagai T, Ibata K, Park ES, Kubota M, Mikoshiba K, Miyawaki A (2002) A variant of yellow fluorescent protein with fast and efficient maturation for cell-biological applications. *Nat Biotech* **20**: 87-90
- Naisbitt S, Kim E, Tu JC, Xiao B, Sala C, Valtschanoff J, Weinberg RJ, Worley PF, Sheng M (1999) Shank, a Novel Family of Postsynaptic Density Proteins that Binds to the NMDA Receptor/PSD-95/GKAP Complex and Cortactin. *Neuron* **23**: 569-582
- Nakayama M, Goto TM, Sugimoto M, Nishimura T, Shinagawa T, Ohno S, Amano M, Kaibuchi K (2008) Rho-Kinase Phosphorylates PAR-3 and Disrupts PAR Complex Formation. *Developmental Cell* **14**: 205-215
- Narimatsu M, Bose R, Pye M, Zhang L, Miller B, Ching P, Sakuma R, Luga V, Roncari L, Attisano L, Wrana JL (2009) Regulation of Planar Cell Polarity by Smurf Ubiquitin Ligases. *Cell* **137**: 295-307
- Nishimura K, Akiyama H, Komada M, Kamiguchi H (2007) betaIV-spectrin forms a diffusion barrier against L1CAM at the axon initial segment. *Mol Cell Neurosci* **34**: 422-430
- Nishimura T, Kato K, Yamaguchi T, Fukata Y, Ohno S, Kaibuchi K (2004) Role of the PAR-3-KIF3 complex in the establishment of neuronal polarity. *Nat Cell Biol* **6**: 328-334
- Noctor SC, Martínez-Cerdeno V, Ivic L, Kriegstein AR (2004) Cortical neurons arise in symmetric and asymmetric division zones and migrate through specific phases. *Nat Neurosci* **7**: 136-144
- Noctor SC, Martínez-Cerdeño V, Kriegstein AR (2008) Distinct behaviors of neural stem and progenitor cells underlie cortical neurogenesis. *The Journal of Comparative Neurology* **508**: 28-44
- O'Donnell M, Chance RK, Bashaw GJ (2009) Axon Growth and Guidance: Receptor Regulation and Signal Transduction. *Annual Review of Neuroscience* **32**: 383-412
- Okabe S, Miwa A, Okado H (2001) Spine formation and correlated assembly of presynaptic and postsynaptic molecules. *Journal of Neuroscience* **21**: 6105-6114
- Olsen O, Moore KA, Fukata M, Kazuta T, Trinidad JC, Kauer FW, Streuli M, Misawa H, Burlingame AL, Nicoll RA, Brecht DS (2005) Neurotransmitter release regulated by a MAL2, Æiliprin-C $\pm$  presynaptic complex. *The Journal of Cell Biology* **170**: 1127-1134



- Ozdamar B, Bose R, Barrios-Rodiles M, Wang H-R, Zhang Y, Wrana JL (2005) Regulation of the Polarity Protein Par6 by TGF $\beta$  Receptors Controls Epithelial Cell Plasticity. *Science* **307**: 1603-1609
- Parrish JZ, Emoto K, Kim MD, Jan YN (2007) Mechanisms that Regulate Establishment, Maintenance, and Remodeling of Dendritic Fields. *Annual Review of Neuroscience* **30**: 399-423
- Perry WL, Hustad CM, Swing DA, O'Sullivan TN, Jenkins NA, Copeland NG (1998) The itchy locus encodes a novel ubiquitin protein ligase that is disrupted in a18H mice. *Nature Genetics* **18**: 143-146
- Peschiaroli A, Scialpi F, Bernassola F, Sherbini ESE, Melino G (2010) The E3 ubiquitin ligase WWP1 regulates [Delta]Np63-dependent transcription through Lys63 linkages. *Biochemical and Biophysical Research Communications* **402**: 425-430
- Pirozzi G, McConnell SJ, Uveges AJ, Carter JM, Sparks AB, Kay BK, Fowlkes DM (1997) Identification of Novel Human WW Domain-containing Proteins by Cloning of Ligand Targets. *Journal of Biological Chemistry* **272**: 14611-14616
- Plant PJ, Lafont F, Lecat S, Verkade P, Simons K, Rotin D (2000) Apical Membrane Targeting of Nedd4 Is Mediated by an Association of Its C2 Domain with Annexin Xiiiib. *The Journal of Cell Biology* **149**: 1473-1484
- Pulido R, Serra-Pag C, Tang M, Streuli M (1995) The LAR/PTP delta/PTP sigma subfamily of transmembrane protein-tyrosine-phosphatases: multiple human LAR, PTP delta, and PTP sigma isoforms are expressed in a tissue-specific manner and associate with the LAR-interacting protein LIP.1. *Proceedings of the National Academy of Sciences of the United States of America* **92**: 11686-11690
- Rajewsky K, Gu H, Kuhn R, Betz UA, Muller W, Roes J, Schwenk F, Schwenk F (1996) Conditional gene targeting. *J Clin Invest* **98**: 600-603
- Reumann S, Babujee L, Ma C, Wienkoop S, Siemsen T, Antonicelli GE, Rasche N, Luder F, Weckwerth W, Jahn O (2007) Proteome Analysis of Arabidopsis Leaf Peroxisomes Reveals Novel Targeting Peptides, Metabolic Pathways, and Defense Mechanisms. *THE PLANT CELL*: tpc.107.050989
- Rhee J, Pirity MK, Lackan CS, Long JZ, Kondoh G, Takeda J, Hadjantonakis A-K (2002) In vivo imaging and differential localization of lipid-modified GFP-variant fusions in embryonic stem cells and mice. *Genesis* **44**: 202/218
- Richardson WD, Kessaris N, Pringle N (2006) Oligodendrocyte wars. *Nat Rev Neurosci* **7**: 11-18
- Rotin D, Kumar S (2009) Physiological functions of the HECT family of ubiquitin ligases. *Nat Rev Mol Cell Biol* **10**: 398-409
- Saito T, Nakatsuji N (2001) Efficient Gene Transfer into the Embryonic Mouse Brain Using in Vivo Electroporation. *Developmental Biology* **240**: 237-246
- Sala C, Piłch V, Wilson NR, Passafaro M, Liu G, Sheng M (2001) Regulation of Dendritic Spine Morphology and Synaptic Function by Shank and Homer. *Neuron* **31**: 115-130
- Sanes JR, Yamagata M (2009) Many Paths to Synaptic Specificity. *Annual Review of Cell and*

*Developmental Biology* **25**: 161-195

- Sapkota GP, Kieloch A, Lizcano JM, Lain S, Arthur JSC, Williams MR, Morrice N, Deak M, Alessi DR (2001) Phosphorylation of the Protein Kinase Mutated in Peutz-Jeghers Cancer Syndrome, LKB1/STK11, at Ser431 by p90RSK and cAMP-dependent Protein Kinase, but Not Its Farnesylation at Cys433, Is Essential for LKB1 to Suppress Cell Growth. *Journal of Biological Chemistry* **276**: 19469-19482
- Sauer B, Henderson N (1988) Site-specific DNA recombination in mammalian cells by the Cre recombinase of bacteriophage P1. *Proceedings of the National Academy of Sciences of the United States of America* **85**: 5166-5170
- Schmitz C, Kinge P, Hutter H (2007) Axon guidance genes identified in a large-scale RNAi screen using the RNAi-hypersensitive *Caenorhabditis elegans* strain nre-1(hd20) lin-15b(hd126). *Proceedings of the National Academy of Sciences* **104**: 834-839
- Schoch S, Castillo PE, Jo T, Mukherjee K, Geppert M, Wang Y, Schmitz F, Malenka RC, Sudhof TC (2002) RIM1[alpha] forms a protein scaffold for regulating neurotransmitter release at the active zone. *Nature* **415**: 321-326
- Schwamborn JC, Puschel AW (2004) The sequential activity of the GTPases Rap1B and Cdc42 determines neuronal polarity. *Nat Neurosci* **7**: 923-929
- Serra-Page C, Medley QG, Tang M, Hart A, Streuli M (1998) Liprins, a Family of LAR Transmembrane Protein-tyrosine Phosphatase-interacting Proteins. *Journal of Biological Chemistry* **273**: 15611-15620
- Sessa A, Mao C-a, Hadjantonakis A-K, Klein WH, Broccoli V (2008) Tbr2 Directs Conversion of Radial Glia into Basal Precursors and Guides Neuronal Amplification by Indirect Neurogenesis in the Developing Neocortex. *Neuron* **60**: 56-69
- Shariff GA (1953) Cell counts in the primate cerebral cortex. *The Journal of comparative neurology* **98**: 381-400
- Shelly M, Cancedda L, Heilshorn S, Sumbre Gn, Poo M-m (2007) LKB1/STRAD Promotes Axon Initiation During Neuronal Polarization. *Cell* **129**: 565-577
- Shi S-H, Cheng T, Jan LY, Jan Y-N (2004) APC and GSK-3[beta] Are Involved in mPar3 Targeting to the Nascent Axon and Establishment of Neuronal Polarity. *Current Biology* **14**: 2025-2032
- Shi S-H, Jan LY, Jan Y-N (2003) Hippocampal Neuronal Polarity Specified by Spatially Localized mPar3/mPar6 and PI 3-Kinase Activity. *Cell* **112**: 63-75
- Shin H, Wyszynski M, Huh K-H, Valtschanoff JG, Lee J-R, Ko J, Streuli M, Weinberg RJ, Sheng M, Kim E (2003) Association of the Kinesin Motor KIF1A with the Multimodular Protein Liprin-alpha. *Journal of Biological Chemistry* **278**: 11393-11401
- Sieburth D, Ch'ng Q, Dybbs M, Tavazoie M, Kennedy S, Wang D, Dupuy D, Rual J-F, Hill DE, Vidal M, Ruvkun G, Kaplan JM (2005) Systematic analysis of genes required for synapse structure and function. *Nature* **436**: 510-517
- Silverman JL, Turner SM, Barkan CL, Tolu SS, Saxena R, Hung AY, Sheng M, Crawley JN (2011)

- Sociability and motor functions in Shank1 mutant mice. *Brain Research* **1380**: 120-137
- Sordella R, Van Aelst L (2008) Dialogue between RhoA/ROCK and Members of the Par Complex in Cell Polarity. *Developmental Cell* **14**: 150-152
- Spruston N (2008) Pyramidal neurons: dendritic structure and synaptic integration. *Nat Rev Neurosci* **9**: 206-221
- Stambolic V, Suzuki A, de la Pompa JL, Brothers GM, Mirtsos C, Sasaki T, Ruland J, Penninger JM, Siderovski DP, Mak TW (1998) Negative Regulation of PKB/Akt-Dependent Cell Survival by the Tumor Suppressor PTEN. *Cell* **95**: 29-39
- Stryker E, Johnson KG (2007) LAR, liprin {alpha} and the regulation of active zone morphogenesis. *Journal of Cell Science* **120**: 3723-3728
- Tai H-C, Schuman EM (2008) Ubiquitin, the proteasome and protein degradation in neuronal function and dysfunction. *Nat Rev Neurosci* **9**: 826-838
- Takamori S, Holt M, Stenius K, Lemke EA, Grønborg M, Riedel D, Urlaub H, Schenck S, Brügger B, Ringler P, Müller SA, Rammner B, Grøtter F, Hub JS, De Groot BL, Mieskes G, Moriyama Y, Klingauf Jr, Grubmüller H, Heuser J, Wieland F, Jahn R (2006) Molecular Anatomy of a Trafficking Organelle. *Cell* **127**: 831-846
- Takeuchi T, Nomura T, Tsujita M, Suzuki M, Fuse T, Mori H, Mishina M (2002) Flp recombinase transgenic mice of C57BL/6 strain for conditional gene targeting. *Biochemical and Biophysical Research Communications* **293**: 953-957
- Tu JC, Xiao B, Yuan JP, Lanahan AA, Leoffert K, Li M, Linden DJ, Worley PF (1998) Homer Binds a Novel Proline-Rich Motif and Links Group 1 Metabotropic Glutamate Receptors with IP3 Receptors. *Neuron* **21**: 717-726
- van Haaften G, Romeijn R, Pothof J, Koole W, Mullenders LHF, Pastink A, Plasterk RHA, Tijsterman M (2006) Identification of Conserved Pathways of DNA-Damage Response and Radiation Protection by Genome-Wide RNAi. *Current Biology* **16**: 1344-1350
- van Roessel P, Elliott DA, Robinson IM, Prokop A, Brand AH (2004) Independent Regulation of Synaptic Size and Activity by the Anaphase-Promoting Complex. *Cell* **119**: 707-718
- Varoqueaux F, Aramuni G, Rawson RL, Mohrmann R, Missler M, Gottmann K, Zhang W, Südhof TC, Brose N (2006) Neuroligins Determine Synapse Maturation and Function. *Neuron* **51**: 741-754
- Werner HB, Kuhlmann K, Shen S, Uecker M, Schardt A, Dimova K, Orfaniotou F, Dhaunchak A, Brinkmann BG, Mühlbauer W, Guarente L, Casaccia-Bonnel P, Jahn O, Nave K-A (2007) Proteolipid Protein Is Required for Transport of Sirtuin 2 into CNS Myelin. *The Journal of Neuroscience* **27**: 7717-7730
- Wiesner S, Ogunjimi AA, Wang H-R, Rotin D, Sicheri F, Wrana JL, Forman-Kay JD (2007) Autoinhibition of the HECT-Type Ubiquitin Ligase Smurf2 through Its C2 Domain. *Cell* **130**: 651-662
- Wilkinson KD, Lee KM, Deshpande S, Duerksen-Hughes P, Boss JM, Pohl J (1989) The neuron-specific protein PGP 9.5 is a ubiquitin carboxyl-terminal hydrolase. *Science* **246**: 670-673
- Wyszynski M, Kim E, Dunah AW, Passafaro M, Valtschanoff JG, Serra-Pagès C, Streuli M,

- Weinberg RJ, Sheng M (2002) Interaction between GRIP and Liprin-[alpha]/SYD2 Is Required for AMPA Receptor Targeting. *Neuron* **34**: 39-52
- Wyszynski M, Kim E, Dunah AW, Passafaro M, Valtschanoff JG, Serra-Pagès C, Streuli M, Weinberg RJ, Sheng M (2002) Interaction between GRIP and Liprin-±/SYD2 Is Required for AMPA Receptor Targeting. *Neuron* **34**: 39-52
- Wyszynski M, Valtschanoff JG, Naisbitt S, Dunah AW, Kim E, Standaert DG, Weinberg R, Sheng M (1999) Association of AMPA Receptors with a Subset of Glutamate Receptor-Interacting Protein In Vivo. *The Journal of Neuroscience* **19**: 6528-6537
- Xu H, Wang W, Li C, Yu H, Yang A, Wang B, Jin Y (2009) WWP2 promotes degradation of transcription factor OCT4 in human embryonic stem cells. *Cell Res* **19**: 561-573
- Xu P, Duong DM, Seyfried NT, Cheng D, Xie Y, Robert J, Rush J, Hochstrasser M, Finley D, Peng J (2009) Quantitative Proteomics Reveals the Function of Unconventional Ubiquitin Chains in Proteasomal Degradation. *Cell* **137**: 133-145
- Yamashita M, Ying S-X, Zhang G-m, Li C, Cheng SY, Deng C-x, Zhang YE (2005) Ubiquitin Ligase Smurf1 Controls Osteoblast Activity and Bone Homeostasis by Targeting MEKK2 for Degradation. *Cell* **121**: 101-113
- Yamatani H, Kawasaki T, Mita S, Inagaki N, Hirata T (2010) Proteomics analysis of the temporal changes in axonal proteins during maturation. *Developmental Neurobiology* **70**: 523-537
- Yi JJ, Barnes AP, Hand R, Polleux F, Ehlers MD (2010) TGF-[beta] Signaling Specifies Axons during Brain Development. *Cell* **142**: 144-157
- Yoshimura T, Kawano Y, Arimura N, Kawabata S, Kikuchi A, Kaibuchi K (2005) GSK-3[beta] Regulates Phosphorylation of CRMP-2 and Neuronal Polarity. *Cell* **120**: 137-149
- Zecevic N, Rakic P (1991) Synaptogenesis in Monkey Somatosensory Cortex. *Cerebral Cortex* **1**: 510-523
- Zhang H, Macara IG (2008) The PAR-6 Polarity Protein Regulates Dendritic Spine Morphogenesis through p190 RhoGAP and the Rho GTPase. *Developmental Cell* **14**: 216-226
- Zhang X, Srinivasan SV, Lingrel JB (2004) WWP1-dependent ubiquitination and degradation of the lung Kr, ppe1-like factor, KLF2. *Biochemical and Biophysical Research Communications* **316**: 139-148
- Zhen M, Jin Y (1999) The liprin protein SYD-2 regulates the differentiation of presynaptic termini in *C. elegans*. *Nature* **401**: 371-375
- Zhen M, Jin Y (2004) Presynaptic terminal differentiation: transport and assembly. *Current Opinion in Neurobiology* **14**: 280-287
- Zhu L-Q, Zheng H-Y, Peng C-X, Liu D, Li H-L, Wang Q, Wang J-Z (2010) Protein Phosphatase 2A Facilitates Axonogenesis by Dephosphorylating CRMP2. *The Journal of Neuroscience* **30**: 3839-3848
- Zitzer H, Hönck H-H, Bächner D, Richter D, Kreienkamp H-J (1999) Somatostatin Receptor Interacting Protein Defines a Novel Family of Multidomain Proteins Present in Human and Rodent Brain. *Journal of Biological Chemistry* **274**: 32997-33001

## CURRICULUM VITAE

Family name: Kishimoto-Suga

Forename: Mika

Sex: Female

Date of Birth: 12 August 1976

Place of Birth: Kyoto

Nationality: Japanese

Present address: Department of Molecular Neurobiology,  
Max-Planck-Institute for Experimental Medicine,  
Hermann-Rein-Str. 3, 37075 Göttingen, Germany

Education:

Faculty of Biology, Georg-August University School of Science (GAUSS), Göttingen  
Department of Molecular Neurobiology, Max Planck Institute for Experimental Medicine,  
Göttingen

PhD Thesis: “The Role of HECT Type Ligases WWP1 and WWP2 in Nerve Cell  
Development and Function”, Sep 2007-2011, under the supervision of Prof. Dr. Nils Brose  
and Dr. Hiroshi Kawabe

Department of Biochemistry, Faculty of Biology, Graduate School of Science and  
Technology, Kobe University, Japan,  
Master of Science, 2001

Department of Biology, Faculty of Liberal Arts and Education, Shiga University, Japan,  
Bachelor of Education, 1999

Research and professional experience:

PhD student at Department of Molecular Neurobiology, Max-Planck-Institute for  
Experimental Medicine, working on “The role of the HECT-type ubiquitin ligases WWP1 and  
WWP2 in nerve cell development and function” with Dr. Hiroshi Kawabe and Prof. Dr. Nils  
Brose, Sep 2009-2011

Assistant professor at Department of Molecular Bio-regulation, Kyoto Pharmaceutical  
University, Japan, working on “Function of novel centrosomal and nuclear envelope protein  
CNEp35/Nup35 in mammalian cells” with Dr. Koji Owada, 2001-2007

